Ovarian Steroid Regulation of the Midbrain Corticotropin Releasing Factor and Urocortin Systems in Macaques

by

Rachel Sanchez Thwing

A DISSERTATION

presented to

Department of Neuroscience
Vollum Institute
Oregon Health and Science University
School of Medicine

in partial fulfillment of the requirements for the degree of

Doctor of Philosophy

June 2010

School of Medicine
Oregon Health and Science University

CERTIFICATE OF APPROVAL

This is to certify that the Ph.D. dissertation of

Rachel Sanchez Thwing

has been approved

by

_____
Cynthia L. Bethea, Ph.D.

_____
Andrey Ryabinin, Ph.D.

_____
Henryk Urbanski, Ph.D.

_____
Oline Ronnekleiv, Ph.D.

_____
Daniel Marks, M.D., Ph.D.

ACKNOWLEDGEMENTS

I am grateful for the guidance and patience of my mentor, Dr. Cynthia Bethea. Her vision and dedication profoundly impacted my perspective. The lessons I learned from her will continue to benefit me throughout my life and career.

I also thank Drs. Andrey Ryabinin, Henryk Urbanski, Oline Ronnekleiv, Dan Marks, and other faculty members of the Neuroscience Graduate Program who taught and advised me throughout these studies. I will strive to make them proud by continuing to pursue research questions and translating science in schools.

I sincerely thank the past and current members of the Bethea lab with whom I have worked the past eight years, especially Arubala Reddy, Stephanie Mirkes, Lisa Smith, Jessica Henderson, Luisa Appleman, Fernanda Lima, Karin Weisheimer, Nurgul Salli, Yukari Tokuyama, and Heidi Rivera. Each member has shared her recipes and knowledge generously and patiently. Thanks also to Diana Gordon who provided me with numerous opportunities to develop my teaching skills with younger students.

The recipient list of my gratitude would not be complete without thanking Dr. Frances Pau at Oregon National Primate Research Center (ONPRC) for help with hormone assays, Dr. Anda Cornea for assistance with the Marianas imaging system, Dr. Ybing Jia of the Molecular Biology core, and Dr. Henryk Urbanski for generously sharing tissues. I am also grateful for the help provided by the surgical team and animal care technicians at ONPRC.

ABSTRACT

A significant number of postmenopausal women report increased anxiety and vulnerability to stress, which has been linked to decreased secretion of ovarian steroids. Communication between the serotonin system and the CRF system determines stress sensitivity or resilience. This study examines the effects of the ovarian steroids, estradiol (E) and progesterone (P) on the CRF system components that impact serotonin neurons in the midbrain of nonhuman primates. Ovariectomized rhesus macaques were treated with placebo, E alone for one month, or E supplemented with P for the last 2 weeks. Quantitative (q)RT-PCR and immunocytochemistry were employed. E±P treatment decreased CRF-R1 and increased CRF-R2 gene expression in hemi-midbrain blocks and in laser captured serotonin neurons. Also in hemi-midbrains, E treatment increased UCN1 and CRFBP gene expression, but supplemental P treatment reversed these effects. E±P suppressed the already very low UCN3 mRNA, but had no effect on UCN2 mRNA. E±P decreased CRF fiber density in the dorsal, interfascicular and median raphe nuclei and decreased CRF-R1 immunostaining in the dorsal raphe. E increased CRF-R2 immunostaining in the dorsal and median raphe. E±P increased UCN1 immunostaining in the cell bodies and increased UCN1 fiber density in the caudal linear nucleus. ERβ, but not ERα was detected in the nucleus of UCN1-positive neurons. While the mechanism of ovarian hormone regulation of the midbrain CRF system requires further investigation, these studies clearly demonstrate another pathway by which ovarian hormones may have positive effects on anxiety and mood regulation.

Chapter 1: Introduction

1.1 Menopause is associated with onset of depressed mood.

The menopause transition is the time in a woman's life when her ovaries decrease the rate of ovulation and her menstrual cycle lengthens (O'Connor et al., 2009). Importantly, ovarian estradiol secretion is normal or at times elevated (Santoro, 2005) during the early stages of the menopause transition. Gradually, over time, ovarian hormone production declines until menstruation ceases altogether. This transition into menopause lasts an average of four years duration (McKinlay et al., 2008), and often negatively impacts the quality of life for many women. After a women's final menstruation, she enters post-menopause, and negative menopause-related symptoms may persist for another 8 to 10 years (Nisar and Sohoo, 2009). Together, the transition into and after menopause lasts twelve or more years of a woman's life and may constitute a window of vulnerability for the development of depression (Soares and Frey, 2010) and stress-related inflammatory responses (Prather et al., 2009).

More than a million women in the United States reach the menopause transition each year, and many of them may live one third or more of their lives post-menopause. This transition is strongly associated with recurrent depression in women with a past history of mood disorders, as well as new onset of depressed mood among women with no history of depression (Freeman et al., 2006). Moreover, women in the menopause transition experience a diminished positive response to the most effective treatment of depression to date, selective serotonin reuptake inhibitors (SSRIs) (Pinto-Meza et al.,

2006). If we more precisely understood the mechanisms by which ovarian hormones regulate brain stress systems during menopause, then we would be able to treat anxious and depressive symptoms in menopausal women more effectively. However, the mechanisms by which the ovarian hormones estradiol (E) and progesterone (P) exert their mood regulating effects need further investigation.

1.2 Hormone replacement therapy and the macaque model of surgical menopause

In addition to changes in mood, irritability and anxiety levels, women transitioning through menopause experience other negative symptoms such as hot flushes, sleep disturbances, night sweats, loss of libido, vaginal dryness, fatigue, difficulty concentrating, and up to 34 less common symptoms. Ultimately, the lack of estrogen leads to osteoporosis, hip fractures and the dowagers' hump with marked curvature of the spine. For women without a prior diagnosis of breast or reproductive tract cancers, hormone replacement therapy (HRT) is an excellent recourse. Unfortunately, there exists an array of formulations that fall under the rubric of HRT, many of which have poorer outcomes and adverse side effects. The most commonly prescribed formulations of HRT in the US are the Wyeth products. Because of the wide usage of the Wyeth products, their efficacy and side effects were examined in a large multiarm clinical trial called the Women's Health Initiative (WHI). The early interpretation of the results from that trial led to grave misunderstandings and underprescription of HRT for millions of needy women.

Premarin[TR] is the Wyeth estrogen formulation, which contains conjugated equine estrogens that are isolated from horse urine. The major estrogen in Premarin[TR] is estriol and there is little bioactive estradiol. The large amount of equine estrogens in this formulation may cause adverse reactions in some women and clinical trials comparing the efficacy and side effects of Premarin[TR] with bioidentical estradiol are lacking. However, Premarin[TR] is only prescribed for women who have had a complete hysterectomy and the Premarin[TR] arm of the WHI study did not find a significant increase in risk for breast cancer at the dosages utilized. Nonetheless, since release of the WHI analysis, Wyeth has decreased the recommended dosage for Premarin[TR] by half.

Provera[TR] is the progestin formulation from Wyeth. It consists of medroxyprogesterone acetate (MPA), which has significantly different effects on numerous end organs in comparison to natural progesterone. In addition, it has some androgenic properties. Moreover, it has frequently been reported to cause depression and anxiety. The estrogen and progesterone combination formulation from Wyeth is called Prempro[TR] and it consists of conjugated equine estrogens plus medroxyprogesterone acetate. MPA blocks the effects of the conjugated equine estrogens on the uterus, but it also blocks the effect of estrogen in other organs, resulting in little beneficial effect and a number of negative side effects including new breast cancers. Prempro[TR] was used in the arm of the WHI for women with an intact uterus, and this arm was suspended early due to adverse cardiovascular events.

In recent years, clinical scientists have finally started to ask why animal studies show beneficial effects of HRT and clinical studies do not. One of the most obvious reasons is that animal studies usually use natural estradiol and progesterone. Formulations of natural estradiol or ethinyl estradiol at low doses are available, but large-scale double blind clinical trials to compare the risks and benefits of natural estradiol in comparison to the Wyeth products are lacking. Obtaining natural formulations of progesterone is not straightforward. Solvay produced a micronized version for many years, but it has been withdrawn from the market.

More recently, evidence has accrued that the first pass of oral estrogens through the liver increases the production of proteins that accumulate in plaques. Therefore, clinicians are beginning to recognize that administration of HRT via skin patches or vaginal rings is superior to oral formulations because the doses can be reduced and there is a decrease in risk for plaque formation.

The time of onset of HRT is also an important consideration. The women enrolled in the WHI study were on average, 15 or more years past menopause, and they had numerous pre-existing conditions. The most troubling outcome of the WHI was related to cardiovascular events, which were significantly higher in the women taking Prempro than in placebo treated controls. Subsequent data from Clarkson and colleagues (Clarkson, 2007) has shown that administration of estrogen after atherosclerosis progression causes plaque inflammation and plaque instability. The disruption of plaques leads to blood clots in peripheral tissues, heart attacks and strokes. Thus,

premenopausal atherosclerosis progression seems to be an important determinant of postmenopausal atherosclerosis. Both monkeys and women with premenopausal estrogen deficiency develop premature atherosclerosis, an effect that can be prevented in both species by estrogen-containing oral contraceptives. During the perimenopausal years, there are robust estrogen benefits. Monkeys given estrogens immediately after surgical menopause have a 70% inhibition in coronary atherosclerosis progression. Estrogen treatment prevented progression of atherosclerosis of women in the Estrogen in the Prevention of Atherosclerosis Trial. A meta-analysis of women younger than 60 years given hormone therapy had reduced total mortality (relative risk = 0.61, 95% CI: 0.39-0.95). In the late menopausal years, there are no or possible deleterious estrogen effects. Monkeys lose cardiovascular benefits of estrogens when treatment is delayed (Clarkson, 2007).

The WHI also reported an increase in cognitive problems in women taking Prempro for the first time, many years after menopause. As highlighted above, the effect of late onset estrogen treatment on plaque inflammation and instability leads to blood borne particles, which could lodge in the microvasculature of the brain and produce ministrokes. Without better assessment, there was no way to discriminate vascular dementia from other types of cognitive decline in the WHI (Harman et al., 2005a).

A recent clinical trial (KEEPS) has been initiated which attempts to control for the type of estrogen formulation, the route of administration and the initiation time after

menopause (Harman et al., 2005b). The KEEPS is designed to explore the hypothesis that early initiation of hormone therapy, in women who are at the inception of their menopause, will decrease the rate of accumulation of atherosclerotic plaque, indicating a likely delay in the onset of clinical cardiovascular disease. The Bethea lab has also proposed a monkey mini-trial to examine the effect of time after ovarietomy on the actions of natural estrogen and progesterone in the serotonin system.

The rhesus monkey is an excellent model for studying neuropsychiatric disorders in humans because rhesus monkeys have neocortex and display psychopathology that appears similar to that of humans (Kalin et al., 2000). Moreover, monkeys and humans have similarities in social behavior, stress-related endocrine function, and brain structure (Kalin et al., 2000). Another important characteristic that monkeys share with humans is that they experience a long period of maternal-infant nurturance that appears to be necessary for emotional, social, and physical development of infants. In fact, subtle differences in maternal-infant interactions are associated with the behavioral reactivity of the developing infant monkey (O'Connor and Cameron, 2006).

The rhesus monkey is also an excellent model for studying the neuropsychiatric effects of hormone replacement therapy (HRT) after menopause because the rhesus has monthly menstrual cycles similar to humans (Bellino and Wise, 2003). Monkeys enter menopause naturally at about 25 years of age and age-related changes in FSH predict their transition into menopause that lasts for approximately four years (Downs and Urbanski, 2006). However, in the model employed for these studies, surgical

ovariectomy of adult females, rather than natural menopause, is used to reduce serum E and P levels to approximate those of women in menopause. This model has several advantages. One, it removes the confounding influence of age on the gene expression levels that we are investigating. Two, it allows for replacement of natural hormones in regimens that mimic those given to postmenopausal women (Hotchkiss, 1994). A disadvantage of using surgical ovariectomy to study the central effects of withdrawal of E and P is that the repercussions of natural menopause on a woman's health may be more complex because of age-related changes and the gradual (rather than abrupt) rate of loss of estradiol and other ovarian factors (Roberts et al., 1997; Bellino and Wise, 2003).

1.3 Estrogen and progestin receptors.

Many of the biological effects of E and P are mediated through the nuclear estrogen and progestin receptors (ER and PR), which are members of the steroid/nuclear receptor superfamily of transcriptional activators (Tsai and O'Malley, 1994). E and P have high affinity for, and are potent activators, of ER and PR, respectively. Nuclear ER and PR function by acting as ligand-dependent genomic transcription factors. To initiate transcription, E and P also require specific coactivators and corepressors in the binding complex (Tetel, 2009). In addition to their genomic mechanisms, ER and PR can also function in the brain as membrane receptors that activate cytoplasmic signaling cascades (Kelly and Ronnekleiv, 2008; Mani, 2008; Micevych and Mermelstein, 2008 766; Roepke et al., 2008; Kuo et al., 2009). However, because we administer one month of HRT to the ovariectomized macaques, we expect that rapid membrane-

mediated actions of E and P on gene and protein expression may have passed during the time-course of our treatment regime. Therefore, we expect that the effects of E and P on gene and protein expression in the experiments described herein were mediated primarily by nuclear ERs and PRs.

Nuclear ERs exist in two forms, α and β, which are transcribed from different genes (Kuiper et al., 1996). The subtypes have different functions in the human brain and in behavior (Bodo and Rissman, 2006), and they also differ in their central distribution within the female brain (Osterlund et al., 2000). Importantly, a new role ERβ is emerging as regulator of anxiety because activation of ERβ reduces anxious behavior on a number of tasks in several species (Bodo and Rissman, 2006).

The primary mechanism of P action in the brain involves its interaction with E-induced, nuclear PRs. In this case, PRs serve as transcriptional factors, regulating the expression of genes and genomic neural networks to initiate or sustain a physiological response (Mani, 2008). Multiple PR isoforms are produced from a single gene on chromosome 11 by transcription from alternative promoters and alternate translation sites, and these isoforms dimerize and bind DNA. Two isoforms, PR-A and PR-B, which are structurally related but functionally distinct, have been identified in rodents, primates, and humans. Recently a third isoform, PR-C, was identified in humans, and PR-C is thought to modulate the transcriptional activity of PR-A and PR-B (Mani, 2008).

In women who have a hysterectomy, E or an estrogen analog is prescribed alone to prevent hot flushes, mood changes and osteoporosis. In women with an intact uterus, P or modified analogs are given in conjunction with E analogs to prevent proliferation of the uterine endometrium. Therefore, in these studies E was administered alone to model HRT for hysterectomized women and E+P was administered to model HRT for women with an intact uterus. We expect that any measurable transcriptional effects due to P treatment in our model would be via E-induced intracellular PRs.

1.4 Serotonin, stress, and depression.

The central serotonin system can be divided into two large subsystems. The rostral raphe nuclei send their projections mainly to the forebrain via ascending pathways, while the caudal raphe system targets areas of the lower brain stem and spinal cord. The dorsal and median raphe nuclei are the two main rostral nuclei and their serotonergic projections travel through the medial forebrain bundle to reach a multitude of pathways in the forebrain (Paxinos, 1990).

The serotonin system modulates a wide range of neural outcomes from emotion to intellect to metabolism; and it is a target of pharmacotherapies, steroid hormones, cytokines, neuropeptides, and trophic factors, which impact the efficacy of serotonin neurotransmission. Epidemiological evidence links exposure to stressful life events with increased risk for depression (Kendler et al., 1999); however, there is significant individual variability in vulnerability to environmental risk factors. Several studies have shown that individuals carrying the short allele of the serotonin transporter gene-linked

polymorphic region have an increased risk of experiencing depression following exposure to stress during adulthood than individuals carrying the long allele (Kendler et al., 2005). Functional analysis indicates that short allele carriers show uncoupling of a feedback circuit in the amygdala and cingulate areas that are important in the extinction of fear after exposure to fearful stimuli (Pezawas et al., 2005). These studies imply that the availability of serotonin after processing stressful or fearful stimuli is low in the short allele carriers and that there is consequently not enough serotonin available for extinction of negative affect. In accordance with this notion, the administration of selective serotonin reuptake inhibitors is the most effective pharmacological intervention for depression and anxiety disorders to date (Owens and Nemeroff, 1994). In opposition to this notion, a 2009 meta-analysis (combining results of several studies) examining the interaction between the serotonin transporter gene and stressful life events on depression yielded no evidence that serotonin transporter genotype couples with stressful life events to increase the risk of depression (Risch et al., 2009).

Recent work in rodent models seeking to identify the molecular mechanisms underlying the gene (short allele of the serotonin transporter gene-linked polymorphic region) by environment (stressful life event) risk factor have aided in our understanding of individual differences in resilience to stress. When wild-type mice and heterozygous serotonin transporter knockout mice were subjected to 3 weeks of chronic psychosocial stress, the heterozygous serotonin transporter knockout mice showed increased vulnerability to the stressor compared to wild-type mice, as evidenced by increased social avoidance and depressed locomotor activity (Bartolomucci et al., 2010).

Heterozygous mice also showed significantly lower levels of serotonin turnover than the wild-type mice did after experiencing the chronic stressor. The rodent studies support the evidence in human studies asserting that low functionality of the serotonin transporter after stressful stimuli increases risk of depression by preventing serotonin-mediated extinction of fear and avoidance behaviors. However, most of the rodent studies were performed with males, presumably because circulating hormones in cycling females confound experimental results, especially those measuring anxious and depressive behavior in rodents. The lack of knowledge about the underlying mechanisms mediating serotonin turnover, stress sensitivity, and depression in the female gender is a significant obstacle against effectively treating stress-related mood disorders in women.

1.5 Anatomy and physiology of the central CRF and UCN systems with a focus on connections with the serotonin system.

*Central CRF anatomy with emphasis on its connections with the raphe***:** The relationship between CRF signaling and serotonin transmission has attracted significant interest. Centrally, the three main sites of CRF production are the paraventricular nucleus of the hypothalamus, the amygdala, and the bed nucleus of the stria terminalis. In the rodent, CRF neurons in the hypothalamic paraventricular nucleus, the amygdala, and the bed nucleus of the stria terminalis project to the dorsal and median raphe nuclei (Luiten et al., 1985a; Luiten et al., 1985b; Portillo et al., 1998), which are the main serotonergic projections to the forebrain. There is also a reciprocal serotonergic projection from the raphe to the hypothalamic paraventricular nucleus (Petrov et al.,

1992; Hanley and Van de Kar, 2003) as well as to the amygdala (Gray 1993). The CRF innervation of the human dorsal raphe nucleus is well documented (Austin et al., 1997; Ruggiero et al., 1999), and one study in humans showed that CRF fibers and terminals apposed serotonin cell bodies and primary dendrites in the raphe region (Ruggiero et al., 1999).

Central UCN anatomy with emphasis on connections with raphe: Across species, there is a large concentration of UCN1 neurons in a perioculomotor region known as the Edinger-Westphal nucleus (EW), and this region is the only brain site where UCN1 expression is conserved across species (Zhao et al., 1998; Bittencourt et al., 1999; Kozicz et al., 2002; Vasconcelos et al., 2003; Lim et al., 2006). May et al. characterized UCN1-immunopositive neurons within the perioculomotor region of the monkey and cat (May et al., 2008), and determined that they form a distinct population of neurons than the cholinergic oculomotor neurons for which the EW was named. The authors therefore proposed that a name distinct from the EW be used to describe UCN1-positive neurons in this area and applied the name perioculomotor urocortin population or $pIII_u$. In the experiments described here, we refer to perioculomotor UCN1-positive neurons as the $pIII_u$.

A UCN1-positive fiber tract originating from the monkey $pIII_u$ and innervating the raphe has been identified in primate and rat brains (Vasconcelos et al., 2003; Weitemier and Ryabinin, 2005), but it is not known whether the raphe sends reciprocal serotonergic innervation to the $pIII_u$, and this question merits further investigation. In

rodents, lesions of perioculomotor urocortin neurons decrease immunoreactive UCN1-positive fibers in the dorsal raphe (Bachtell et al., 2004). This supports a role of UCN1-induced modulation of the raphe.

UCN2 gene expression in the rodent brain appears to be predominantly in the arcuate and paraventricular nuclei (PVN) of the hypothalamus, as well as the locus coeruleus and the nucleus of the solitary tract (NTS) (Reyes et al., 2001). The human stresscopin-related peptide (SRP) shares 76% sequence identity with mouse UCN2 (Hsu and Hsueh, 2001). Both rodent UCN2 and human SRP bind selectively to CRF-R2 (Hsu and Hsueh, 2001; Reyes et al., 2001) rather than CRF-R1.

In the rat brain, central production of UCN3 appears to be predominantly in the hypothalamus and medial amygdala (Li et al., 2002), although UCN3 mRNA signal has also been detected in the posterior bed nucleus of the stria terminalis (BST) as well as the superior paraolivary nucleus of the brainstem (Lewis et al., 2001). Recent close examination of UCN3 distribution in rodents has revealed close anatomical association between UCN3 terminal fields and CRF-R2 in the hypothalamus, lateral septum, and medial amygdala (Jamieson et al., 2006).

CRF receptors are anatomically distributed in the dorsal raphe serotonin system. In rodents, CRF-R1 and CRF-R2 receptors have been observed in the dorsal raphe nucleus and CRF has complex and opposing effects depending on the dose used and the endpoint examined (Pernar et al., 2004; Waselus et al., 2009). The primate raphe

reportedly expresses both CRF-R1 and CRF-R2, but sources disagree as to whether CRF-R1 is abundantly expressed in raphe (Sanchez et al., 1999; Kostich et al., 2004), and it remains to be determined which CRF receptors are more abundant on serotonin neurons.

CRF and UCN system physiology within the raphe serotonin system: Ovarian hormones may modulate signaling within the CRF system by modulating any one of several key components within the network: CRF-related ligands (CRF, UCN1, UCN2, UCN3), receptors, and binding proteins**.** As shown in **Figure 1** below, CRF and urocortins mediate their effects by activating two known G-protein coupled receptors, CRF-R1 and CRF-R2 (Dautzenberg and Hauger, 2002). CRF has a higher affinity for CRF-R1 than CRF-R2. In contrast, the urocortins bind CRF-R2 with higher affinity than they bind CRF-R1 (Vaughan et al., 1995). In addition, CRF and UCN1 also interact with a binding protein, CRF-BP, with an affinity comparable to that of their affinity to their respective CRF receptor (Behan et al., 1995). CRF-BP binds CRF or UCN1 extracellularly and is thought to prevent receptor activation by binding up the ligand (Behan et al., 1996; Kemp et al., 1998).

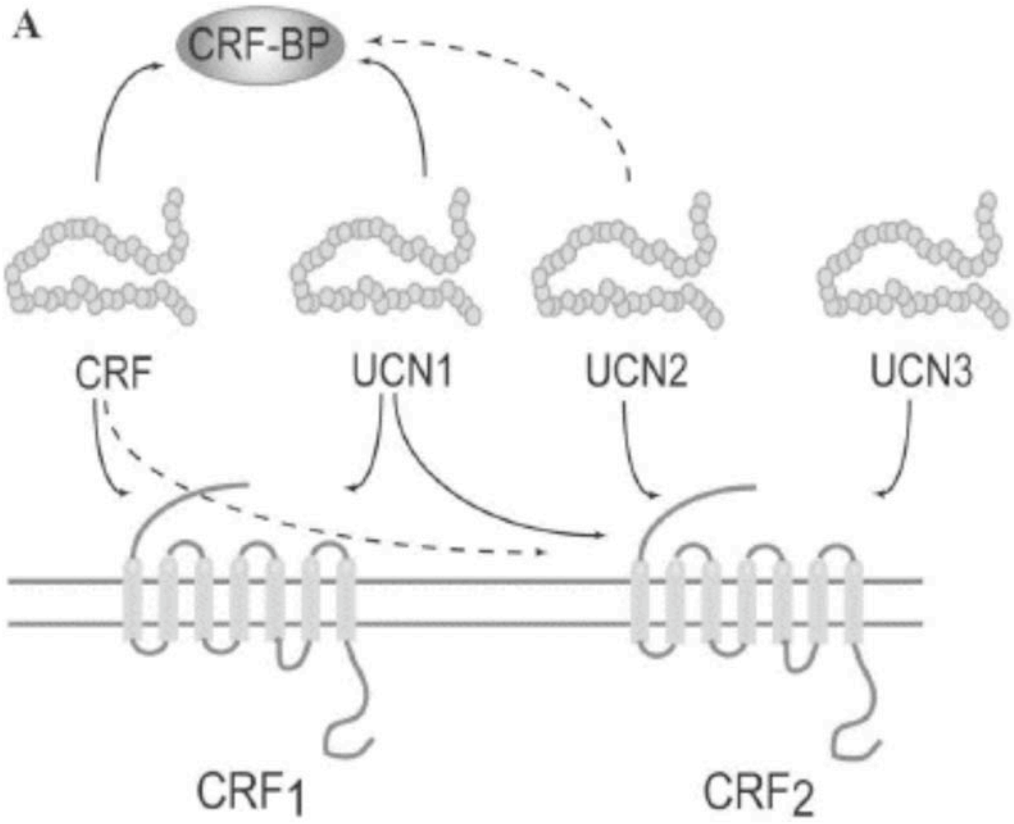

Figure 1. Schematic representation of relative binding affinities of mammalian corticotropin-releasing factor-like peptides, their receptors, and the CRF binding protein (CRF-BP). Solid lines with arrows indicate high affinity binding, while dashed lines with arrows indicate lower affinity binding. Reproduced from Boorse and Denver (2006) with permission from Elsevier Inc.

The distribution of the CRF-R1 and CRF-R2 receptors is distinct and implies diverse physiological functions, as evidenced by the divergent phenotypes of CRF-R1- and CRFR2-null mice (Smith et al., 1998; Timpl et al., 1998; Muller et al., 2003; Keck et al., 2005; Refojo et al., 2005; Pastor et al., 2008). In the raphe specifically, pharmacologically engaging either CRF receptor differentially affects serotonin release and behavior. The current model supports a neurotransmitter role for endogenous CRF on both receptor subtypes, facilitating contrasting behaviors (Valentino and Commons, 2005; Waselus et al., 2009). It implies that CRF released in low concentration would activate CRF-R1, thus toning down the activity of the dorsal raphe and decreasing serotonin release. In contrast, higher pharmacological concentrations of CRF would engage CRF-R2, thus activating the dorsal raphe and increasing serotonin release. In addition, in unstressed rats CRF-R1 and CRF-R2 are differentially distributed within the DR, with CRF-R1 being prominent in the plasma membrane and CRF-R2 being cytoplasmic. Stress experience reverses this distribution, such that CRF-R2 is recruited to the plasma membrane and CRF-R1 internalizes. As a consequence of this stress-induced cellular redistribution of CRF receptors, neuronal responses change, and this provided a cellular mechanism for switching strategies for coping with stressors. Although this model seems to work, it negates the possibility that another member of the CRF neuropeptide family with a much higher affinity for CRF-R2 could activate this receptor as well (Kozicz, 2010).

Recently, Neufeld-Cohen et al. (2010) demonstrated that UCN1 and UCN2 double deficient mice show a robust anxiolytic phenotype, an altered stress response, and

modified serotonergic activity in anxiety circuits (Neufeld-Cohen et al., 2010), and these studies point to an important role of the urocortins in modulating the raphe serotonin system. Their study is an important step towards understanding the integrated action of CRF/CRF-R1 and UCNs/CRF-R2 within the dorsal raphe, and it provides evidence to build a more satisfying model. In this model CRF would activate CRF-R1 neurons and facilitate the translocation of CRF-R2 from the cytoplasm to the plasma membrane of dorsal raphe neurons. The now membrane-bound CRF-R2 could be engaged by either UCN1 or UCN2 (Kozicz, 2010), both of which both project to the raphe through the $pIII_u$ and locus coeruleus, respectively (Reyes et al., 2001; Weitemier and Ryabinin, 2005). UCN1 or UCN2 activation of CRF-R2 would increase serotonin release (into fear/anxiety areas) and promote passive coping responses to stress such as depressive-type behaviors (Waselus et al., 2009).

UCN2 and UCN3 were isolated in humans and rodents within the last five years, and less is known about the full extent of their physiological functions. A stimulus for hypothalamic UCN2 and UCN3 release is intracerebroventricular injection (icv) of parathyroid hormone-related protein, a protein produced by many tumors (Asakawa et al., 2010). Once released, central UCN2 and UCN3 mediate cachexia and anorexia (Fekete et al., 2006; Kamdi et al., 2009; Thammacharoen et al., 2009). It has been suggested that the primary role of urocortin 3 in the rodent is as a neuromodulator linking stress-induced anxiety and energy homeostasis (Jamieson et al., 2006; Kuperman et al., 2010), and results from a 2010 study (Deussing et al., 2010) suggest a

novel role for UCN3 related to the processing of social cues and to the establishment of social memories.

1.6 Estradiol and progesterone modulate serotonin system and serotonin related gene expression.

This laboratory has shown that the ovarian steroids, estradiol (E) and progesterone (P) increase serotonin neural function (Bethea et al., 2002) and protect serotonin neuronal health in monkeys (Bethea et al., 2009). We found that one month of E ± P treatment increases gene transcription of the rate-limiting enzyme of central serotonin synthesis, tryptophan-hydroxylase 2 (*TPH-2*) (Sanchez et al., 2005). Panels 1-8 in **Figure 2** illustrate *TPH-2* in situ hybridization signal in eight levels of the dorsal raphe (each 250 µm apart) from an E+P-treated animal. The levels pictured are arranged rostrally to caudally and represent the extent of the dorsal raphe analyzed in placebo-, E-, P-, and E+P-treated animals. **Figure 3-upper panel** depicts radiolabeled *tryptophan hydroxylase 2* mRNA signal in representative photomicrographs from placebo-, E-, P-, and E+P-treated animals at three levels of the rostral raphe region. There is an obvious increase in *tryptophan hydroxylase 2*-signal intensity in the animals treated with E, P, and E+P compared to the placebo-treated ovariectomized controls (labeled SPAY in this picture). When the *TPH-2* mRNA signal was quantified (**Figure 3-lower panel**) across eight rostro-caudal levels of the dorsal raphe, there was an overall significant increase in TPH-2 signal intensity in the dorsal raphe of the hormone treated animals compared to placebo-treated controls. This implies that serotonin neurons in female

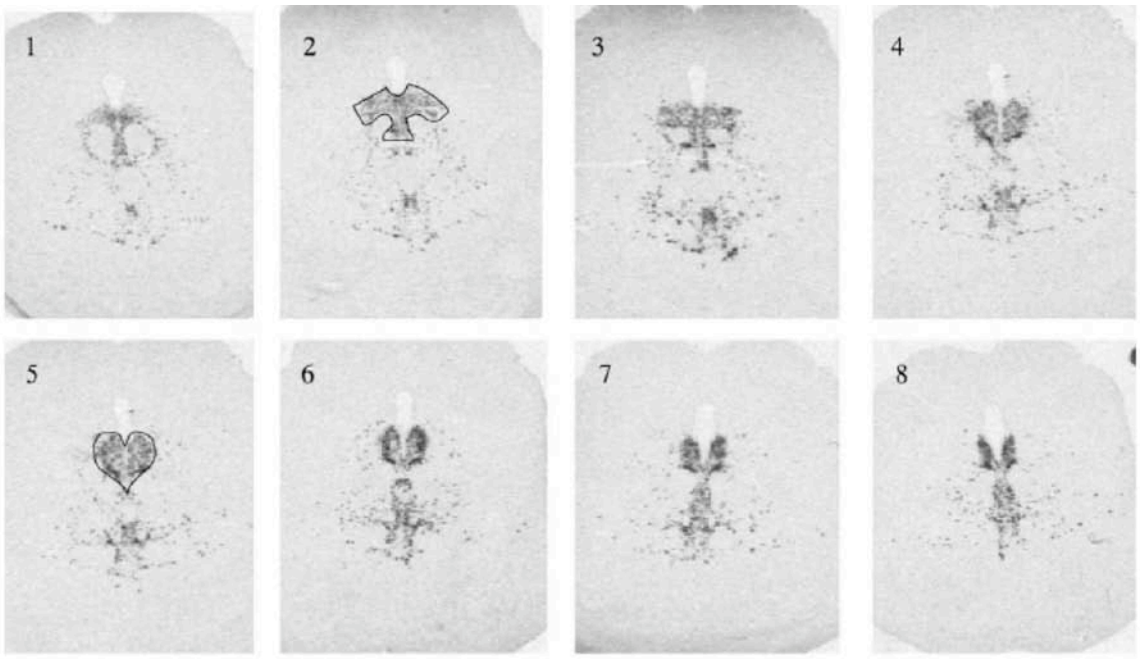

Figure 2. Representative photomicrographs of *tryptophan hydroxylase 2 (TPH-2)* in situ hybridization signal in the monkey midbrain. Panels 1-8 illustrate the appearance of radiolabeled *TPH-2* mRNA signal on film autoradiograms from an E+ P- treated animal. Each level of the raphe that was analyzed was located 250 um caudal to the previous level. Collectively, the levels of the raphe pictured here represent a region spanning 2 mm of dorsal raphe nucleus. Panels 2 and 5 illustrated the area template that was applied for optical density analysis. Each level had a different template that was applied to all animals. Reproduced from Sanchez et al. (2005) with permission from Elsevier.

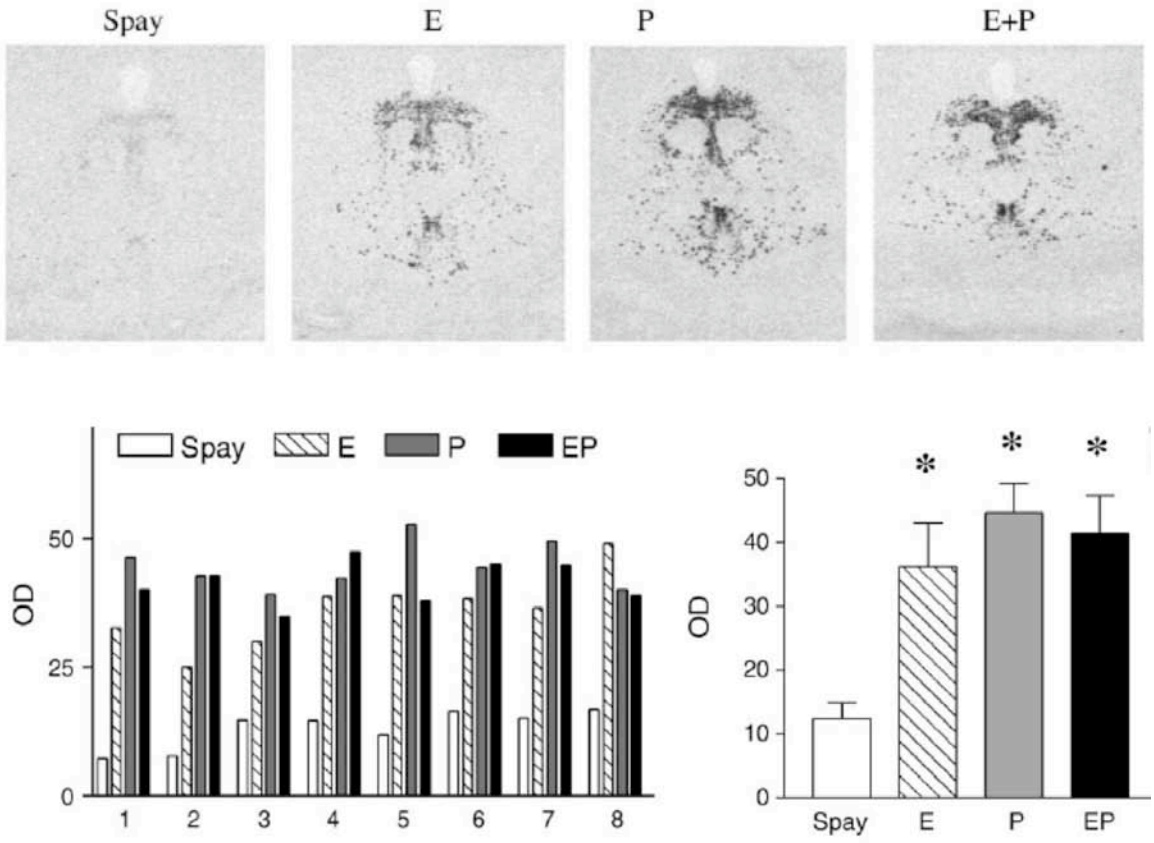

Figure 3. Upper Panel: Depicts four representative S^{35}-labeled *TPH-2* autoradiograms from raphe sections in placebo- (labeled Spay in this figure) and hormone-treated animals. There is a notable increase in *TPH-2* signal intensity in the hormone-treated animals compared to the placebo-treated controls. **Lower Panel:** When the *TPH-2* signal was quantified by densiometric analysis, E, P, and E+P treatments significantly increased overall *TPH-2* mRNA expression in the raphe compared to placebo-treated controls (ANOVA, $p < 0.004$). Reproduced from Bethea and Centeno (2008) with permission from Nature Publishing Group.

monkeys respond to one month of ovarian hormone treatment by increasing serotonin production. This greater availability of serotonin may translate to improved mood and stress resilience in these animals, and this question certainly merits further investigation.

When we extrapolate our findings about the effects of E and P on the primate dorsal raphe serotonin system to make predictions about the transition into menopause for women, we expect that withdrawal from circulating E and P would depress overall central serotonin availability. It follows, then, that drugs targeting the serotonin system would improve depressive symptoms in women, but women transitioning into menopause are less responsive to SSRIs (Pinto-Meza et al., 2006). This further underscores the importance of improving treatment options for anxiety and depression in menopausal women.

1.7 CRF system and models of depression

CRF-immunoreactivity is elevated in the dorsal raphe of depressed suicide subjects (Austin et al., 2003), and this evidence supports the hypothesis that CRF in the dorsal raphe may be particularly important in the pathophysiology of affective disorders. Although human studies elucidating the mechanisms of CRF regulation of serotonin are scarce, much work has been done in rodents to shed light on the relation between CRF system activation and its regulation of the raphe serotonin system

In rodents, exposure to inescapable shock causes many stress-related behaviors and pathologies associated with depression such as: reduced food and water intake and an increase in gastric lesions (Weiss, 1971), reduced aggression and increased social defeat (Wood et al., 2010), neophobia (Minor et al., 1994), and increased escape latency when escape is possible (Maier et al., 1982; Desan et al., 1988; Drugan et al., 1989). One particular model of behavioral depression in which rats experience escapable or inescapable shock provides particular insight into a behavior called "learned helplessness" that can be detected as early as 4 hours post stressor (Maier and Watkins, 2005). Dr. Stephen Maier and colleagues have recently discovered that blocking CRF-R2 activation in the dorsal raphe nucleus prevents uncontrollable stressor-induced learned helplessness. The body of literature on this model is immense, but to sum a few significant points and theories of the authors: Antagonizing CRF-R2 during the inescapable shocks prevents massive serotonin release to fear perception areas such as the basolateral amygdala. Their elegant design has produced work suggesting that uncontrollable stress activates CRF-R2 in the rodent raphe and increases release of serotonin from the raphe into the amygdala, as measured in microdialysate in the amygdala. The authors suggest that depletion of serotonin stores during the stressor reduces the rat's ability to learn to escape in a paradigm 4 and 8 hours later where escape is possible (Maier and Watkins, 2005).

While we know that E and E+P treatments after ovariectomy enhance serotonin neuron survival (Tokuyama et al., 2008), and that CRF signaling network interacts with the raphe serotonin neurons in rodent models of depression (Maier and Watkins, 2005),

we do not know the whether E and P affect CRF receptor signaling in serotonin neurons of the primate.

1.8 Estradiol and progesterone decrease hypothalamic CRF gene and protein expression.

This laboratory has shown that E and P increase CRF gene and protein expression in the hypothalamic paraventricular nucleus (PVN) of rhesus monkeys (Bethea and Centeno, 2008). **Figure 4** shows the CRF mRNA autoradiographic signal in representative sections from an animal in each treatment group. The autoradiographic signal for CRF mRNA is markedly denser in the sections from the hormone-treated animals. The results of this analysis are shown in **Figure 5.** The overall group average of CRF optical density per section was significantly reduced by ovarian hormone treatment. **Figure 6** illustrates representative montages of hypothalamic sections from placebo, E-, P-, and E + P-treated ovariectomized monkeys immunostained with an antibody against human CRF. CRF staining is more robust and covered a larger area in the placebo-treated control animal compared to the hormone-treated animals. The staining was quantified and the results of the analysis are illustrated in **Figure 7**. Each of the treatment groups exhibited a significant decrease compared to the placebo group, but there was no difference between treatment groups.

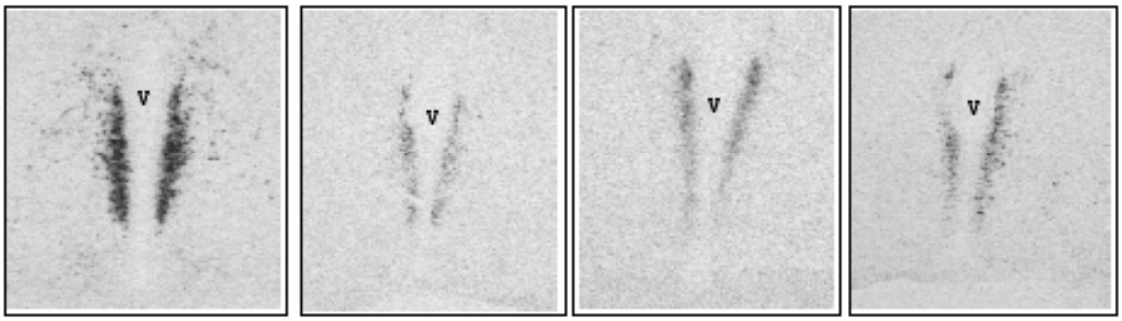

Figure 4. in situ hybridization autoradiograms of the paraventricular nucleus at level 2 from representative ovariectomized monkeys treated with placebo (OVX), E, P, or E+P for 1 month. Reproduced from Bethea and Centeno (2008) with permission from Nature Publishing Group.

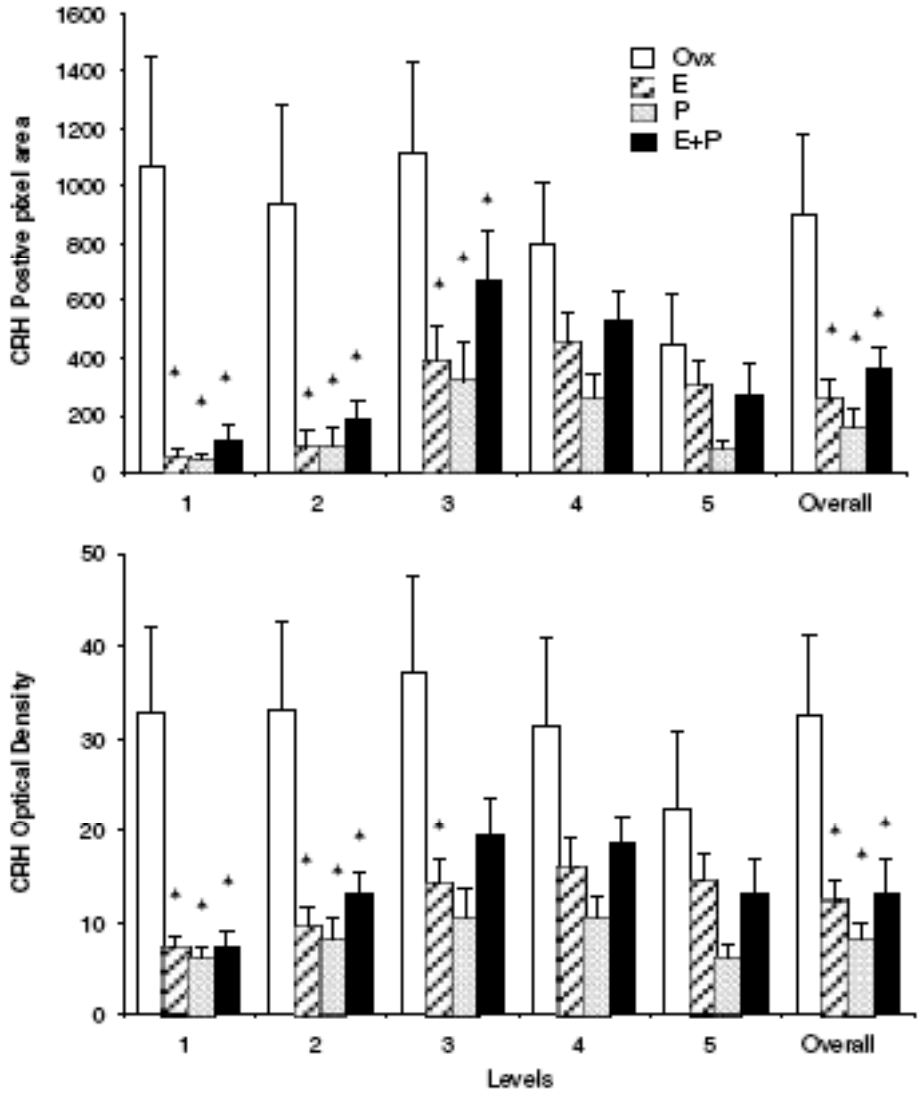

Figure 5. Analysis of *CRF* mRNA signal on autoradiograms across five levels of the paraventricular nucleus in four treatment groups (n = 4 animals/group). The upper panel represents the positive pixel area covered by the signal ± SEM. The lower panel illustrates optical density of the *CRF* signal ± SEM. E, P and E+P treatments significantly decreased *CRF* mRNA signal in the paraventricular nucleus in levels 1, 2, and 3 and in the overall average. The asterisks indicate significant differences by Student-Neuman-Keuls post-hoc pairwise comparison with $p < 0.02$. Reproduced from Bethea and Centeno (2008) with permission from Nature Publishing Group.

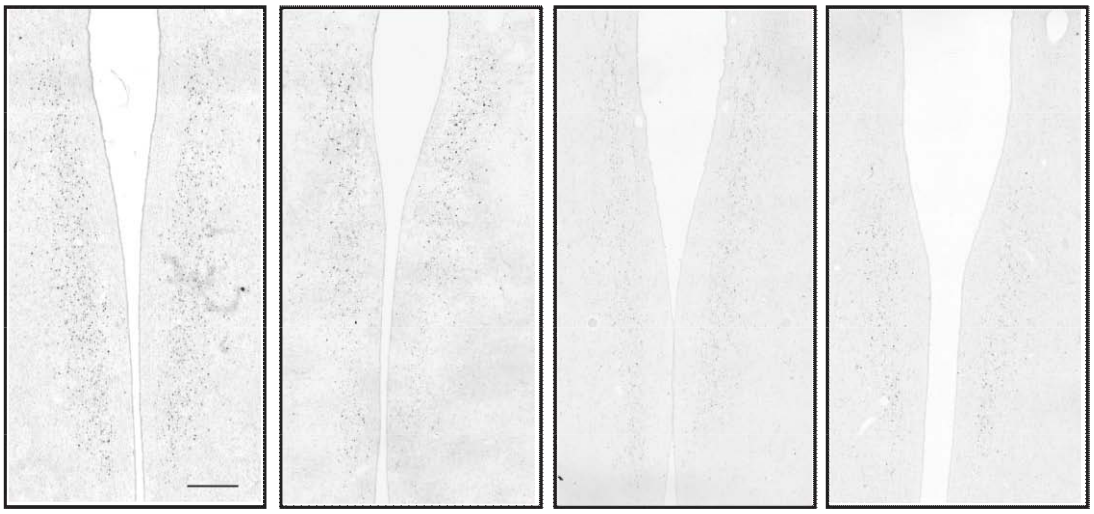

Figure 6. Stereology montages of level 1 of the paraventricular nucleus from ovariectomized monkeys treated with E, P, or E+P. CRF immunostaining is in black and white. The CRF-immunopositive signal was segmented from background and the area of the signal was computed in pixels for further quantitative analysis. Scale bar, 500 μm. Reproduced from Bethea and Centeno (2008) with permission from Nature Publishing Group.

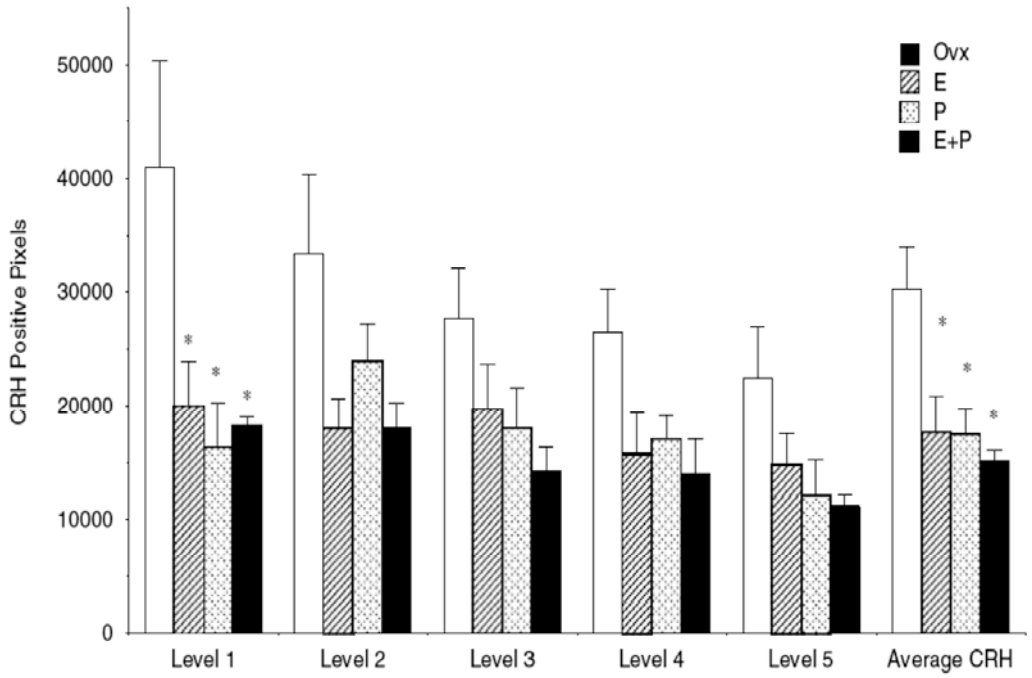

Figure 7. Analysis of CRF-positive pixels across five levels of the paraventricular nucleus in each treatment group (n=4 animals/group). The average CRF-positive pixel area was computed for each animal and then the mean of the animals was obtained for each group. Ovarian hormone treatment significantly reduced the average CRF-immunopositive signal. The asterisks represent a significant difference from the control group by Student-Neuman-Keuls post-hoc pairwise comparison with $p < 0.002$. Reproduced from Bethea and Centeno (2008) with permission from Nature Publishing Group.

1.9 Overall rationale and hypotheses.

Information about the effect of ovarian steroids on the CRF and serotonin systems in the nonhuman primate brain is lacking, but evidence from our lab using a monkey model of ovarian hormone treatment after ovariectomy suggests that E and P can impact the function of CRF neurons. It is known that CRF neurons project from the PVN to the midbrain (Portillo et al., 1998), and that the raphe has CRF receptors (Pernar et al., 2004), but it is not known whether the hormone-treatment-induced decrease in CRF-positive gene and protein expression in the hypothalamus is transmitted to the midbrain raphe serotonin system. I hypothesized that E ± P treatments would decrease CRF-positive fiber innervation in the dorsal raphe nucleus. The results of these experiments will be discussed in **Chapter 3**. If treatment with E ± P does in fact decrease CRF-positive fibers innervating the raphe, then this may be an avenue whereby ovarian hormones decrease inhibition of the dorsal raphe serotonin system, effectively increasing availability of serotonin.

E ± P-treatments may also impact the CRF system components in the raphe by modulating gene or protein expression of CRF receptors. If ovarian hormones regulate CRF-R1 or CRF-R2 gene expression in raphe serotonin neurons, then this would be another potential mechanism of regulating overall central serotonin availability. Therefore, I further hypothesized that E ± P-treatments would decrease CRF-R1 gene expression in the dorsal raphe. Conversely, I hypothesized that E ± P treatments would increase UCNs/CRF-R2 gene expression. To determine whether E ± P treatments impact gene expression of CRF receptors, I used quantitative reverse transcriptase-

polymerase chain reaction (qRT-PCR) on cDNA reverse transcribed from RNA previously isolated from the microdissected raphe-containing midbrains of animals treated with placebo, E, and E+P. I also assessed whether mature CRF-R1 and CRF-R2 peptides are expressed in monkey raphe. I used stereological analysis to quantify the increase or decrease in mature CRF receptor expression caused by ovarian hormone treatment. Also, because any overall effect of ovarian hormones on expression of mature CRF receptors would also be impacted by expression of the binding proteins, I determined whether E ± P regulate CRF binding protein. The results of these experiments will be addressed in **Chapter 4**.

There is evidence in the literature that ERs mediate transcription of UCN1 (Haeger et al, 2006). Therefore, I also hypothesized that E ± P would increase overall gene expression of *UCN1* in the monkey dorsal raphe nucleus. Because UCN1 is an endogenous activators of CRF-R2 and previous work demonstrated a UCN1 projection to the raphe, it follows that an increase in UCN1 expression would increase serotonin levels. To determine whether ovarian hormone treatment affects gene expression of the other *UCNs* in the primate midbrain, qRT-PCR was performed on total RNA extracted from a block of midbrain tissue containing the dorsal raphe nucleus using primers specific for *UCN1, UCN2* and *UCN3* transcripts. Because only half of the UCN1-producing neurons in the $pIII_U$ are located within the rostral boundary of the dorsal raphe midbrain block tissue in the Bethea laboratory dissection, I repeated the qRT-PCR assay using RNA isolated from $pIII_U$-containing hemi-midbrains of female monkeys treated with placebo, E, or E+P (kindly donated by Dr. Henryk Urbanski).

Immunocytochemistry was used to determine whether E ± P modulate the expression of mature UCN1 expression in the midbrain, and whether UCN1-positive neurons in the midbrain co-localize with estrogen receptor beta (ERβ). Finally, I assessed whether E and E+P regulated UCN1-positive fiber intensity in the dorsal raphe. The results of these experiments will be discussed in **Chapter 5**.

In summary, the proposed study aims to describe the effects of ovarian hormone treatment on CRF system signaling components in the midbrain that impact serotonin neurons. Since CRF and serotonin are widely known to play a role in the stress response and depression, this work will provide important information enabling us to improve treatment options for anxiety and depression in menopausal women.

Chapter 2: General Methods

2.1 Animals

Adult female rhesus monkeys (*Macaca mulatta*) were born in China. The ages of the animals were determined by dental exam to be between 7 and 14 years. They weighed between 4 and 8 kg, and were in good health.

2.2 Ovariectomy

Adult female monkeys were ovariectomized by the surgical personnel of ONPRC according to accepted veterinary surgical protocol. Steroid hormone treatments were initiated 3 to 22 months after ovariectomy (mean time = 9.9 months ± 2.65 months). **Tables 1, 2, and 3** show the mean amount of time between ovariectomy and placebo or hormone treatment for the three groups of animals (36 animals total) used in the experimental assays described here. In the first group of animals used in the immunohistochemical experiments, there were 5 animals in each treatment group (n=15). In the second group of animals used in the Sybr Green qRT-PCR experiments, there were 3 animals in each treatment group (n=9). In the third group of animals used for Taqman qRT-PCR, there were 4 animals in each treatment group (n=12).

2.3 Treatments

In this model of surgical menopause with and without HRT, all animals are ovariectomized and then divided into placebo, E or E + P treatment groups as illustrated in **Figure 8.** Animals were treated with either placebo (OVX control group; n=12), or

Table 1. Formalin fixed brains used in IHC

Group	Number	Months OVX to Treatment
OVX	21372	6.6
	22854	5.8
	22150	9.1
	21417	3.5
	21702	3.7
		Mean = 5.7 ± 1.0
E	20867	5.4
	22141	5.6
	22106	8.4
	21634	3.5
	20681	3.7
		Mean = 5.3 ± 0.8
EP	20581	4.9
	21380	7.3
	23473	3.8
	20811	3.5
	21657	3.7
		Mean = 4.6 ± 0.7
		Overall Mean = 5.2 ± 0.9 months

Table 2. Bethea RNA-later perfused brains for Sybr qRT-PCR

Group	Number	Months OVX to Treatment
OVX	20870	6.0
	20831	30.8
	21342	22.1
		Mean = 19.6 ± 7.3
E	21637	7.5
	20982	19.5
	21357	20.1
		Mean = 15.7 ± 4.1
EP	21613	7.1
	21656	21.9
	21696	22.1
		Mean = 17.0 ± 7.0
Overall Mean = 17.4 ± 6.1 months		

Table 3. Urbanski's brains used for TaqMan qRT-PCR

Group	Number	Months OVX to Treatment
OVX	22842	9.3
	23459	7.8
	23463	5.1
	22864	9.6
		Mean = 8.0 ± 1.0
E	22139	6.8
	22868	10.3
	22887	5.3
	22841	4.7
		Mean = 6.8 ± 1.3
EP	22833	7.4
	22823	7.5
	22871	7.0
	22881	5.1
		Mean = 6.8 ± 0.6
Overall Mean = 7.2 ± 1.0 months		

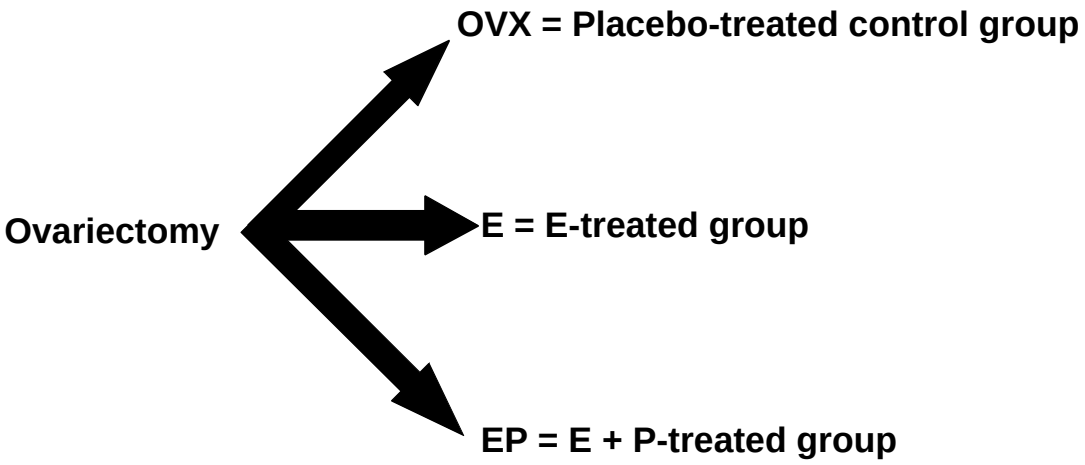

Figure 8. Diagram illustrating the three groups of animals evaluated in this study. All animals were ovariectomized and treated with either placebo (OVX-control group), estradiol (E group), or estradiol plus progesterone (EP group) for one month.

treated with 17β -estradiol (E) for 28 days (E group; n=12), or with E for 28 days supplemented with progesterone (P) for the final 14 of the 28 days (EP group; n=12). The spayed control monkeys received empty Silastic capsules subcutaneously (s.c.). The E-treated monkeys were implanted with 4.5-cm E-filled Silastic capsules (i.d. 0.132 in.; o.d. 0.183 in.; Dow Corning, Midland, MI) filled with crystalline 17β -estradiol [1,3,5 (10)-estratrien-3,17-β -diol; Steraloids, Wilton, NH]. The E+P- treated monkeys received an E-filled capsule followed by one 6-cm capsule filled with crystalline P (pregnen-4-ene-3,20-dione; Steraloids) 14 days later. All capsules were placed in the periscapular area under ketamine anesthesia (ketamine HCl, 10 mg/kg, s.c.; Fort Dodge Laboratories, Fort Dodge, IA).

2.4 Necropsy

The monkeys were euthanized at the end of the treatment periods according to procedures recommended by the Panel on Euthanasia of the American Veterinary Association. Each animal was sedated with ketamine, given an overdose of pentobarbital (25 mg/kg, intravenously), and exsanguinated by severance of the descending aorta. A blood sample was obtained at necropsy for determination of E and P concentrations in serum at the time of death (see E and P assay section below). Brain perfusion and processing of animal tissue was done in consecutive sets containing one animal from each of 3 groups (OVX, E, and EP). Each set was processed together. All necropsies occurred between the hours of 10 a.m. and 1 p.m.

2.5 Serum estradiol and progesterone assays

After one month of either placebo or hormone treatment, circulating estradiol (E) and progesterone (P) levels were determined by chemiluminescence (**Table 4**). Serum E and P levels in all animals in the E and EP groups were within an acceptable range that is physiologically relevant for the intent of our model, which is to study the effects of combined hormone replacement therapy of estrogen and progestin (HRT) after menopause. Brenner et al. previously established that this exact treatment with E and P elicited complete maturational and functional responses of the primate endometrium (Brenner et al., 1974). Our OVX-control animals had very low levels serum estradiol (<12 pg/ml) and progesterone (<0.09 ng/ml) at necropsy, which were characteristic for untreated women after menopause (Schunkert et al., 1997). Animals within the E and E+P groups achieved serum E levels at necropsy between 78-155 pg/ml. These levels correspond to estradiol levels in women during the mid-to-late-follicular phase of the normal menstrual cycle (Baptista et al., 1999; Hotchkiss, 1994). Moreover, 70 pg/ml of bioidentical or natural E is achieved by the FemRing^{TR} 0.1mg/day, a vaginal implant for treatment of menopausal symptoms (product information). Our E+P animals achieved serum P levels of 4-8 ng/ml, and serum P levels within this particular range are considered to be moderate. Premenopausal women exhibit serum P levels above 12 ng/ml in the mid-luteal phase (when P peaks) and below 2 ng/ml in the early follicular phase, when serum P is at its lowest (Hotchkiss, 1994; Baptista et al., 1999).

Assays for E and P were performed using the Roche Diagnostics 2010 Elecsys clinical platform (Alameda, CA, USA) validated for E and P in non-human primate

Table 4. Serum concentrations of estradiol and progesterone at necropsy.

Experiment	Groups	Estradiol pg/mL	Progesterone ng/mL
IHC	OVX	9 ± 1.7	0.1 ± 0.02
	E	79 ± 7.1	0.2 ± 0.02
	EP	89 ± 12.7	3.8 ± 0.73
Sybr green qRT-PCR	OVX	12 ± 0.7	0.1 ± 0.04
	E	153 ± 9.4	1.1 ± 0.07
	EP	154.3 ± 8.9	7.7 ± 0.31
Taqman qRT-PCR	OVX	10 ± 4.0	< 0.02
	E	117 ± 6.7	< 0.02
	EP	130 ± 9.5	3.8 ± 0.40

serum. The Elecsys system uses electrochemiluminescence detection technology by combining an antigen-antibody reaction (on the surface of a streptavidin-coated paramagnetic microparticle) with an electrochemical reaction (on the surface of an electrode) to generate luminescence. Briefly, a biotin-labeled antibody (against E or P) and a ruthenium-labeled antibody (against E or P) are incubated with the serum sample. The immunocomplex is captured by the streptavidin-coated microparticles, which have a high biotin binding capacity. The microparticles with bound immune complexes are uniformly deposited on the electrode within the electrochemiluminescent measuring cell. Finally, E or P is quantified by applying a voltage to the electrode and measuring the electrochemiluminescent signal.

Prior to these analyses, E assays on this platform were compared with traditional RIA's as previously described (Hess et al., 1981). To validate the Elecsys platform for E, the ONPRC Endocrine Services Laboratory measured E with both methods in 192 samples obtained daily from female rhesus monkeys during normal menstrual cycles. The correlation coefficient between the two methods was r = 0.965 and the data from the two assays were compatible with the stage of the cycle. When the individual serum concentrations for E were normalized to the day of the preovulatory surge, the results were in agreement both qualitatively and quantitatively with published literature for rhesus monkeys. Analysis of E in a pool of serum from ovariectomized rhesus macaques provided concentrations of <12 pg/ (n=15). Individual samples of macaque serum containing large concentrations of E were diluted with this ovariectomized pool and assayed with the Roche instrument; such dilutions yielded parallel dilution curves

for E assays. Intra-assay and inter-assay coefficients of variation for the E assays did not exceed 10%. The lower limit of detection of E by the Elecsys is 5 pg/ml. Serum E levels at necropsy can be found in **Table 4**.

Assays for P were also performed utilizing a Roche Diagnostics 2010 Elecsys assay instrument as described above. Prior to these analyses, P assays on this platform were compared with traditional RIA's as previously described (Hess et al., 1981). To validate this platform for P, the laboratory measured P in 220 samples obtained daily from the rhesus monkeys during normal menstrual cycles. The correlation coefficient between the two methods was r = 0.984 and the data were compatible with stage of the cycle. When the individual serum concentrations for both P were normalized to the day of the preovulatory surge, the results were in total agreement both qualitatively and quantitatively with published literature for rhesus monkeys. Analysis of P in a pool of serum from ovariectomized rhesus macaques provided concentrations of <0.09 ng/ (n=15). Individual samples of macaque serum containing large concentrations of P were diluted with this ovariectomized pool and assayed with the Roche instrument; such dilutions yielded parallel dilution curves for both P assays. Intra-assay and inter-assay coefficients of variation for the P assays did not exceed 10%. The lower limit of detection of serum P by the Elecsys is 0.03 ng/ml. Serum progesterone levels at necropsy can be found in **Table 4**.

The three groups of animals used in this dissertation were prepared several years apart by different people. To determine whether there was a treatment (OVX, E, EP) by experiment (IHC, Sybr Green, Taqman) interaction on the outcome of serum E and P levels, I performed a 3 X 3 two-way ANOVA and used Bonferroni posttests. For serum E levels, treatment by experiment interaction accounted for approximately 4.89% of the total variance and P value = 0.0021, which was considered very significant. Within the E and E+P groups, the animals used for Sybr Green and Taqman assays had significantly higher serum E levels at necropsy than did the IHC animals. For serum P levels, treatment by experiment interaction accounted for approximately 8.54% of the total variance and P value < 0.0001, which was also considered extremely significant. Within the E+P group, the animals used for Sybr Green assays had significantly higher serum P levels at necropsy than did the IHC animals.

Thus, in all experiments there was a treatment by experiment interaction such that treated animals in the qRT-PCR groups had significantly higher serum E or P levels at necropsy than did the animals in the IHC experiment. These different groups of animals were processed several years apart and the variation is derived from how different individuals pack the Silastic implants, which is difficult to control. Although it is questionable whether the range makes a significant difference physiologically, it is possible that transcriptional effects of E and P may be greater in the qRT-PCR animals compared to the IHC animals, causing the differences between the treatment groups in the qRT-PCR experiments to be greater.

2.6 Perfusions

Formaldehyde perfusions: Following euthanasia, fifteen animals (n=5/group) were perfused with formaldehyde and processed for immunocytochemistry. The left ventricle of the heart was cannulated and the head of each animal was perfused with 1 liter of 0.9% saline followed by 7 liters of 4% formaldehyde in 3.8% borate, pH 9.5. This buffer has a high pH and it was empirically found to provide optimal signal for immunocytochemistry of tyrosine hydroxylase (Berod et al., 1981) and for in situ hybridization assays (Simmons et al., 1989). This buffer has been routinely employed in the Bethea laboratory in order to use valuable macaque brains for both in situ hybridization and immunocytochemistry. In addition, the Bethea laboratory has examined numerous antibodies for specific staining with tissue perfused with formaldehyde containing borate. In general, immunocytochemistry has been outstanding although it should be noted that the tissue sections are washed exhaustively in neutral KPBS prior to staining. Both perfusion solutions were made with DEPC-treated water (0.1% pyrocarbonate) to minimize ribonuclease contamination. The brains were removed from the cranium and blocked. The dissected midbrain block displayed the rounded central canal on its anterior surface and the wing-shaped canal on its caudal surface; it extends from the Edinger-Westphal nucleus through the dorsal raphe nucleus.

RNA-Later perfusions: Nine animals (n=3/group) were perfused with RNAlater (Ambion Inc., Austin, TX) and processed for mRNA extraction. The left ventricle of the heart was cannulated, and the head of each animal was perfused with 2 liters of cold

RNA-later buffer and 1 liter Ribonuclease-free cold saline. The brain was removed from the cranium and blocked. The dissected midbrain block was further microdissected and a small piece of tissue was harvested, which extended from the middle of the central gray to the decussation of the cerebellar peduncles. This piece, which we call the dorsal raphe region, was the width of the central gray and contained the major portion of the dorsal raphe (5 mm wide, 6 mm high, and 3 mm thick). The tissue was immediately frozen in liquid nitrogen and stored at -80° C. For RNA extraction, the frozen block was dropped directly into TriReagent (Sigma, St. Louis, MO; see section 2.10 for more details).

Saline perfusion and RNA later immersion. The brains of the animals donating tissue for the Taqman qRT-PCR were perfused with 1 liter 0.9% saline, removed and dissected. The pontine midbrain was bisected along the midline (saggital plane) yielding the hemi-midbrain tissue block (gift of Dr. Henryk Urbanski). One side was immersed in 1 x RNAlater for one week at 4ºC, and then frozen in aluminum foil at -80ºC until RNA extraction.

2.7 Brain cryoprotection for immunohistochemistry

The tissue blocks for immunohistochemistry were post-fixed for 3 hours in 4% paraformaldehyde, then transferred to 0.02M potassium phosphate buffered saline (KPBS), pH 7.5, containing 10% glycerol (overnight), followed by 20% glycerol and 2% dimethyl sulfoxide at 4° C for 3 days. After infiltration, the block was frozen in isopentene, cooled to -55° C, and stored at -80° C for up to 6 months until sectioning.

2.8 Brain sectioning for immunohistochemistry

Coronal sections (25 μm) were cut through the perioculomotor region, the dorsal raphe, and median raphe on a sliding microtome, which had been cooled to -20° C with dry ice. Serial sections were collected in a cryoprotectant buffer (30% ethylene glycol and 20% glycerol in 0.05M PBS) and then frozen at -20° C until processing with immunohistochemistry. Midbrain sections were collected in ten boxes and each box contained 24 sections that were 250 μm apart. After the first section was collected in Level 1 of Box #1, the next section was stored in Level 1 of Box #2 and so on. Collecting tissue in this manner allows for ten or more experimental assays in which a representative set of 24 midbrain sections at 250 μm apart are assayed across the entire rostro-caudal extent of dorsal raphe region, about 2.5 mm.

2.9 Immunohistochemistry

Midbrain sections were removed from cryoprotective storage and washed in KPBS for an hour. They were blocked in the appropriate serum for an hour, and then in avidin and biotin for 20 minutes (Vector labs, Burlingame, CA). All of the primary antibodies were examined at increasing titers to determine the optimal signal over background staining. Each primary antibody was diluted in 0.02 M KPBS/ 2% normal rabbit or goat serum/ 0.4% Triton X-100 and exposed to the experimental tissue for 48 hours at 4° C. Two days later, sections were washed in KPBS for an hour. The appropriate secondary antibody (Vector labs, Burlingame, CA) was diluted 1:200 in KPBS/0.4% Triton X-100 and incubated with the tissue for 60 minutes. After another KPBS wash, the sections were incubated in ABC solution (Vector labs) for one hour and washed in buffer again.

Sections were then incubated in 0.02M KPBS with 0.05% DAB and 0.003% H_2O_2. Finally, the sections were washed, mounted on slides, dehydrated through a graded series of ethanol dipped in xylene, and coverslipped in DPX mountant for stereological analysis.

The **CRF** antibody was a gift from Dr. Wylie Vale (Salk Institute, La Jolla, CA) and was raised in rabbit against human CRF conjugated to human alpha globulin. Hence, an additional blocking step with 1% human alpha globulin (Sigma G-2011) for 20 minutes was required. A 1/15,000 dilution of the rabbit anti-human CRF IgG was used in 0.02 M KPBS/ 2% normal goat serum/ 0.4% Triton X-100. Also, 0.1% human alpha globulin was added to the primary antibody solution. The secondary antibody was biotinylated goat anti-rabbit IgG, and the primary antibody was visualized with DAB as a brown precipitate. The antiserum to CRF has been extensively characterized and previously applied to primate (Bassett and Foote, 1992).

The **UCN 1** antibody (Sigma-Aldrich, St. Louis, MO; Catalog No. U4757) was raised in rabbit against amino acids 25-40 of the human peptide. This primary antibody was used at 1/15,000 dilution in 0.02 M KPBS/ 2% normal goat serum/ 0.4% Triton X-100. An additional blocking step with 3% bovine serum albumin in 0.02 M KPBS was applied for an hour. The secondary antibody was biotinylated goat anti-rabbit IgG, and the primary antibody was visualized with DAB as a brown precipitate. The antiserum to UCN1 has been extensively characterized and previously applied to primate and human brain (Ryabinin et al., 2005 343; May et al., 2008).

The **CRF-R1** antibody (Santa Cruz Biotechnology, Santa Cruz, CA; Catalog No. 12381) was an affinity purified goat polyclonal antibody raised against an internal region of CRF-R1 of human origin. The primary antibody was diluted 1/500 in 0.02 M KPBS/ 2% normal rabbit serum/ 0.4% Triton X-100 and exposed to the experimental tissue for 48 hours at 4° C. The secondary antibody was biotinylated rabbit anti-goat IgG, and the primary antibody was visualized with DAB as a brown precipitate. For the absorption control, the minimum concentration of CRF-R1 antibody required to obtain signal (1/2000 dilution) was reabsorbed with a blocking peptide (500 µg; Santa Cruz Biotechnology, Santa Cruz, CA; Catalog No. 12381-P) at 4° C overnight. The CRF-R1 antibody and the preabsorbed antibody were incubated on adjacent tissue sections for 48 hours at 4° C. Two days later, the tissue was incubated with secondary antibody and processed using a VECTASTAIN Elite ABC kit from Vector laboratories, Inc. (Burlingame, CA).

The **CRF-R2** antibody (Chemicon International, Billerica, MA; Catalog No. AB9139, lot 0602022158) was raised in rabbit against the first extracellular domain of human CRF-R2. The primary antibody was diluted 1/750 in 0.02 M KPBS/ 2% normal goat serum/ 0.4% Triton X-100 and exposed to the experimental tissue for 48 hours at 4° C. The secondary antibody was biotinylated goat anti-rabbit IgG, and the primary antibody was visualized with DAB as a brown precipitate. For the absorption control, the experimental concentration of the primary antibody (1/750 dilution) was preabsorbed with a blocking peptide (1000 µg; Lifespan Biosciences LS-P502, Seattle, WA) at 4° C

overnight. The CRF-R2 antibody and the preabsorbed antibody were incubated on adjacent tissue sections for 48 hours at 4° C. Two days later, the tissue was incubated with secondary antibody and processed using VECTASTAIN Elite ABC kit from Vector Laboratories (Burlingame, CA).

2.10 Double Immunohistochemistry

Localization of estrogen receptor beta (ERβ) and UCN1 in the $pIII_u$ was sought using double label IHC. Sections (25um) of the $pIII_u$ were obtained from an extra monkey and stored in cryoprotectant at -20°C until the day of assay. For assay, sections were mounted on slides. The slides were washed in 0.02M KPBS, blocked in normal goat serum, avidin, and biotin, and incubated at 4°C overnight with anti-human ERβ IgG (mouse monoclonal, 1:100, Serotec). The next day, the slides were washed in KPBS, incubated with biotinylated goat anti-mouse secondary antibody, and then washed again before incubation with ABC solution (Vector labs). A solution of 10 ml 0.05M Tris containing 395 g nickel ammonium sulfate, 7 mg diaminobenzidine (DAB; 0.07%), and 2 µL 30% hydrogen peroxide (0.006%) was prepared and 500 µl was placed onto the sections for 10 minutes. The antigen-antibody complex was visualized as a purple nuclear stain. This nuclear ERβ stain was fixed in 4% paraformaldehye/0.1M phosphate for one hour. This was followed by rinsing in 0.02 M KPBS and blocking with normal goat serum (NGS), avidin, and biotin. The slides were incubated at 4°C for 48 hours with rabbit anti-UCN1 polyclonal antiserum. Two days later, the slides were washed in KPBS, and then incubated with goat anti-rabbit biotinylated secondary antibody. After incubation with ABC solution, a solution of 0.02M KPBS containing

0.05% DAB and 0.003% hydrogen peroxide was prepared and 500 µl was placed onto the sections for 2 minutes. The reaction was terminated with a KPBS wash. Slides were vacuum dried overnight, then dehydrated, dipped in xylene, and coverslipped in DPX mountant. Specificity of the antibody has previously been confirmed by Western blotting to identify ERβ specific bands using protein lysates of mammary and prostate cancer cell lines (Shaaban et al., 2003).

2.11 RNA extraction and Reverse Transcription

Sybr Green qRT-PCR assays: RNA was obtained from the microdissected raphe area of nine RNA-later perfused rhesus midbrains containing the DRN by homogenizing the DRN block in TriReagent. The RNA was cleaned with a Qiagen RNAeasy column (Valencia, CA). The quality of the RNA from the Qiagen column was examined on an Agilent Bioanalyzer Nanochip. The ratio of 18 S to 28S RNA was above 1.78, which is considered to be of acceptable quality for all RNA assays. The quantity of RNA was checked with a Nanodrop Spectrometer (ND-1000 Nanodrop Spectrophotometer) and the concentration was adjusted to ~ 1 µg/ µl. Complementary DNA (cDNA) synthesis was performed using 5 µg of extracted RNA, Oligo-dT 15 primer (Invitrogen Life Technologies, Carlsbad, CA) and Moloney murine leukemia virus reverse transcriptase (100 U/µg RNA, Invitrogen) at 42ºC for 1 hour.

TaqMan qRT-PCR assays: RNA was obtained from the microdissected hemi-midbrain block of 12 rhesus midbrains (previously infiltrated with RNAlater) and homogenized using TriReagent. The RNA was further cleaned with a Qiagen RNAeasy

column (Qiagen, Valencia, CA). The quality of the RNA from the Qiagen column was examined on an Agilent Bioanalyzer Nanochip. The ratio of 18 S to 28S RNA was above 1.78, which is considered to be of acceptable quality for all RNA assays. The quantity of RNA is checked with a Nanodrop Spectrometer (ND-1000 Nanodrop Spectrophotometer) and the concentration is adjusted to be ~ 1 µg/ µl. Complementary DNA (cDNA) synthesis was performed using 5 µg of extracted RNA, Oligo-dT 15 primer (Invitrogen Life Technologies, Carlsbad, CA) and Superscript III reverse transcriptase (200 U/µg of RNA, Invitrogen Life Technologies) at 42º C for 1 hr.

2.12 Quantitative (q)RT-PCR

For the Sybr Green qRT-PCR assays, the cDNA samples from ovariectomized animals treated with placebo, E, or E+ P (n=3/group) were subjected to qRT-PCR for: CRF, UCN1, UCN2, UCN3, CRF-R1, and CRF-R2. The specific primer sequences used to examine the *CRF, UCN1, UCN2,* and *UCN3* genes of interest were generated from human sequences and have previously been used for qRT-PCR quantification in the monkey (Xu et al., 2006). Forward and reverse primers for *CRF-R1* and *CRF-R2* were designed carefully. The probe set ID was obtained from the sequences used in the Rhesus custom Affymetrix chip. The Netaffix program enabled the retrieval of an annotated list of genes of interest and provided direct access to the Gen Bank sequence at the National Center for Biotechnology Information (NCBI). Thus, using Netaffix, the oligonucleotide location on each monkey gene sequence was identified. Based on the oligoset distribution, a target area of each gene of interest was selected. The target sequences were then uploaded into Primer Express software and the

primers were chosen for optimum Sybr Green RT-PCR quantification (i.e., optimum primers do not have high incidence of primer dimer formation). The primers were obtained from Invitrogen Life Technologies. The primer sets and NCBI Gene accession numbers used in the Sybr Green RT-PCR experiments are in **Table 5**.

Dynamo Sybr Green qPCR Mix (MJ Research, Watertown, MA) was used to conduct the first qRT-PCR experiment. This mix contains a modified DNA Taq Polymerase and Sybr Green I fluorescent dye, which is specific for double-stranded DNA. The fluorescence was detected with an ABI 7700 thermal cycler during 40 cycles.

A pool of rhesus RNA from various tissues was used as the standard. The reactions had final volume of 20 µL. Each contained increasing (x 10) concentrations (from 10 to 1000 pg of cDNA) of sample cDNA, 100 nM of forward and reverse primers, and the 1 X Dynamo PCR mix. The 50-100 ng cDNA added to the reaction mix was approximated from the amount of RNA used for reverse transcription.

Sybr Green-based detection for qRT-PCR works if only one gene-specific amplicon is generated during the reaction. Sybr Green detection also uniquely allows you to check the specificity of the PCR using dissociation curves. Validation of qRT-PCR was done by analyzing the dissociation curves of all the samples. As an example, the

Table 5. Accession IDs and primers used in Sybr green qRT- PCR quantification

Gene ID	Accession ID	Primers	Amplicon
CRF	NM_000756	Primer F: CGCTGCTCTTATGCCATTT Primer R: AACACCTGGAAACGGAAACT	163
CRF-R1	NM_001032803	Primer F: CGTGGTCCAGCTAACCATGA Primer R:CGTAGTACAGCTTCCCAATGGC	251
CRF-R2	XM_001085987	Primer F: CACAGTGTGAGCCCATTTTGG Primer R: TTCGCAGGATAAAGGTGGTGA	196
UCN1	NM_003353	Primer F: GACCTCACCTTTCACCTGCT Primer R: TGCCCCGCATCCCAACTCT	174
UCN2	NM_0033199	Primer F: GCTCGCGCATTGTCCTATC Primer R: CTCCAGGTCTTCCCATCCAG	188
UCN3	NM_053049	Primer F: GGACCGTTTCCATAGAGAG Primer R: AGTGGACTTCCCTCCGCA	173

dissociation curve for UCN1 is reproduced in **Figure 9**. Most real-time instruments usually plot melting curves as a first derivative. The inflection point in the melting curve then becomes a peak. Single peaks indicate a single product, as seen in **Figure 9**. Similar results were obtained with all of the primer sets. Multiple peaks usually indicate multiple products, which can have many sources such as primer dimers, genomic contamination, or unreported splice variants of the gene of interest. We also verified that only a single amplicon was produced in the reaction by running all PCR products on an agarose gel.

A standard curve with the rhesus pool was generated for all genes of interest and GAPDH (Glyceraldehyde 3-phophate dehydrogenase), an endogenous control sequence that codes for an enzyme in the glycolytic pathway that is not affected by 1 month of E or P treatment in our model. The slope of the standard curve was used to calculate the relative pg of each transcript of interest in the total RNA from each raphe nucleus. GAPDH gene expression was used to normalize expression of the individual transcripts and the results are expressed as a ratio. Thus, the ratio of gene of interest/GAPDH was calculated to determine relative abundance of the gene of interest. The ratio of gene of interest/GAPDH was further normalized by calculating expression in the treated groups relative to the OVX control group. **Figure 10A** illustrates a representative amplification plot for CRF-R1 executed in triplicate with Syber Green on one animal from each treatment group. Amplification plots are plotted with regression curves because cycle time is lower when [RNA] is higher, and cycle time is plotted against the log ratio of concentration to generate an amplification curve for the

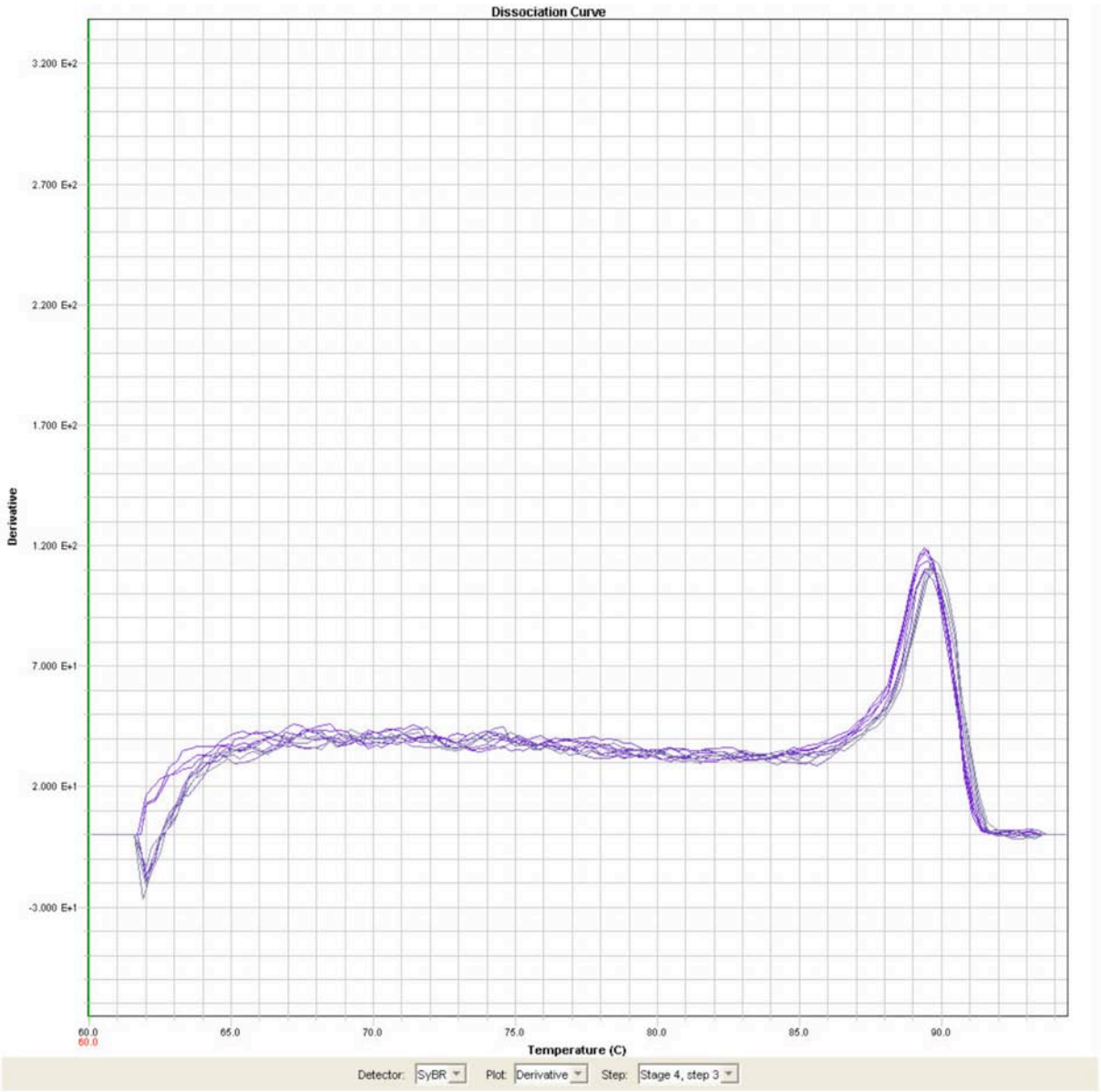

Figure 9. Dissociation curve for UCN1. Sybr green detects the specificity of the PCR using dissociation curves. After the 40 reaction cycles, a temperature ramp like the one shown (above) is created. The real-time PCR instrument plots dissociation curves as a first derivative, causing the inflection point of the melting curve to become a peak. Single peaks indicate a single product whereas multiple peaks indicate multiple products. In the derived dissociation curve for the UCN1 PCR (above), as well as for all PCR reactions in the Sybr green assays, the dissociation curve showed only one peak.

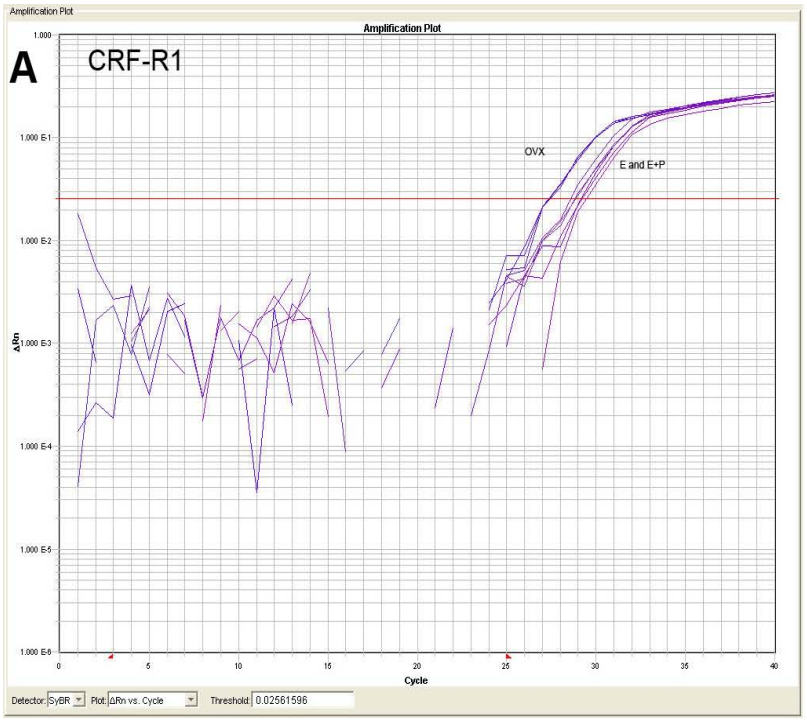

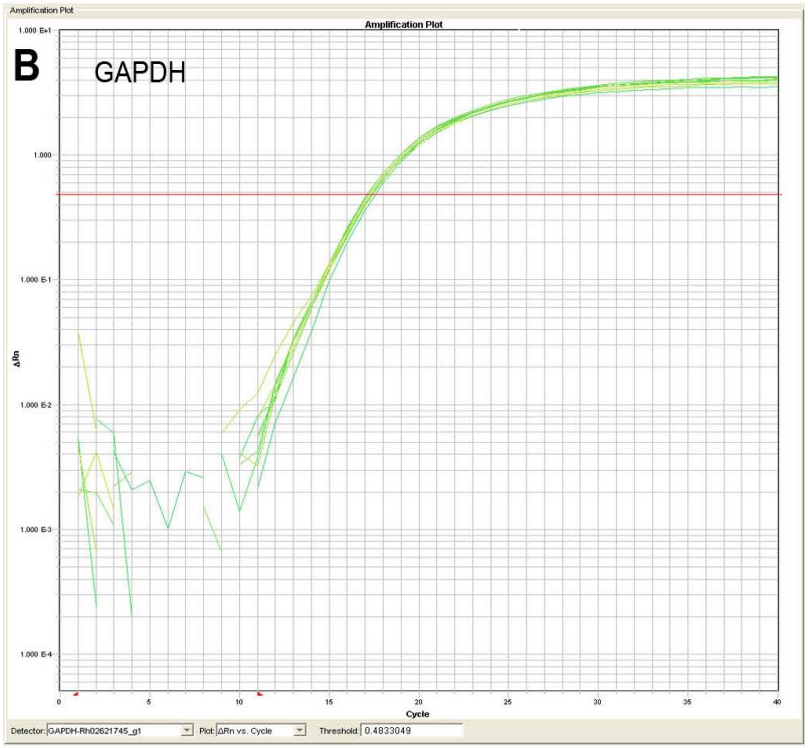

Figure 10A. Regression curve amplification plots for CRF-R1. Cycle time is plotted against the log ratio of concentration to generate a regression curve for the unknown, which in this case is CRF-R1. In this example, RNA extracted from the midbrain block of one animal from each treatment group in the Bethea set of midbrain blocks was assayed in triplicate with Sybr Green. The triplicate wells of the OVX sample reached threshold (red horizontal line) earlier (i.e. with lower cycle times) than the triplicate wells of the E-treated or E+P treated animals. This is because the OVX sample contained more CRF-R1 amplicon. Conversely, the triplicate wells of the E and E+P treated animals needed more cycle times in the qRT-PCR assay to reach threshold than did the OVX animal, indicating that they contained less CRF-R1 cDNA than the OVX animal. This raw data is included in the final analysis of CRF-R1 shown in Figure 18 A.

Figure 10B. Regression curve amplification plots for GAPDH. Cycle time is plotted against the log ratio of concentration to generate a regression curve for the unknown, which in this case is GAPDH. In this example, RNA extracted from the midbrain block of one animal from each treatment group in the Bethea set of midbrain blocks was assayed in triplicate with the Taqman for comparison to the earlier Sybr Green data. The cycle times for the OVX, E- and E+P treated animals are superimposed. This example was used for internal reference only and was not used for normalization of data in this thesis.

unknown. In this example, the three OVX wells reached threshold (red horizontal line) earlier (i.e., with lower cycle times) than the three E or E+P wells because they contained more CRF-R1 DNA amplicon. Conversely, the wells from animals in the E and E+P groups cycled more times in the qRT-PCR assay to reach threshold than did the OVX group, so these animals contained less CRF-R1 DNA amplicon than the OVX group.

For animals used in the Taqman qRT-PCR assays, cDNA samples from the 12 animals (previously reverse transcribed from the RNA isolated from microdissected hemi-midbrains) were subjected to qRT-PCR for the following genes of interest: CRF-BP, UCN1, UCN2, UCN3, CRF-R1, and CRF-R2. Tryptophan hydroxylase 2 (TPH-2) was also examined as a physiological positive control for E and P regulation of gene expression. 25 ng of cDNA from each of the 12 animals (previously reverse transcribed from the isolated RNA from the 12 monkey hemi-midbrains) was loaded onto the Taqman custom low-density array containing 384 wells. The array was custom designed to analyze 31 cDNA probe sets in triplicate with 4 samples/plate (Applied Biosystems Inc., Foster City, CA) according to the manufacturer's specifications. The cards contained proprietary primer sets for amplification of CRF-R1, CRF-R2, CRF-BP, UCN1, UCN2, UCN3, and TPH-2. [Additional probe sets were present for another inquiry.] The ABI primer set identification numbers, context sequences that bound probe, and the NCBI gene reference numbers are listed in **Table 6**.

Table 6. Accession numbers and context sequences used in TaqMan array

Gene ID	Accession ID	Context Sequence
CRF-R1	NM_001032803.1 AB078141.1	GACAATGAGAAGTGCTGGTTTGGCA
CRF-R2	XM_001085987.1	AGTACAACACGACCCGGAATGCCTA
CRF-BP	XM_001106453.1 XM_001106396.1	GGGCGGCGACTTCCTGAAGGTATTT
UCN1	XM_001092424.1 XM_001092536.1	GCCGAGCAGAACCGCATCATATTCG
UCN2	XM_001097967.1	AGAAGAAGCTGGTGGCGCCTGACCT
UCN3	XM_001104616.1	GTCCACTCTCAGGGAGAGATGCCGA

Four different concentrations of the Rhesus pool cDNA were loaded onto the Taqman array. Each concentration of standard and the 12 experimental samples was amplified in triplicate for each probe set. The fluorescent reporter on the probe was FAM (Flourescein amidite; Molecular Probes, Eugene, OR). The cards also contain the passive reference dye, ROX. The cycle threshold (Ct) is determined by the log linear increase in fluorescence and quenching of the probe at a specific cycle. qRT-PCR was performed on an ABI 7900 thermal cycler (Applied Biosystems Inc.) during 40 cycles. A standard curve was generated from the different concentrations of the rhesus pool. The slope of the curve was used to calculate the relative picograms of each transcript. Then, the ratio of each transcript to GAPDH was calculated. Finally, the ratio of gene of interest to GAPDH was normalized by determining the fold difference in expression between the E and the E+P groups relative to the OVX group. For illustration only, **Figure 10B** shows the GAPDH cycle times of one animal from each treatment group of the Sybr Green experimental animals, but measured with the Taqman array. The cycle times were similar. This data is used for illustration because these three animals were included on one plate of a multi-plate assay and the data was accessible for plotting. Due to a software limitation, data on different plates are not simultaneously accessible and are plotted in separate files.

2.13 Statistical Analyses

Immunohistochemistry: Sections were morphologically matched between animals using anatomical reference points and a rhesus monkey brain atlas. The Marianas stereological workstation with Slidebook 4.2 was used for analysis. Serial sections were

examined through the rostro-caudal extent of the dorsal raphe with a 500- μm interval between sections. Serial levels of the perioculomotor region, dorsal raphe (DRN), and median raphe (MR) were analyzed. A montage of the region at each level was built by the workstation. The immunostain appeared as either negative-nucleus neuronal staining (cells) or beaded varicosities (fibers) throughout the serial sections of the perioculomotor region, the DRN, and MR. The immunostained-positive pixel area was quantified using a Marianas Stereology Workstation and Slidebook 4.2. A montage (10 x) of the region of interest was constructed and positive pixels were segmented and quantified. The total area analyzed was recorded to ensure that it did not vary between animals during the analysis. Results are expressed in percent positive pixels, which were computed by dividing the number of immunostained positive pixels by the total number of pixels in the area analyzed. Differences in percent positive fibers and cells between the groups were determined with ANOVA followed by a post-hoc Student-Neuman-Keuls test using Prism Statistical software (Graph-Pad Software, Inc., San Diego, CA, USA) and $p < 0.05$ was considered statistically significant.

For cell counting, each immunopositive neuron was marked using a bull's eye icon. Then, the total number of immunopositive cells was tallied by the software program and reported. An example of counting immunopositive cells using Slidebook 4.2 is illustrated in **Figure 11**.

qRT-PCR: A standard curve was generated for each primer set using a pool of rhesus tissues, and the slope of the curve was used to calculate the relative pg of each

transcript in the total RNA from all midbrain blocks. The ratio of gene of interest/*GAPDH* was calculated to determine the relative abundance of the gene of interest. Finally, this ratio of gene of interest/GAPDH in the treated groups was normalized by the OVX control group (Ponchel et al., 2003; Sanchez et al., 2005). Differences in the relative abundance of mRNA of the gene of interest between the groups were determined with ANOVA followed by a post-hoc Student-Neuman-Keuls test using Prism Statistical software (Graph-Pad Software, Inc., San Diego, CA, USA) and $p < 0.05$ was considered statistically significant.

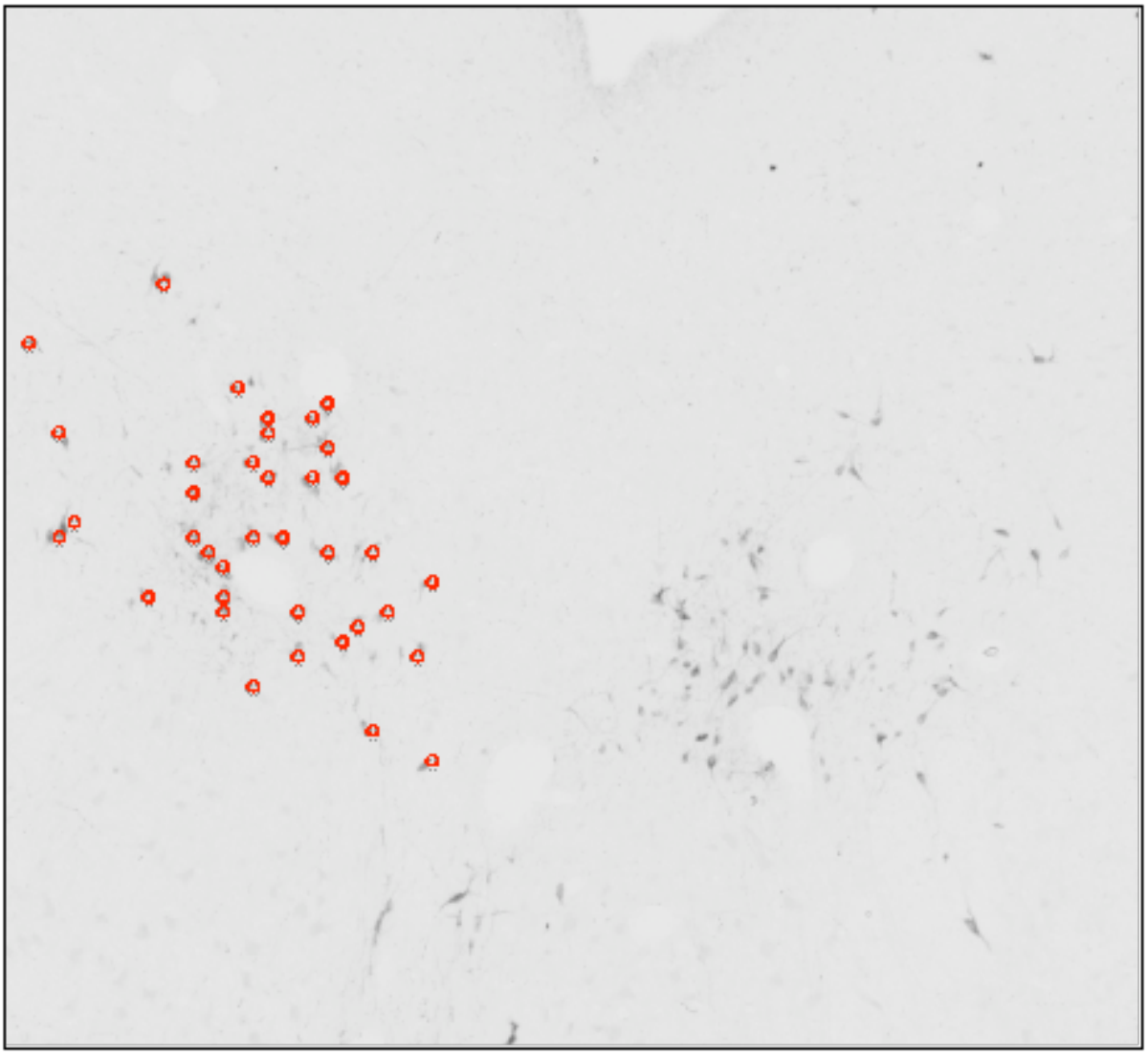

Figure 11. High magnification image of UCN1-positive neurons in the monkey perioculomotor region. A montage of the area of interest was created using Slidebook and individual UC1-positive neurons were marked with a red circle by the operator. After each cell is manually marked, the software computes and records the number of UCN1-positive cells detected in each montage.

Chapter 3: Estradiol and progesterone decrease Corticotropin-releasing factor (CRF) input to the monkey raphe nuclei

3.1 Introduction

Since the discovery of CRF as the initiator of the adrenocorticotropin (ACTH) response to stress (Vale et al., 1981), the presence of CRF-containing axon terminals and receptors outside of the pituitary has led to the idea that CRF coordinates multiple limbs of the stress response (Bale and Vale, 2004). The ability of centrally administered CRF to mimic many of the autonomic and behavioral aspects of the stress response underscores the notion that central CRF release initiates several stress response pathways independent of the Hypothalamic-Pituitary- Adrenal (HPA) axis. The serotonin neurons within the dorsal raphe nucleus system are a compelling target of CRF given the established role of this system in stress-related psychiatric disorders (Cowen, 1993; Lesch, 2001).

Although much of what we know regarding CRF regulation of the dorsal raphe is based on rodent studies, CRF innervation of the human dorsal raphe nucleus is well documented. Dual labeling suggests that CRF fibers directly interact with 5-HT-containing processes in the human raphe (Ruggiero et al., 1999). And in line with the theory that CRF in the dorsal raphe may be particularly important in the physiology of affective disorders, CRF-immunoreactivity is elevated in the dorsal raphe in the post-mortem brains of depressed suicide subjects (Austin et al., 2003).

In our primate model of hormone treatment after ovariectomy, we have shown that one month of E or E+P treatments alter gene and protein expression in serotonin neurons in a manner that indicates serotonin neurotransmission is elevated (Bethea et al., 2002). We have also shown that one month of E ± P treatment decreases CRF gene and protein expression in the PVN (Bethea and Centeno, 2008). Most of what is known about CRF innervation of the dorsal raphe derives from rat studies, which indicate that CRF immunoreactive axon terminals in the dorsal raphe project from subcortical regions such as the PVN, bed nucleus of the stria terminalis, and central nucleus of the amygdala (Poulin et al., 2008). We hypothesized that the decreased expression of hypothalamic CRF gene and protein seen in the PVN of hormone treated animals (compared to placebo-treated controls) would translate into decreased CRF delivery to the serotonin cell bodies in rhesus macaques. The present study used immunohistochemistry (IHC) to identify CRF-positive fibers in the monkey dorsal raphe nucleus and stereological and statistical analysis of the area covered by the fibers (called CRF fiber density) to determine whether E and P treatments decrease CRF innervation onto the raphe serotonin system of ovariectomized macaques. Because CRF-positive cell bodies or mRNA have been identified in the dorsomedial subnucleus of the dorsal raphe of rats (Commons et al., 2003) as well as the median raphe of voles (Lim et al., 2006), we also sought to confirm that the source of CRF innervation into the dorsal raphe serotonin system in our model was extrinsic and not derived from the dorsal raphe itself. We used qRT-PCR to determine if E and E+P treatments had any effect on CRF mRNA expression in the monkey midbrain.

3.2 Experiments

Experiment A. *Immunochistochemistry (IHC) experiment to identify and quantify CRF-positive fibers in dorsal raphe*.

Methods: Four sections of the dorsal raphe from animals in each treatment group (n=5/group) were immunostained with an antibody against human CRF, courtesy of Dr. Wiley Vale. The anti-CRF immunostaining appeared as beaded varicosities throughout the four serial sections (500 µm apart) of the dorsal raphe nucleus. These levels spanned approximately 2 mm of the caudal region of the raphe. We quantified the immunostained-positive pixel area by constructing a montage of the region of interest, and then segmenting and quantifying the immunoreactive pixel area. Results are expressed in percent positive pixels, which were computed by dividing the number of immunostained positive pixels by the total number of pixels in the area analyzed. Differences in the percent of positive fibers and pixels between the groups were determined with ANOVA followed by Student-Neuman-Keuls test.

Results: The greatest amount of CRF-positive fiber staining was toward the caudal region of dorsal raphe and spanned approximately 2 mm. We analyzed four levels of the dorsal and median raphe nucleus for each animal in the three treatment groups (n=5/group). The dorsal raphe was divided into 2 regions called the dorsal raphe and the interfascicular raphe. **Figure 12** depicts representative stereology montages of the dorsal and interfascicular raphe from ovariectomized monkeys treated with placebo, E,

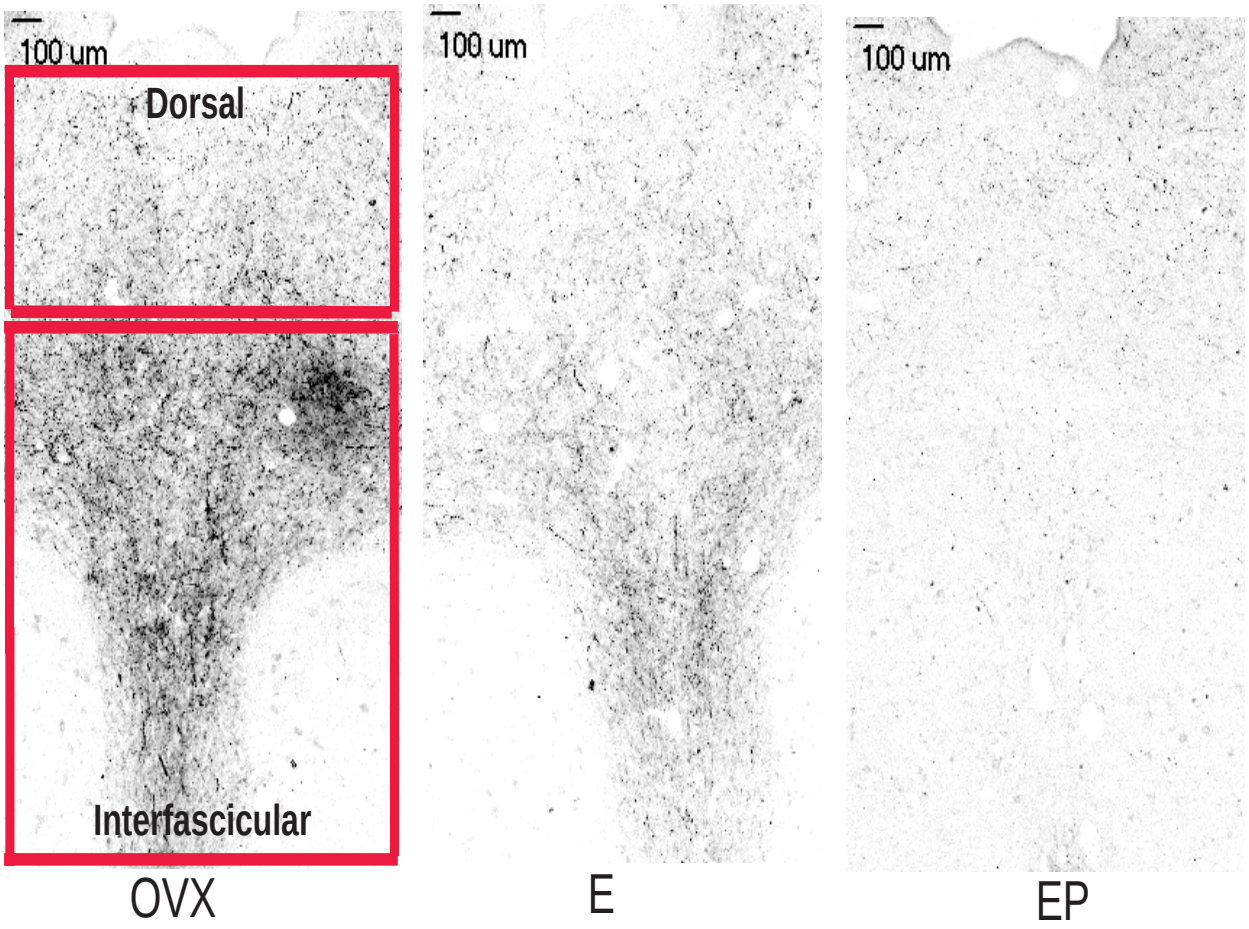

Figure 12. Representative stereological montages of dorsal raphe nucleus fibers from OVX-, E-, and E+P-treated animals immunostained with anti-human CRF. Red boundaries mark the two areas of the DRN that were analyzed. The upper box outlines the dorsal region of the dorsal raphe nucleus. The lower box outlines the interfascicular region of the dorsal raphe nucleus.

and E + P. The CRF-immunopositive pixels were quantified using a Marianas Stereology Workstation and Slidebook 4.2. **Figure 13** depicts CRF-immunopositive fibers in the dorsal and interfascicular raphe after segmentation. Once the CRF-positive pixels are segmented, they are quantified. The total area analyzed was measured and held constant to ensure that it did not vary between animals during the analysis. Results are expressed in percent CRF-positive pixels, which were computed by dividing the number of CRF-positive pixels by the total number of pixels in the area analyzed.

We found CRF-positive fibers to be densest adjacent to the ventricle (dorsally) and in lateral aspects of the dorsal raphe. As illustrated in **Figure 14**, E and E+P significantly decreased the percent of CRF-positive pixels in the dorsal segment of the dorsal raphe nucleus in all four levels analyzed (ANOVAs range $p < 0.0001$ to 0.0006; error bars are omitted for clarity). When the levels were combined, there was an overall decrease in the mean percent positive pixel area per level with administration of E and E+P compared to placebo-treated controls (ANOVA, $p<0.0001$).

In addition, E and E+P significantly decreased the percent of CRF-positive pixels in the interfascicular segment of the dorsal raphe nucleus in all four levels analyzed (ANOVAs range $p < 0.0001$ to 0.02; error bars are omitted for clarity). When the interfascicular levels of the dorsal raphe nucleus were combined, E and E+P significantly decreased the mean percent of CRF-positive pixels compared to OVX placebo-treated controls (ANOVA, $p<0.0001$).

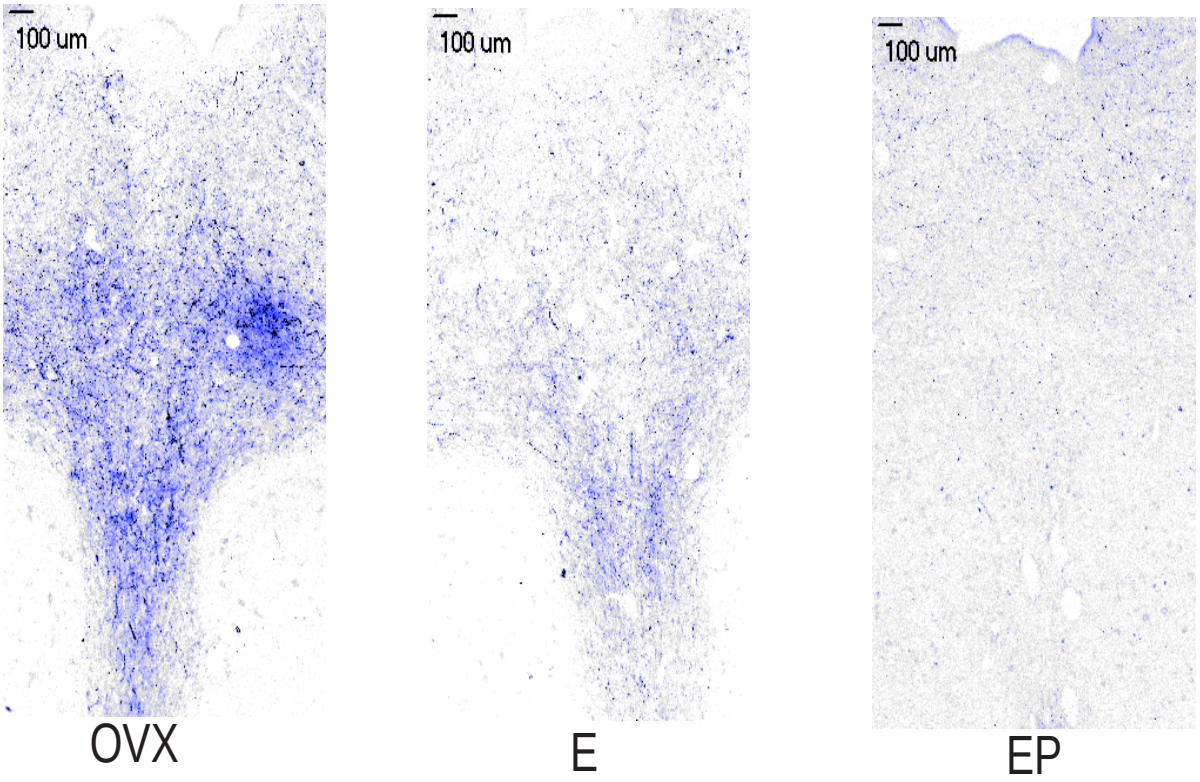

Figure 13. Segmenting CRF-positive fibers in the dorsal raphe nucleus. Representative montages of CRF-positive fibers in OVX- (control), E-, and E + P-treated animals after segmentation.

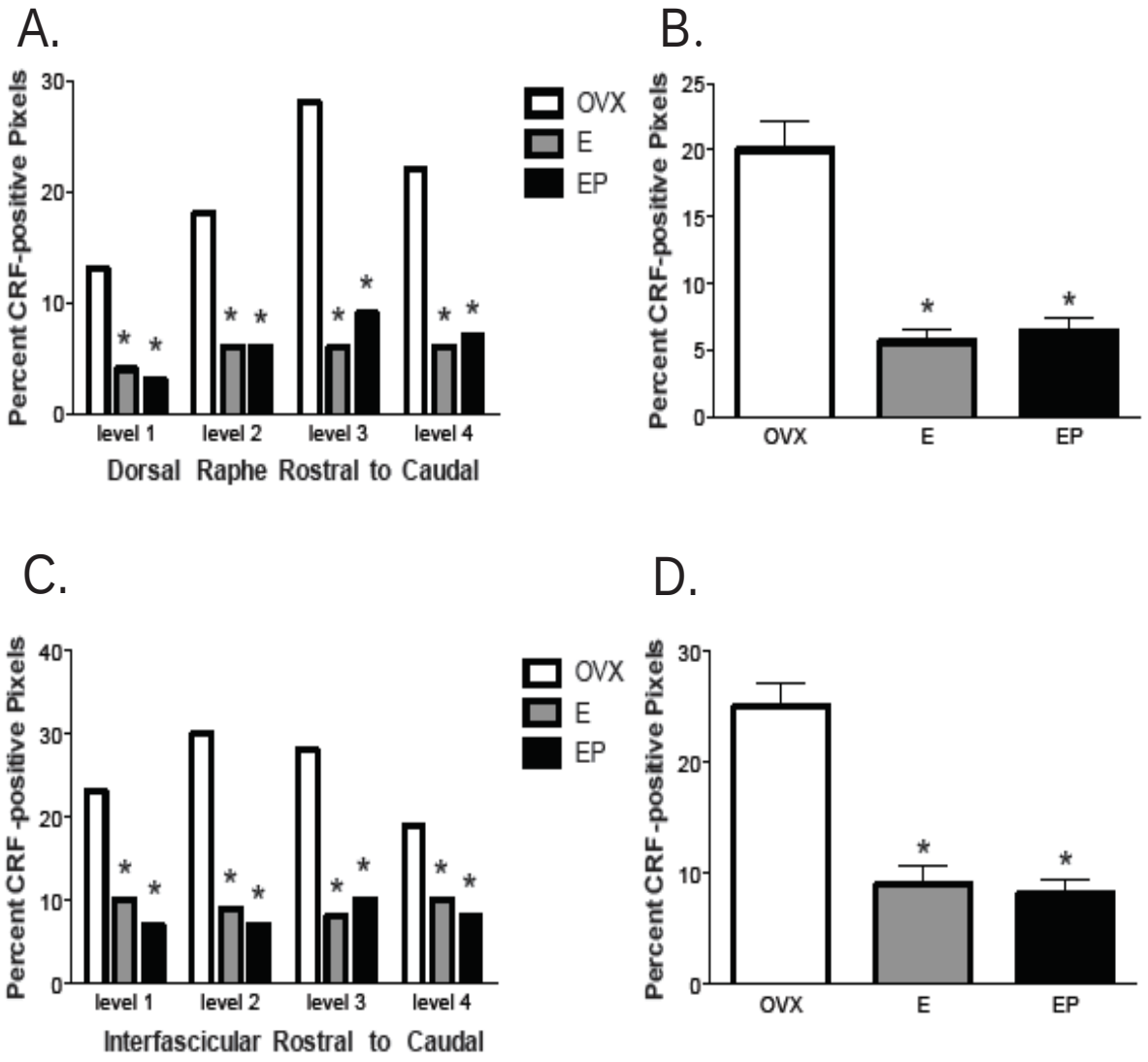

Figure 14. Histograms representing the percent of CRF-positive pixels within the dorsal raphe nuclei for the animals in each treatment group (n=5/group). **A**. E and E + P significantly decreased the percent of CRF-positive pixels in the dorsal segment of the dorsal raphe nucleus in all four levels analyzed. **B**. When levels were combined, E and E + P significantly decreased the mean percent of CRF-positive pixels compared to OVX placebo-treated controls. **C**. E and E + P significantly decreased the percent of CRF-positive pixels in the interfascicular segment of the dorsal raphe nucleus in all four levels analyzed. **D**. When the interfascicular levels of the dorsal raphe nucleus were combined, E ± P significantly decreased the mean percent of CRF-positive pixels compared to OVX placebo-treated controls. The asterisks represent a significant difference from the control group by Student-Neuman-Kuels post-hoc comparison with $p<0.05$.

CRF-positive fibers within the median raphe were also segmented, quantified, and analyzed. **Figure 15** illustrates representative levels of the median raphe for animals in each treatment group (n=5/group). As illustrated in **Figure 16**, E and E+P significantly decreased the percent of CRF-positive pixels in the median raphe in all four levels analyzed (ANOVAs range $p < 0.0001$ to 0.02; error bars are omitted for clarity). When the levels were combined, there was an overall decrease in the mean percent positive pixel area per level with administration of E and E+P compared to placebo-treated controls (ANOVA $p < 0.05$).

Experiment B. *qRT-PCR to determine CRF expression in dorsal raphe*

Methods: We hypothesized that the CRF fibers in the dorsal raphe were derived from cell bodies that were located elsewhere, particularly the hypothalamus and the amygdala. To rule out the possibility that CRF in the fibers under analysis was synthesized in the dorsal raphe, qRT-PCR was used on a small block of brain tissue containing the dorsal raphe that was collected from 9 monkeys (n=3/group) and perfused with RNA later. The microdissected raphe block from each animal was homogenized, and the RNA was extracted. Forward and reverse primers were designed from the human sequence of CRF (see **General Methods** for details about RNA extraction, primers, and PCR conditions). qRT-PCR was conducted with the Dynamo Sybr Green qPCR Mix. A standard curve was generated using a pool of rhesus tissues and the slope of the curve was used to calculate the relative ρg of *CRF* transcript in the

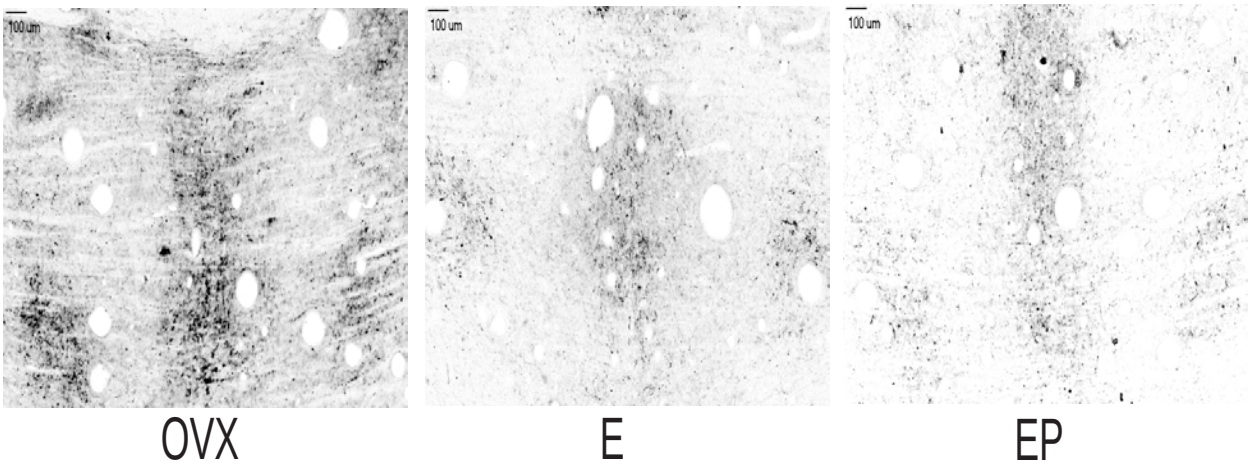

Figure 15. CRF staining in the median raphe nucleus. Representative stereological montage of median raphe fibers from OVX, E, and E + P animals immunostained with anti-human CRF.

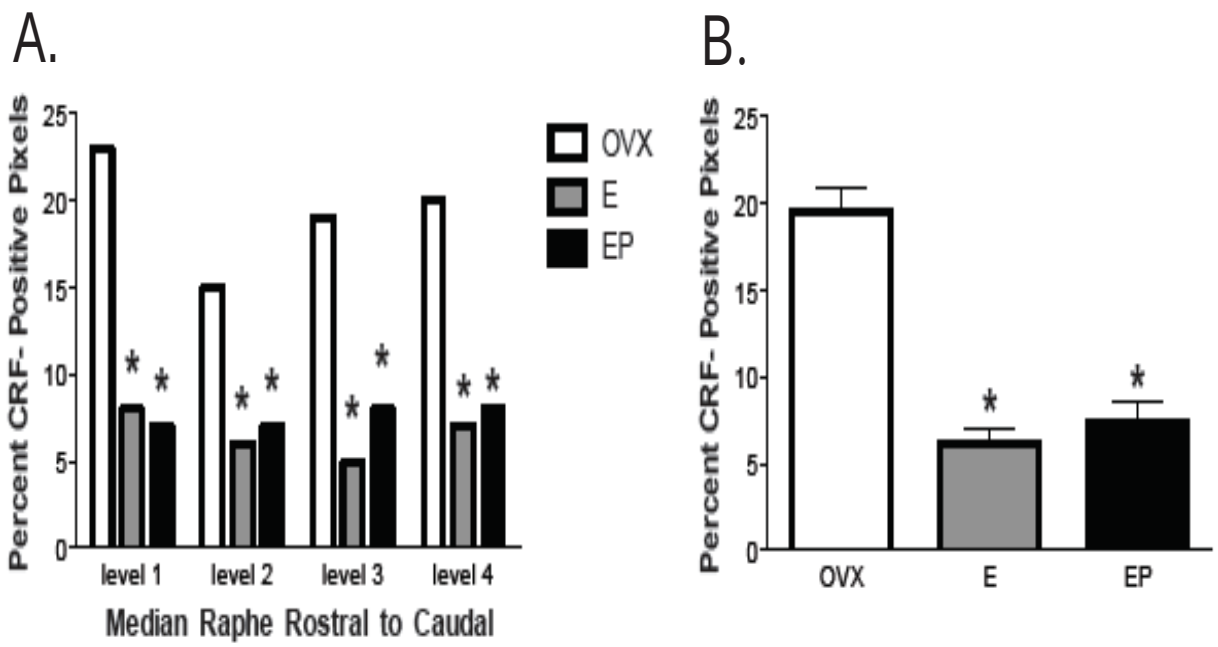

Figure 16. Histograms representing the percent of CRF-positive pixels within the median raphe for the animals in each treatment group (n=5/group). **A**. E ± P significantly decreased the percent of CRF-positive pixels in all four levels analyzed. **B**. When the levels were combined, E ± P significantly decreased the percent of CRF-positive pixels compared to OVX placebo-treated controls. The asterisks represent a significant difference from the control group by Student-Neuman-Kuels post hoc comparison with $p<0.05$.

total RNA from each animal's midbrain. Then, the ratio of *CRF/GAPDH* was calculated and calibrated to the OVX-control group to determine the relative abundance of *CRF* in the microdissected raphe-containing areas of the two hormone-treated groups compared to the OVX-control.

Results: When the relative abundance of CRF mRNA was calculated in the placebo-, E, and E+P- treated animals; the E and E+P groups did not differ significantly in CRF mRNA expression compared to placebo-treated controls (**Figure 17**), as there was too much variance of CRF expression within each group. However, there was a trend indicating that ovarian hormone treatment increased CRF mRNA in the dorsal raphe and this outcome of this experiment may have reached significance with sufficient power.

3.3 Discussion

In the current study, we report that the treatment of ovariectomized monkeys with E ± P for one month reduces CRF fiber innervation in the dorsal and median raphe nuclei of ovariectomized macaques. Based on anatomical studies in rats, these CRF-positive fibers in the caudal raphe project mainly from the caudal two-thirds of the PVN, the bed nucleus of the stria terminalis (BST), the central amygdala, or lateral hypothalamus (Waselus and Van Bockstaele, 2007; Poulin et al., 2008). This supports our previous work showing the E and P treatments significantly decreased the expression of CRF mRNA and protein across five levels of the PVN compared to placebo-treated controls

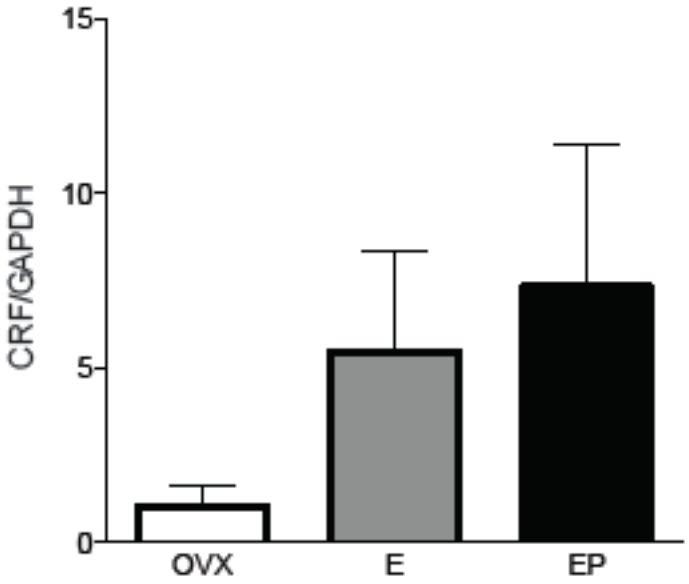

Figure 17. Histogram representing the relative abundance of *CRF* in RNA extracted from the microdisected raphe area of OVX female monkeys treated with placebo, E, or E+P for 1 month (n=3 animals/group). These results are normalized to the OVX (placebo-controlled) treatment group. Although E and E+P treatments tended to increase the relative abundance of midbrain *CRF* RNA, these differences were not significant between any two of the three treatment groups.

(Bethea and Centeno, 2008). This information suggests that E and P can impact the function of CRF neurons innervating the dorsal raphe serotonin system. This is important because it indicates that ovarian hormone treatment decreases CRF input to the dorsal raphe serotonin system. CRF preferentially binds to CRF-R1 over CRF-R2, and activation of CRF-R1 is thought to decrease release of serotonin from the raphe (Valentino et al., 2009). It is attractive to speculate that E- and P-induced decrease of CRF input to CRF-R1 within the raphe serotonin system would increase serotonin release and decrease anxiety.

An alternative interpretation of the observed E- and E+P- induced decrease of CRF input to the raphe observed in this experiment is that removal of ovarian steroids interfered with CRF release from axon terminals, resulting in the increase in CRF-fiber density we saw in the OVX condition. In this scenario, E and P treatments may potentially increase CRF release from axon terminals. This interpretation of the results is highly unlikely given that E and P markedly decreased CRF gene and protein expression in the neuronal cell bodies where the majority of the axons originate. Altogether, the data show that E+P decrease CRF gene and protein expression in the PVN, which in turn sends axons to the raphe that reflect reduced CRF gene and protein expression.

One study in rats reports that in addition to being targeted by CRF-containing axon terminals, the dorsomedial subnucleus of the dorsal raphe nucleus also contains a small population of CRF-positive neuronal cell bodies (Commons et al., 2003). Notably, CRF

immunoreactive cell bodies were only detected in the centromedial dorsal raphe nucleus of rats treated with colchicine (Commons et al., 2003), which was necessary for visualization of CRF immunolabeling of somatodendritic processes of the DR, but CRF immunoreactive cell bodies were not present in DR from rats not treated with the colchicine. Instead, untreated rats showed CRF immunoreactivity primarily in axon terminals, with the densest innervation being the dorsolateral aspects of the caudal dorsal raphe nucleus (Kirby et al., 2000). Likewise, CRF mRNA has been detected in the median raphe of voles (Lim et al., 2006), although the amount of labeled CRF mRNA is much lower in the median raphe compared to more densely labeled regions such as the PVN.

Unlike rodents (Commons et al., 2003; Lim et al., 2006), CRF cell bodies were not observed in the monkey raphe nuclei. However, CRF cell bodies were observed far laterally outside of the raphe nuclei. To verify that the source of CRF innervation into the dorsal raphe nucleus serotonin system in our model was extrinsic and not derived from the DR itself, we used Sybr Green quantitative polymerase chain reaction (qRT-PCR) to measure CRF mRNA in microdissected midbrains from OVX, E, and E+P groups (n=3/group). Surprisingly, E, with or without P, treatment tended to increase CRF mRNA expression in the midbrain block, although the individual variance among animals in each group prevented statistical significance. This is interesting and inconsistent with the fact that the CRF fiber innervation to the raphe decreases with E and P treatments. The relative expression was near the limits of detection of the assay suggesting that CRF mRNA was minimal. Also, we cannot rule out the possibility that

the distant lateral CRF cell bodies in the block of tissue contributed to the results. A further limitation of this assay was the small number of animals in each group (3/group), and consequently there was insufficient power. However, with additional animals it may be discerned that ovarian steroids increased CRF expression in the midbrain population, raising the intriguing possibility that not all CRF neurons respond to ovarian steroids in the same fashion. Future studies in the monkey could more closely examine the effect of ovarian steroids on the small CRF neuronal populations in the midbrain.

In the literature, there are two nonhuman primate studies assessing the effects of circulating E and P on the expression of CRF in the PVN of the hypothalamus. Interestingly, the two studies report opposite results of E action on the CRF-producing neurons in the PVN (Roy et al., 1999; Bethea and Centeno, 2008). In our model of ovarian hormone treatment after surgical menopause, E treatment decreased CRF mRNA, but in the Roy et al. study, E treatment increased CRF mRNA expression in the PVN. These confounding results may be better explained by the difference between the models that each study employs. The animals in the Roy et al. paper were treated with implants containing concentrations of E and P intended to mimic the 28-day natural menstrual cycle in women; they sacrificed the monkeys in the E group at a time point intended to model mid-follicular phase E levels, but the serum E concentrations that are reported are suspiciously low. Serum E levels at necropsy in our animals were 78-155 ± pg/ml and are nearly twice those of monkeys in the Roy et al. study (37.2 ± 3.1 pg/ml). The serum E levels achieved by the monkeys in our model are more physiologically

relevant for studying the effects of combined hormone replacement therapy of estrogen and progestin after menopause. Nonetheless, the serum levels of E and P in our hormone treated monkeys are well below surge levels in normal cycling women and monkeys (Brenner et al., 1974). One emerging concept in the CRF field is that acute and chronic estrogen replacement have different effects on CRF expression in rodents. We speculate that the treatment used in the Roy study may be similar to an acute injection in rats, whereas our treatment may mimic a more chronic treatment in rats.

The mechanism by which E and P decrease CRF input to the dorsal raphe serotonin system requires further investigation. Ovarian hormones may act directly on CRF neurons in the PVN to decrease CRF gene expression. Although the human CRF promoter contains five half ERE sites (Vamvakopoulos and Chrousos, 1993), questions remain regarding the presence and type of nuclear estrogen receptors (ERα or ERβ) in primate CRF neurons. ERβ was detected in CRF neurons of rats (Miller et al., 2004), but ERα was reported in human CRF neurons (Bao et al., 2005). Further characterization of the steroid receptor compliment of CRF neurons in different species and at different levels of the PVN is needed.

Our laboratory has shown that E ± P increases tryptophan hydroxylase (TPH) production in the dorsal raphe nucleus (Bethea et al., 2000; Sanchez et al., 2005) and serotonin release in the hypothalamus (Centeno et al., 2006). Serotonin neurons express ERβ and progestin receptors (PR) for mediation of the action of ovarian hormones (Gundlah et al., 2000). Thus, serotonin innervation of the PVN could mediate

the decrease in CRF expression, but either an inhibitory serotonin receptor or an inhibitory GABA interneuron would be required. In this way, E and P would increase serotonin, which would stimulate GABA interneurons to inhibit CRF expression or release by CRF neurons.

This study raises the question of whether different populations of CRF neurons express ovarian steroid receptors and respond in a similar manner to ovarian steroid treatment. The BST and amygdala contain important populations of CRF neurons and they also send projections to the raphe nuclei. Future studies to measure CRF mRNA and quantify CRF-positive cells in the BST and amygdala are warranted to determine whether E and P treatment also decreased CRF innervation to the dorsal and median raphe nuclei by the BST and amygdala.

In summary, one month of E ± P treatment significantly reduced CRF immunoreactive fibers in the dorsal raphe nucleus of ovariectomized monkeys. Regardless of the mechanism by which ovarian hormones decrease CRF fiber innervation in dorsal raphe nucleus, the resultant decrease in CRF input to the dorsal raphe serotonin system may be an important avenue whereby ovarian steroids modulate serotonin dysfunction in affective disorders. The impact of ovarian steroids on the function of the central stress-related signaling systems is of significant importance to women because of their transition into menopause and their concomitant increase in depression and other stress-related diseases.

Chapter 4: Estradiol and progesterone modulate CRF receptor expression in monkey raphe nuclei.

4.1 Introduction

CRF regulates the serotonin system in the dorsal raphe nucleus through corticotropin-releasing factor receptor subtypes 1 and 2 that have opposing effects on the activity of the serotonin system (Pernar et al., 2004). In rats, low doses of CRF are more selective for CRF-R1 and decrease extracellular serotonin in dorsal raphe forebrain targets (Kirby et al., 2000; Price and Lucki, 2001). Alternatively, higher doses of CRF engage CRF-R2 receptors in the dorsal raphe and thereby increase extracellular serotonin (Kirby et al., 2000; Price and Lucki, 2001; Pernar et al., 2004). Although the opposing actions of CRF-R1 and CRF-R2 activation in the raphe have been well characterized in rat models of stress-induced depressive behaviors, their opposing actions in the raphe serotonin system of macaques and humans is lacking. Further, immunohistochemical and *in situ* hybridization studies conducted in primates disagree as to whether monkey raphe expresses CRF-R1 (Sanchez et al., 1999; Kostich et al., 2004).

The opposing actions of CRF-R1 and CRF-R2 in the dorsal raphe are hypothesized to facilitate active and passive behavioral coping styles, respectively (Valentino and Commons, 2005). For example, CRF-R2-mediated activation of the dorsal raphe promotes passive behavior strategies such as learned helplessness (Hammack et al., 2003). In contrast, low doses of CRF, which selectively activate CRF-R1, promote an active escape response in the same behavioral paradigm (Hammack, 2003).

Much work has been done in the rodent to elucidate the opposing roles of CRF receptor types 1 and 2 and their regulation of serotonin function in the raphe. Recently, Waselus et al. used electron microscopy and immunofluorescence to determine that acute swim stress causes differential trafficking of CRF-R1 and CRF-R2 in the raphe serotonin neurons. In the unstressed condition, CRF-R1-immunoreactivity was more prominent on the plasma membrane of raphe neurons while CRF-R2-immunoreactivity was more prominent internally within the cytoplasm. Twenty-four hours after a swim test, which is considered an acute stress for rodents, the distribution of CRF-R immunoreactivity was reversed, such that CRF-R2 was recruited to the plasma membrane and CRF-R1 was internalized (Waselus et al., 2009). As a consequence of this stress-induced redistribution of CRF receptors, neuronal responses to CRF and related ligands change from inhibition to a CRF-R2-mediated excitation. The authors speculate that during the initial exposure to acute stress, CRF-R1 is more prominent on serotonin neurons, and consequently serotonin neurons are inhibited from releasing serotonin during the stressor. Activation of this circuit is adaptive and would promote an active coping style immediately after exposure to the stressor, presumably because serotonin stores are adequate to facilitate the learning of escape behaviors when escape is possible (Amat et al., 2004). On the other hand, twenty-four hours after an acute stressor, an unknown mechanism mediates the recruitment of CRF-R2 to the membrane of serotonin neurons. Repeated exposure to stress would cause an overall excitation of serotonin neurons, with increased release into fear perception areas of the amygdala. Continued activation of this circuit would promote passive coping styles (or

poor escape-learning when escape is possible) two to four days after the stressor because serotonin stores would be depleted (Amat et al., 2004). This provides a cellular mechanism for switching behavioral strategies while coping with stressors.

Although much of what we know about the regulation and expression patterns of CRF-R1 and CRF-R2 comes from rodent studies, two studies in primates report that CRF-R2 is expressed more robustly in the monkey raphe than CRF-R1 (Sanchez et al., 1999; Kostich et al., 2004). However, the distribution of CRF-R1 and CRF-R2 in the female monkey has not been described and this lack of knowledge is a significant obstacle in our understanding of CRF and serotonin system interactions in women. In the experiments described here, we determined whether E and E+P treatments affect CRF-R1 and CRF-R2 gene expression in the raphe, and more importantly, we determine E ± P regulation of mature CRF-R1 and CRF-R2 expression.

There are other components of the CRF-signaling system that affect central CRF receptor binding and consequent activation of the behavioral sequelae following stress exposure. One of these, corticortopin-releasing factor binding protein (CRF-BP) is a soluble protein that binds CRF and prevents it from activating receptors. Because CRF binds CRF-R1 preferentially, it is generally thought that CRF-BP functions to prevent CRF-R1 activation (Van Den Eede et al., 2005). In rodents CRF-BP transcription significantly increases in the basolateral amygdala following an acute stressor (Herringa et al., 2004), and this supports the endogenous role of CRF-BP as a neuropeptide that protects against prolonged activation of CRF receptors. Evidence indicates that E

positively regulates CRF-BP expression in hypothalamic neurosecretory cells via ERα and ERβ (van de Stolpe et al., 2004). There is also one study that positively identifies CRF-BP mRNA in the rodent raphe (Potter et al., 1992). If CRF-BP is expressed in the primate raphe and also regulated by E, we predict that animals in the E group will have significantly higher CRF-BP expression in the raphe hemi-midbrains than animals in the OVX placebo-treated control group.

To adequately assess the impact of E and E ± P treatment on the CRF-receptor activation in the dorsal raphe nucleus, we sought to determine the effect of one month of E and E+P treatment on gene and protein expression of both receptors (CRF-R1 and CRF-R2) as well as the gene expression of CRF-BP. First, we used qRT-PCR to quantify the expression of CRF-R1, CRF-R2, and CRF-BP mRNAs in the microdissected raphe area of animals in each treatment group. If the receptor or binding protein transcripts were abundantly expressed in raphe and appeared to be regulated by E or E+P, we then assessed E ± P regulation of the mature form of each receptor or binding protein using immunocytochemistry. We hypothesized that compared to placebo-treated control animals, E ± P treatments would decrease gene and protein expression of CRF-R1 and increase gene and protein expression of CRF-R2 in the raphe region of ovariectomized monkeys. This regulation would lead to an increase in serotonin as previously observed. If CRF-BP was detectable in the microdissected midbrains of animals in this study, we predicted that E ± P would increase CRF-BP expression.

4.2 Experiments

Experiment C. *Quantitative RT- PCR quantifying CRF-R1 mRNA expression in the microdissected raphe area.*

Methods: Two qRT-PCR experiments were performed. Initially, Sybr Green qRT-PCR was used to quantify CRF-R1 in the microdissected raphe area collected from 9 monkeys (n=3/group) perfused with RNA later. Forward and reverse primers were designed from the monkey sequence of CRF-R1 and qRT-PCR was conducted with the Dynamo Sybr Green qPCR Mix. **Table 5** includes the primer sequences and gene accession ID of CRF-R1 used for Sybr Green qRT-PCR quantification. The primers amplified a 251-bp segment corresponding to the 1st extracellular loop and the 3rd transmembrane domain of mature CRF-R1. In the Bethea laboratory, we have found that primers amplifying segments of DNA about 200-bp to 250-bp in size optimize our Sybr Green qRT-PCR results. A standard curve was generated using a pool of rhesus tissues and the slope of the curve was used to calculate the relative pg of CRF-R1 transcript in the total RNA from each animal's midbrain. Then, the ratio of CRF-R1/GAPDH was calculated to determine relative abundance of CRF-R1 in the DRN-containing raphe area (please see **Chapter 2** for specific details on Sybr Green qRT-PCR methods). Finally, this ratio of CRF-R1/GAPDH was normalized by determining the fold difference in expression between the E and the E+P group relative to the OVX control group.

In the second qRT-PCR experiment, we used TaqMan qRT-PCR to assess CRF-R1 gene expression in the hemi-midbrain of OVX-, E- and E + P-treated animals (n=4/group). Accession numbers and context sequences used to quantify CRF-R1 in the TaqMan array are listed in **Table 6**. Again, a standard curve was generated using a pool of rhesus tissues and the slope of the curve was used to calculate the relative pg of CRF-R1 transcript in the total RNA from each animal's midbrain. Then, the ratio of CRF-R1/GAPDH was calculated to determine relative abundance of CRF-R1 in the DRN-containing raphe area (please see **Chapter 2** for specific details on Taqman qRT-PCR methods). Finally, this ratio of CRF-R1/GAPDH was normalized by determining the fold difference in expression between the E and the E+P group relative to the OVX control group.

Results: The animals in the E and E+P groups expressed significantly less CRF-R1 mRNA compared to the placebo-treated controls. **Figure 18** illustrates results from the two separate quantitative PCR experiments. The first experiment was performed as described above with Sybr Green (**Figure 18-top)**. When levels of CRF-R1 cDNA were corrected to GAPDH and normalized to the OVX control group, one month of E or E+P treatment significantly decreased CRF-R1 gene expression compared to OVX placebo-treated controls (ANOVA, $p < 0.001$). In the second qRT-PCR experiment, a TaqMan custom expression array was used to assess CRF-R1 expression in the hemi-midbrain of OVX-, E-, and E+P-treated animals (**Figure 18-bottom)**. When levels of CRF-R1 cDNA were corrected to GAPDH and normalized to the OVX control group, one month of E and E+P treatments significantly decreased CRF-R1 gene expression compared to

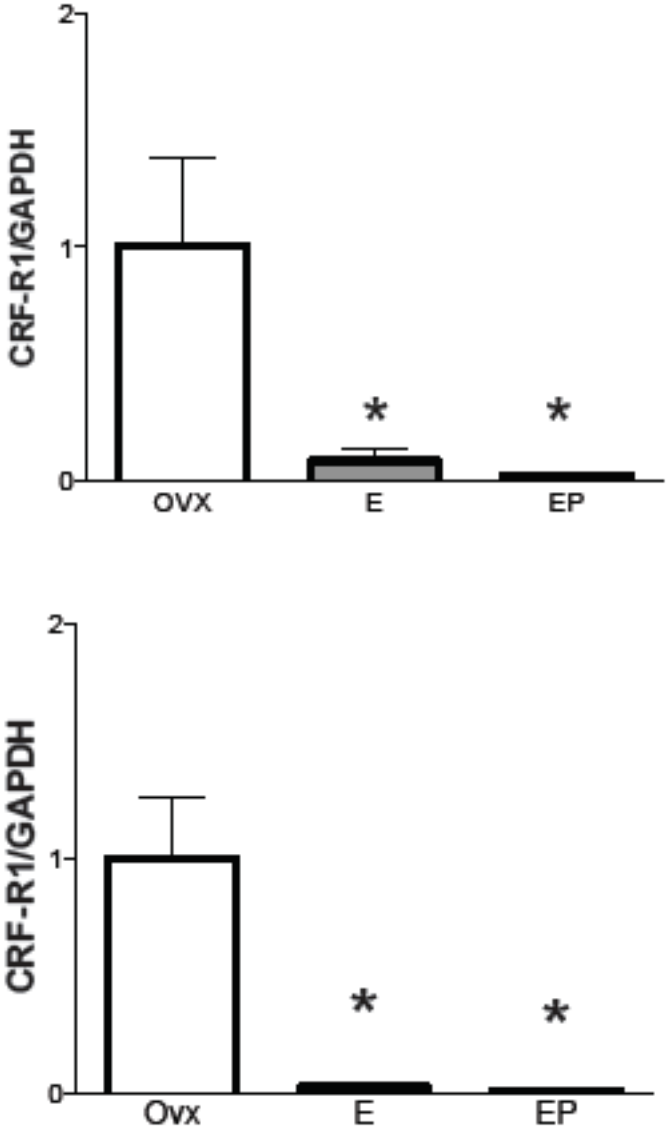

Figure 18. Upper: Histogram representing the relative abundance (normalized to OVX group) of *CRF-R1* in RNA extracted from the microdisected raphe area of OVX female monkeys treated with placebo, E, or E+P for 1 month (n=3 animals/group). **Lower:** Histogram representing the relative abundance of *CRF-R1* in RNA extracted from the hemi-midbrain block of OVX female monkeys treated with placebo, E, or E+P for 1 month (n=4 animals/group). The asterisks represent a significant difference from the control group by Student-Neuman-Keuls post-hoc comparison with $p<0.05$. Both the E and E + P treatment groups showed decreased expression of CRF-R1 when compared to the OVX control group.

OVX placebo-treated controls in the hemi-midbrain of ovariectomized macaques (ANOVA, $p < 0.001$).

Experiment D. *Immunohistochemistry (IHC) experiment to identify and quantify CRF-R1-positive cells and pixels in the dorsal raphe*.

Methods: To determine if the change in CRF-R1 mRNA translated to protein expression and to further assess whether E or E+P treatment decrease CRF-R1 expression in the dorsal raphe, we immunostained the dorsal raphe nucleus with an antibody made against a peptide spanning an internal region of human CRF-R1. **Figure 19-A** depicts the dorsal raphe nucleus immunostained with the CRF-R1 antibody diluted 1/500 in phosphate buffered saline, the dilution of antibody used in all experimental assays. Because the expression of CRF-R1 in macaque raphe is disputed (Sanchez et al., 1999; Kostich et al., 2004), we ran preabsorption control experiments to ensure antibody specificity. **Figure 19-B** depicts the CRF-R1-positive signal in an OVX animal incubated in anti-CRF-R1 antibody diluted 1/2000, the minimal concentration needed to observe signal. **Figure 19-C** depicts the adjacent section of the same animal incubated in antibody diluted 1/2000 and preabsorbed with 100 µg CRF-R1 peptide. Five levels of the dorsal raphe nucleus at 500 µm intervals were examined in OVX, E and E+P treated animals (n=5/group) for CRF-R1 immunostaining. Slidebook 4.2 was used to segment the images (illustrated in **Figure 20**) and to quantify the percent of CRF-R1 positive pixels in the dorsal raphe area. We measured and recorded the area of the raphe analyzed to ensure that it did not vary across animals.

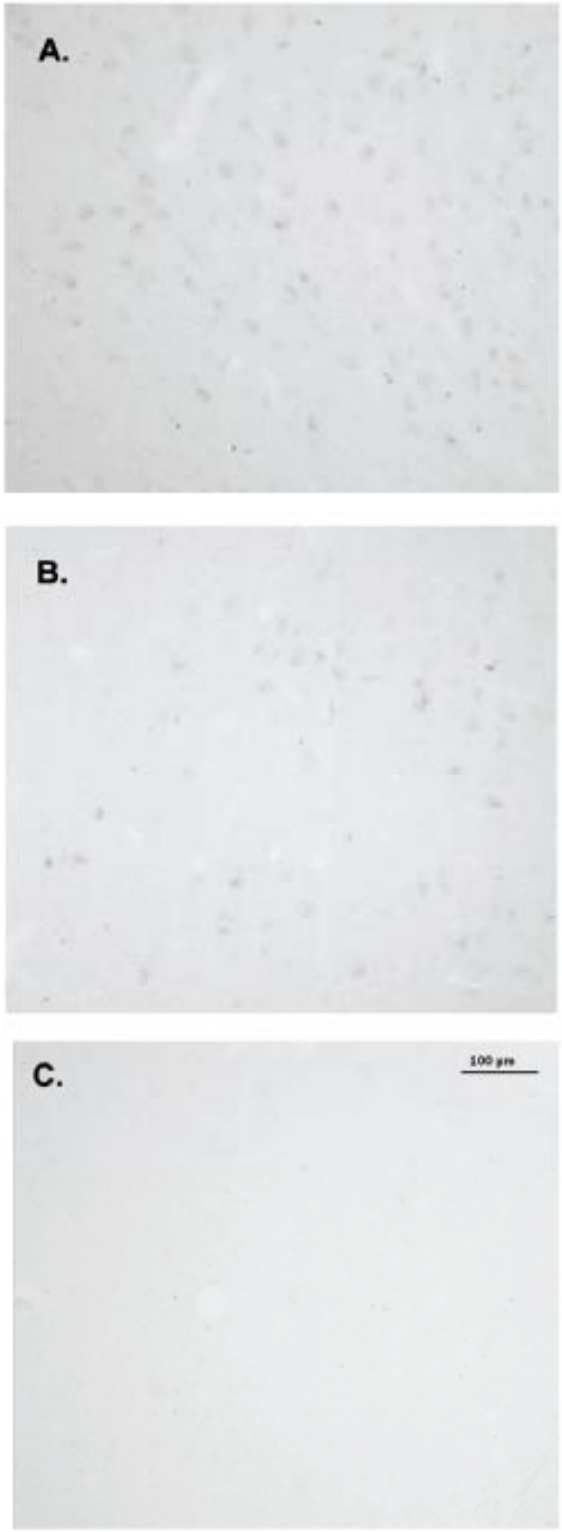

Figure 19. Absorption control experiments for antibody against CRF-R1. **A**. Dorsal raphe nucleus from OVX (control) animal immunostained with the CRF-R1 antibody diluted 1:500 in phosphate buffered saline. **B.** CRF-R1-positive signal in an OVX animal incubated in 1:2000 dilution of the primary antibody. **C**. To serve as a negative control, the 1:2000 dilution of the primary antibody was preabsorbed with 100 μg CRF-R1 peptide for 24 hours before incubation with raphe tissue from the same level of the OVX animal. Scale bar, 100 μm.

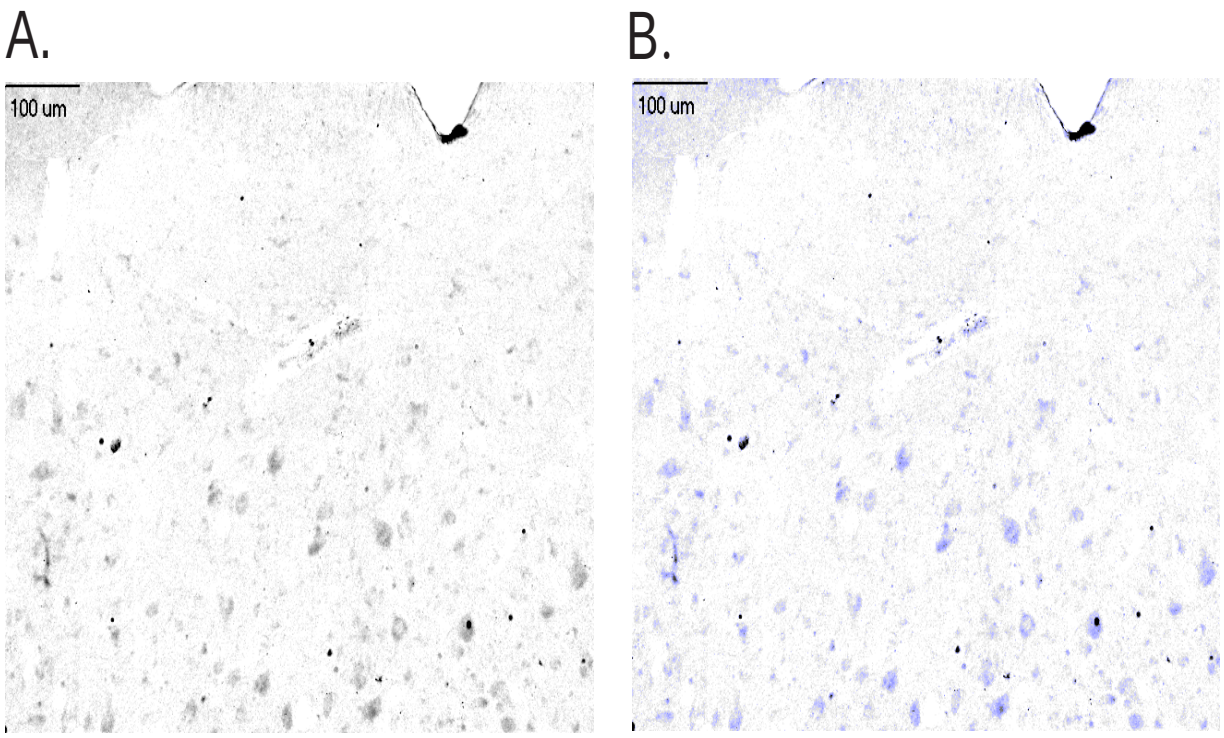

Figure 20. Representative stereological montage of the dorsal raphe nucleus immunostained with an antibody raised in goat against human CRF-R1. **A**. CRF-R1-positive signal in the dorsal raphe from an OVX animal **B**. Representative montage of CRF-R1-positive signal after segmentation with Slidebook 4.2

Results: The quantification of CRF-R1 positive pixel area as percent of total area in the dorsal raphe is illustrated in **Figure 21.** E and E + P significantly decreased the percent of CRF-R1-positive pixels in the third level of the dorsal raphe nucleus (ANOVA, $p < 0.0025$; **Figure 21-A**). When the levels were combined as illustrated in **Figure 21-B**, there was an overall decrease in the mean percent positive pixel area per level with administration of E and E+P compared to ovariectomized placebo-treated controls (ANOVA $p<0.03$).

Experiment E. *Real time PCR quantifying CRF-R2 mRNA expression in the microdissected raphe area*.

Methods: We hypothesized that E and E+P treatment would increase the abundance of CRF-R2 in the raphe area of ovariectomized macaques. Initially, Sybr Green qRT-PCR was applied to the microdissected raphe area collected from 9 monkeys (n=3/group) perfused with RNA later as described above. Forward and reverse primers were designed from the rhesus sequence of CRF-R2 and qRT-PCR was conducted with the Dynamo Sybr Green qPCR Mix. **Table 5** includes the primer sequences and gene accession ID of CRF-R2 used for real time Sybr Green PCR quantification. The primers amplified a 196-bp segment corresponding to exons 3 and 4 within the N-terminal extracellular domain of mature CRF-R2.

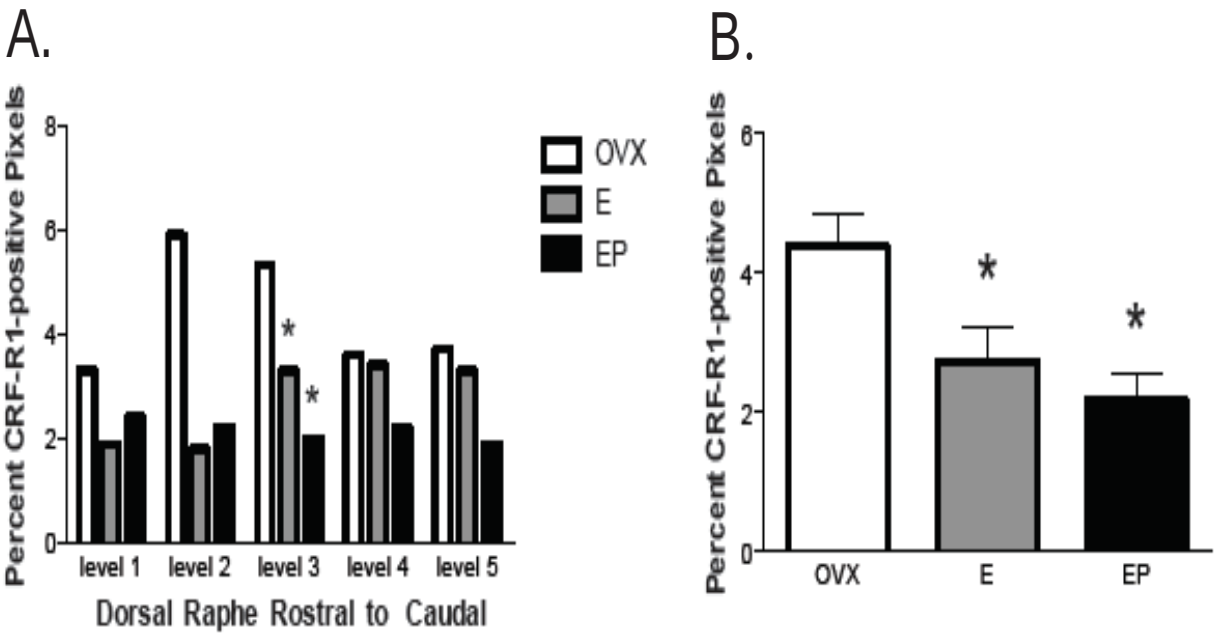

Figure 21. Histograms representing the percent of CRF-R1-positive pixels within the dorsal raphe nucleus for the animals in each treatment group (n=3/group). **A**. E and E+P significantly decreased the percent of CRF-R1-positive pixels in the third level of the dorsal raphe nucleus. The asterisks represent a significant difference from the control group by Student-Neuman-Keuls post-hoc comparison with $p<0.05$. **B**. When levels were combined, E and E+P significantly decreased the mean percent of CRF-R1-positive pixels compared to OVX placebo-treated controls. The asterisks represent a significant difference from the control group by Student-Neuman-Kuels post-hoc comparison with $p<0.05$.

In the second qRT-PCR experiment, TaqMan qRT-PCR as described above was applied to assess CRF-R2 gene expression in the hemi-midbrain of OVX-, E- and E + P-treated animals (n=4/group). Accession numbers and context sequences used to quantify CRF-R2 in the TaqMan array are listed in **Table 6.**

In each assay, a standard curve was generated using a pool of rhesus tissues and the slope of the curve was used to calculate the relative pg of CRF-R2 transcript in the total RNA from each animal's midbrain. Then, the ratio of CRF-R2/GAPDH was calculated to determine relative abundance of CRF-R2 and normalized to the OVX control group.

Results: The expression of CRF-R2 was significantly higher in the E-treated animals than in OVX controls. **Figure 22** illustrates the results from two separate quantitative PCR experiments. The first experiment was performed as described above with Sybr Green. When levels of CRF-R2 cDNA were corrected to GAPDH and normalized to the OVX control group, E treatment significantly increased CRF-R2 gene expression compared to OVX placebo-treated controls (ANOVA, $p < 0.001$) . Supplementation with P reversed the effect of E and the CRF-R2 expression in the E+P group was not different from the OVX control group **(Figure 22-top)**. In the second qRT-PCR

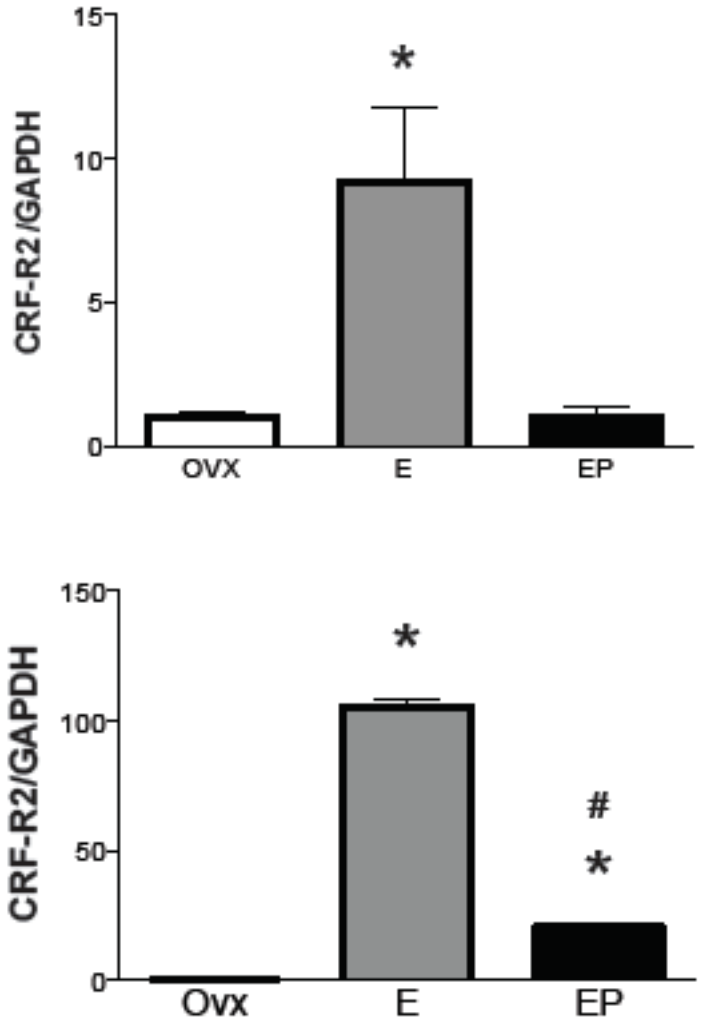

Figure 22. Upper: Histogram representing the relative abundance of *CRF-R2* in RNA extracted from the microdisected raphe area of OVX female monkeys treated with placebo, E, or E+P for 1 month (n=3 animals/group). **Lower**: Histogram representing the relative abundance of *CRF-R2* in RNA extracted from the hemi-midbrain block of OVX female monkeys treated with placebo, E, or E+P for 1 month (n=4 animals/group). In both the Sybr green and TaqMan assays, the E group showed increased expression of *CRF-R2* when compared to the OVX control group. The asterisks represent a significant difference from the control group by Student-Neuman-Keuls post-hoc comparison with $p<0.05$. The hatched bar represents a significant difference from the E-treated group with $p<0.05$.

experiment with hemi-midbrains from different animals, a TaqMan custom array was used to assess CRF-R2 expression in the hemi-midbrain of OVX-, E-, and E+P- treated animals **(Figure 22-bottom)**. The relative expression of CRF-R2 was significantly increased by E treatment compared to the OVX control group and then significantly reduced by P treatment. However, expression in the P group remained significantly higher than in the OVX control group (ANOVA $p < 0.001$).

Experiment F. *Immunohistochemistry (IHC) experiment identifying and quantifying CRF-R2-positive cells and pixels in the dorsal and median raphe*.

Methods: To determine if the increase in CRF-mRNA expression translated to protein expression and to further assess whether E treatment increases CRF-R2 expression in the dorsal and median raphe nuclei, the dorsal raphe nucleus was immunostained with an antibody made against a synthetic peptide spanning the first extracellular domain of human CRF-R2 (Chemicon, AB9139). To ensure antibody specificity, we ran preabsorption controls. **Figure 23-A and 23-B** depict the CRF-R2-positive signal in and E-treated animal incubated in anti-CRF-R2 antibody diluted 1/750 at low and high magnifications. **Figure 23-C** depicts an adjacent section from the same animal incubated in antibody diluted 1/750 and preabsorbed with 1.0 mg CRF-R2 peptide (Lifespan Biosciences LS-P502). We sought to achieve a concentration of peptide that was 1000 X greater than antibody, which insures that all binding sites for CRF-R2 on the antibody are saturated before incubation with the experimental tissue. **Figure 24** depicts high magnification photomicrographs of the dorsal (**A**) and median (**B**) raphe

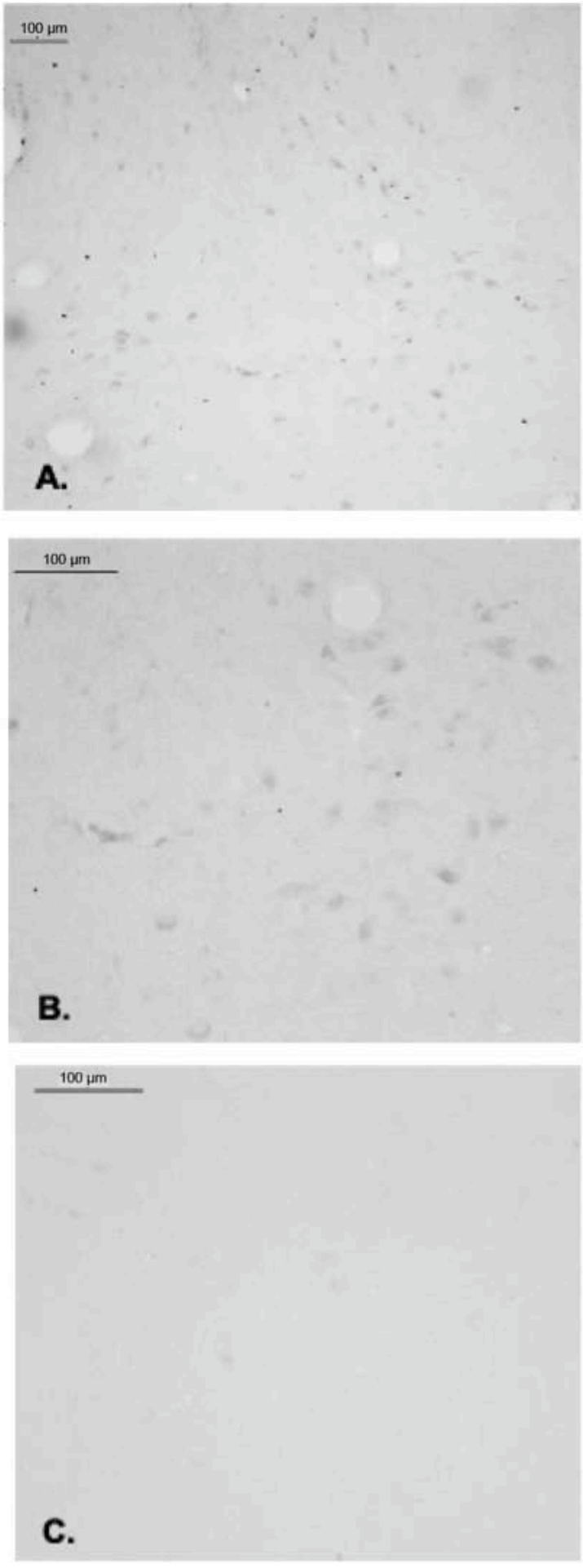

Figure 23. Absorption control experiments for CRF-R2 antibody. **A**&**B.** CRF-R2-positive signal in an E+P-treated animal incubated with a 1:750 dilution of the primary antibody. **C**. To serve as a negative control, the 1:750 dilution of the primary antibody was preabsorbed with 1 mg CRF-R2 peptide for 24 hours before incubation with raphe tissue from the same level of the EP animal. Scale bar, 100 µm.

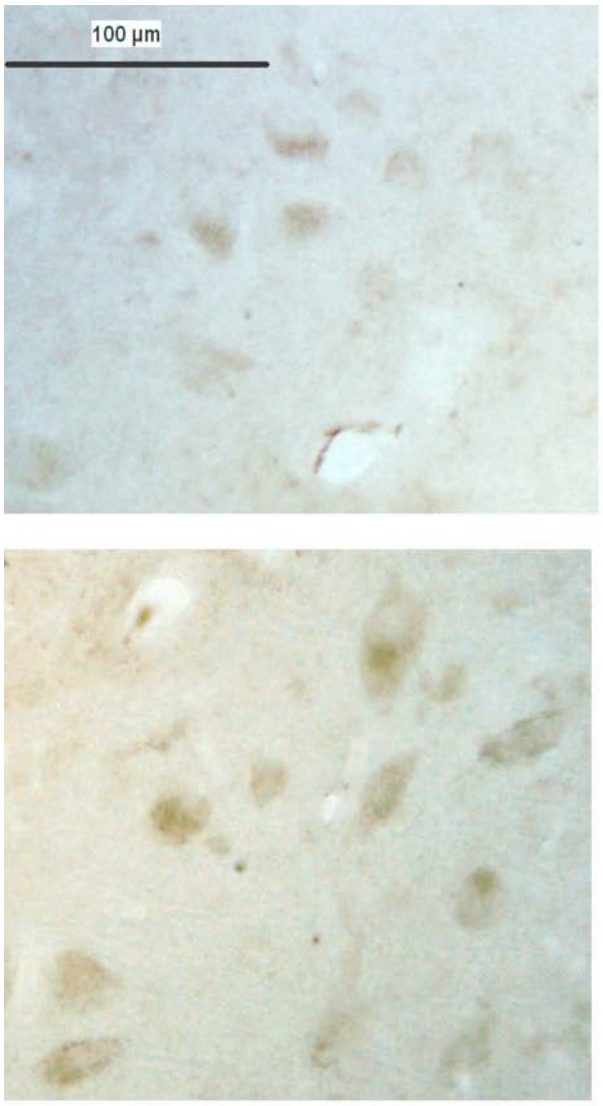

Figure 24. Representative sections of the dorsal and median raphe nuclei immunostained with an antibody raised in rabbit against human CRF-R2. Upper panel: CRF-R2-positive signal in the dorsal raphe from an E-treated animal. Lower panel: CRF-R2-positive signal in the median raphe nucleus in the same animal. Scale bar, 100 µm.

nuclei immunostained with the CRF-R2 antibody diluted 1/750 in phosphate buffered saline.

Five levels of the dorsal raphe spanning about 1 mm, and three levels of the median raphe spanning about 500 μm, at 500 μm intervals were examined for CRF-R2 immunostaining. We used Slidebook 4.2 to segment the images and quantify the percent CRF-R2 positive pixels in the dorsal and median raphe nuclei. We measured and recorded the area of the raphe analyzed to ensure that it did not vary across animals.

Results: As illustrated in **Figure 25-A,** the E-treated group showed a significantly higher percent of CRF-R2-positive pixels in the dorsal raphe nucleus compared to OVX control or E+P-treated groups in 4 of 5 levels (ANOVAs range $p < 0.0001$ to 0.014; error bars are omitted for clarity). When all levels were combined (**Figure 25-B**), there was an overall increase in the mean percent positive pixel area with administration of E compared to the OVX group or the E+P group (ANOVA $p<0.05$). Similarly, when we quantified CRF-R2 positive pixels across 3 levels of the median raphe, the E-treated group showed a significantly higher percent of CRF-R2-positive pixels in the median raphe nucleus compared to OVX placebo- or E+P-treated groups at all 3 levels (ANOVAs range $p < 0.0001$ to 0.018; error bars are omitted for clarity; **Figure 26-A**). When all levels were combined (**Figure 26-B**), there was an overall increase in the mean percent positive pixel area of the median raphe with administration of E compared to the OVX group or the E+P group (ANOVA $p < 0.0001$).

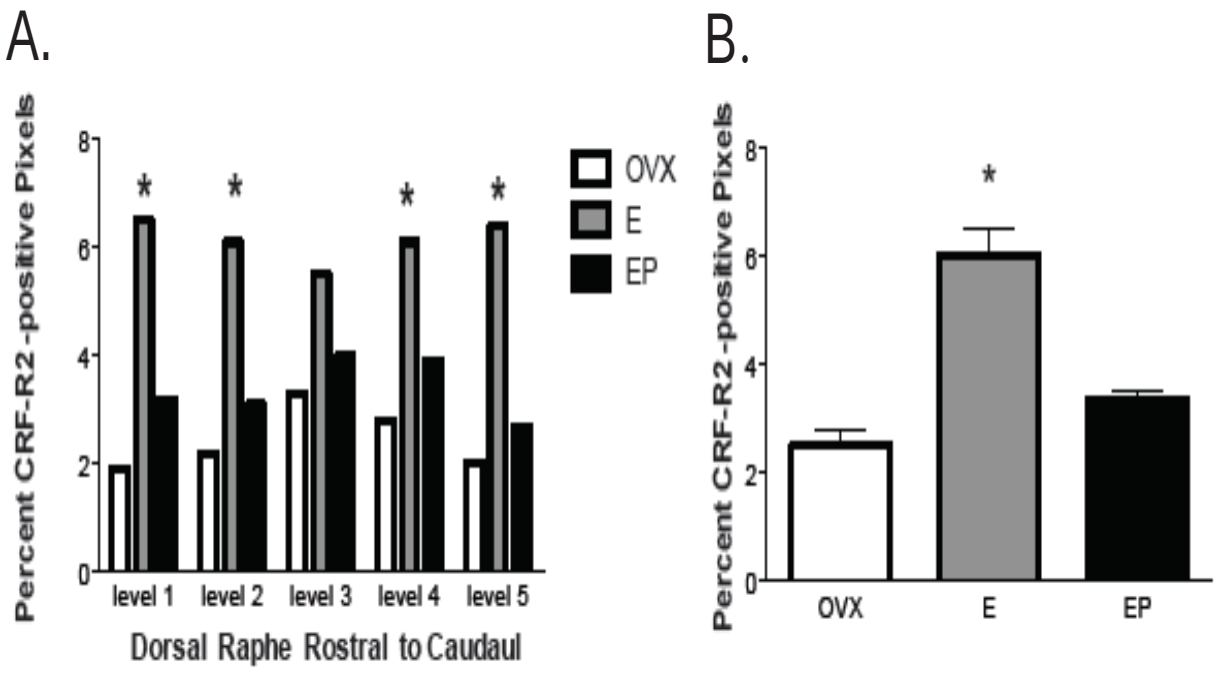

Figure 25. Histograms representing the percent of CRF-R2-positive pixels in the dorsal raphe nuclei from ovariectomized monkeys treated with placebo (OVX), estradiol (E) or estradiol + progesterone (E+P) for one month (n=5/group). **A.** The E-treated group showed a significantly higher percent of CRF-R2-positive pixels in the dorsal raphe nucleus compared to OVX placebo- or E+P-treated groups in 4 of 5 levels examined. **B.** When all 5 levels were combined, E and E+P significantly increased the mean percent of CRF-R2-positive pixels compared to OVX placebo-treated controls. The asterisks represent a significant difference from the control group by Student-Neuman-Kuels post-hoc comparison with $p<0.05$.

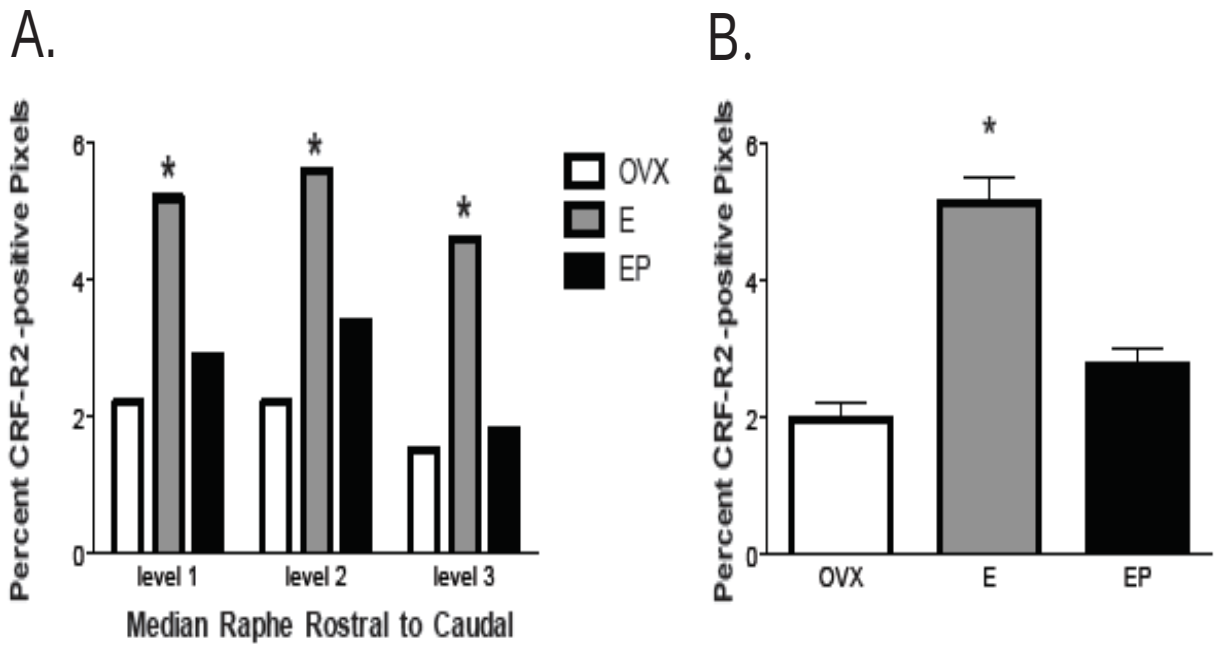

Figure 26. Histograms representing the percent of CRF-R2-positive pixels in the median raphe nuclei from ovariectomized monkeys treated with placebo (OVX), estradiol (E) or estradiol + progesterone (E+P) for one month (n=5/group). **A.** The E-treated group showed a significantly higher percent of CRF-R2-positive pixels in the median raphe nucleus compared to OVX placebo- or E+P-treated groups at all 3 levels examined. **B.** When all 3 levels were combined, E treatment significantly increased the mean percent of CRF-R2-positive pixels compared to OVX placebo-treated controls. The asterisks represent a significant difference from the control group by Student-Neuman-Kuels post-hoc comparison with $p<0.05$.

Experiment G.*TaqMan real-time PCR quantifying CRF-BP mRNA expression in the hemi-midbrain block.*

Methods: In order to quantify the effect of E and E+P on CRF-BP expression in the raphe, we used the TaqMan custom expression array to assess CRF-BP expression in the hemi-midbrain of OVX-, E- and E + P-treated animals. Accession numbers and context sequences used to quantify CRF-BP in the TaqMan array are listed in **Table 6.**

Results: As illustrated in **Figure 27,** one-month of E treatment significantly increased CRF-BP gene expression in the hemi-midbrain of ovariectomized macaques, and additional P treatment (for the last 14 days) significantly decreased gene expression of CRF-BP in the hemi-midbrain.

4.3 Discussion

E ± P decreased CRF-R1 gene and protein expression in the dorsal raphe.

One month of E ± P treatment decreased CRF-R1 mRNA in the microdissected raphe area. The pattern of neuronal staining observed is highly suggestive that CRF-R1 is on serotonin neurons. Indeed, review of microarray data obtained with laser captured serotonin neurons indicated that CRF-R1 mRNA was present in serotonin neurons (unpublished). Future experiments could seek to confirm this with double ISH or IHC. Nonetheless, serotonin neurons express nuclear ERβ and PR, which could transduce the action of E and P on CRF-R1 gene expression. Hence the simplest, and

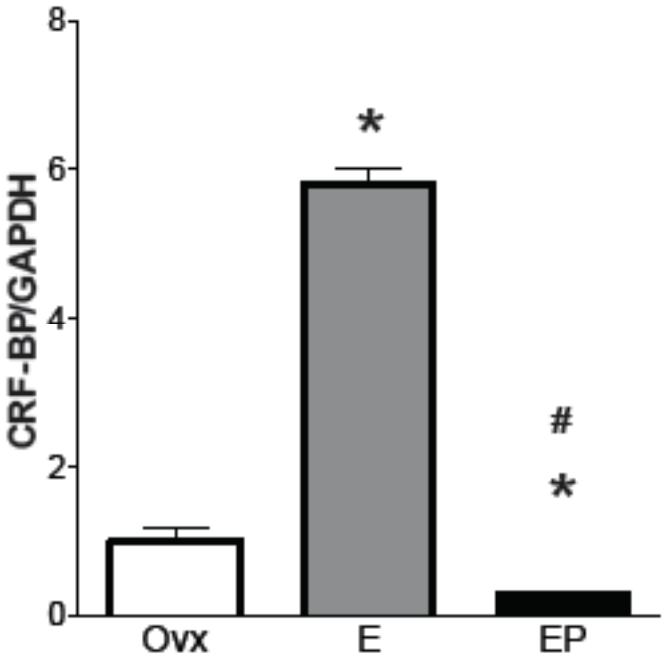

Figure 27. Histogram representing the relative abundance of *corticotropin-releasing binding protein (CRF-BP)* in RNA extracted from the hemi-midbrain block of OVX f monkeys treated with placebo, E, or E+P for 1 month (n=4 animals/group). E trea increased expression of *CRF-BP* compared to the OVX placebo-treated control group treatment decreased *CRF-BP* expression when compared to the OVX placebo-treated group. The asterisks represent a significant difference from the control group by St Neuman-Keuls post-hoc comparison with $p<0.05$.

therefore most likely, explanation (Occam's razor) is that E modulates CRF-R1 gene expression on serotonin neurons directly through a nuclear ER. However, the mechanism by which ERβ inhibits gene expression may involve inhibitory protein-protein interaction with other transcription factors as discussed in Chapter 6.

An alternative explanation is that E regulation of CRF-R1 gene expression is secondary to E regulation of the ligands. For example, high levels of CRF expression (and presumably) release into the raphe of ovariectomized, placebo-treated control animals may cause an up regulation of CRF-R1 expression through a mechanism involving agonist-induced upregulation of a receptor. There are several g-protein coupled receptors that are upregulated after agonist exposure through alternate mechanisms (Thomas et al., 1992; Hoffman et al., 1996; Whiteaker et al., 1998), and one example is via agonist-induced receptor sequestration to the membrane.

Whether ovarian steroids decrease gene expression of CRF-R1 directly via ER activation, or via an agonist-dependent mechanism, our results indicated that ovarian hormone treatment after ovariectomy reduced CRF-R1 gene expression in the microdissected raphe area. Importantly, the E-induced decrease in overall midbrain expression of CRF-R1 mRNA was translated to a decrease in CRF-R1 protein expression in raphe. These results are significant because they indicate that ovarian hormone treatment may ameliorate stress-induced activation of CRF-R1 in the dorsal raphe, and this may be an additional avenue whereby E ± P increase serotonin neural activity. E ± P treatments would therefore be expected to increase overall serotonin

availability and reduce depressive symptoms. In support of this theory, rats that exhibit proactive behavior in resisting defeat to a social stressor show signs of decreased efficacy of both CRF receptors (Wood et al., 2009).

E treatment increased CRF-R2 gene and protein expression in the dorsal raphe.

E- treated animals expressed more CRF-R2-positive pixels in the dorsal and median raphe than OVX control animals. We would expect that increased CRF-R2-positive cells in the raphe would increase overall serotonin availability in these animals. Consistent with this, activating CRF-R2 in the dorsal raphe with the selective agonist urocortin 2 increases dorsal raphe neuronal activity and serotonin efflux in forebrain targets (Amat et al., 2004; Pernar et al., 2004; Staub et al., 2005; Lukkes et al., 2008). Indeed, *in vitro* electrophysiological evidence in the rat has shown the existence of a subpopulation of serotonergic neurons in the ventral and interfascicular region of the caudal dorsal raphe on which CRF has an excitatory effect on serotonin release (Lowry and Moore, 2006). If E treatment increases serotonin availability by increasing CRF-R2 expression and activation of raphe serotonin neurons, then this would be a mechanism by which E modulates depressive symptoms.

Again, the CRF-R2 staining pattern is highly indicative of serotonin neurons and CRF-R2 was detected in RNA from laser captured serotonin neurons (unpublished). Since serotonin neurons express ERβ and PR, it is attractive to speculate that the effects of E and P on CRF-R2 are mediated by the nuclear steroid receptors.

The mechanisms of action of activated ER and PR on CRF-R1 and CRF-R2 are likely different. Classically E acts through nuclear ERs that bind to E response elements (EREs) and stimulate gene transcription. The stimulatory effect of E was observed in the expression of CRF-R2 at the gene level, which was translated to the protein level. This was consistent with an action of activated ER acting as a transcription factor.

Interestingly, supplemental P treatment reversed the E-induced increase in CRF-R2 mRNA and protein in the dorsal and median raphe. When E stimulates gene expression, supplemental P administration can have different effects depending on the gene, the ratio of E/P achieved in the serum, and the isoforms of progestin receptor (PR) in the cell type. At the ratio of 1/50 typically achieved with our implants, P has been observed to block E -stimulated PR gene expression in the pituitary, but to have no effect on E-stimulated PR gene expression in the hypothalamus of the same animals (Bethea et al., 1996). This may be due to the differential prevalence of PR-A and PR-B in pituitary and brain (Bethea and Widmann, 1998). In this study, P was observed to block the effect of E on CRF-R2 gene and protein expression, and this may also be due to differential prevalence of the two PR isoforms across the extended raphe nuclei.

It should be noted that the probes for the Sybr Green real time PCR for CRF-R2 experiment would detect sCRFR2α and CRF-R2γ gene products as well as CRFR2α (sCRF-R2α). sCRF-R2α is a soluble slice variant of CRF-R2 that was identified and characterized in the mouse brain, and high levels of *sCRF-R2α* gene expression were reported in the olfactory bulb, cortex, and midbrain regions. The translated protein

includes the majority of the first extracellular domain encoded by CRF-R2α, but it is followed by a unique 38-aa hydrophilic C- terminus resulting from a frame shift produced by deletion of exon 6 that causes a conformational change such that secreted CRF-R2α protein is soluble. Thus, secreted CRF-R2α does not insert into the membrane, nor is it connected to downstream enzymatic machinery. Presumably, secreted sCRF-R2α binds CRF-related ligands and prevents activation of CRF receptors. In support of this theory, purified sCRF-R2α protein inhibits cellular responses to CRF and urocortin 1 (Chen et al., 2005b). Immunohistochemical studies using primary antiserum raised in rabbits immunized with a synthetic peptide fragment encoding the unique C-terminal tail (amino acids 113-143) of mouse sCRF-R2α indicate that raphe nuclei lacked sCRF-R2α-immunopositive cell bodies and fibers (Chen et al., 2005b). Because this study is aimed at regulation of CRF system components in the raphe serotonin system, we did not expect to see a significant effect of E on sCRF-R2α gene expression in the raphe-containing microdissected midbrains.

In future studies it would be possible to design primers that could determine the percentage of the CRF-R2 splice variants known to translate into mature receptors (CRF-R2α and CRF-R2γ) as well as, the percentage of CRF-R2 splice variants destined to become decoy receptors (sCRFR2α). This is because sCRFR2α is identical to CRFR2α with the exception of a deletion of exon 6. We could detect *CRF-R2α* and *CRF-R2γ* by designing primers for an amplicon spanning exon 6. In another assay, we could design primers corresponding to the splice junction of exons 5 and 7 to quantify abundance of *sCRF2α*.

We did not pursue the qRT-PCR to assess the effect of E ± P on *sCRFR2α* gene expression in our 3 groups of animals, largely because the report of this transcript in rodents appeared late in the investigation and the presence in monkey was not confirmed. We also did not attempt to identify mature sCRFR2α with immunohistochemical techniques because available evidence indicates that rodent raphe nuclei lack sCRF-R2α-immunopositive cell bodies and fibers (Chen et al., 2005b). One outcome of the E ± P -induced increase in CRF-R2 mRNA is an increase in overall expression of CRF-R2; the activation of which increases serotonin release by the raphe. If sCRF-R2α were highly expressed in the monkey raphe area, then an alternative outcome of the E ± P-induced increase in CRF-R2 mRNA could be an increase in the decoy receptor for CRF-R2, which would decrease activation of CRF-R2 and potentially decrease overall serotonin release. This scenario is unlikely since a decrease in serotonin was not observed with E±P treatment.

E increased CRF-BP gene expression in the raphe of ovariectomized monkeys.

CRF-BP expression may play a role in the pathogenesis of depression (Van Den Eede et al., 2005) and most evidence suggests that *CRF-BP* expression is regulated by acute stress . Therefore, we did not expect E or E + P to modulate CRF-BP expression because our animals are not stressed prior to necropsy. However, there are estrogen response element-half sites in the CRF-BP promoter (van de Stolpe et al., 2004), so it was important to verify whether E modulates CRF-BP expression in our model of ovarian hormone treatment after ovariectomy.

The E-induced upregulation of CRF-BP expression in the raphe was a novel finding. If the outcome of an E-induced increase in CRF-BP gene expression is translated to the functional protein level, then this could be a means whereby E prevents further activation of CRF-R1. A decrease in activation of CRF-R1 would increase serotonin release by the raphe, and this protective action of E merits further investigation.

Interestingly, supplemental P decreased CRF-BP expression in the microdissected raphe area of ovariectomized monkeys compared to OVX controls, and the mechanism whereby P reverses the effects of E on CRF-BP warrants further investigation.

In summary, E treatment had opposing effects on gene and protein expression of CRF-R1 and CRF-R2 in the raphe serotonin system, supporting the theory that E treatment promotes serotonin availability and increases access to stress-coping behavioral strategies. In addition to down regulating mature CRF-R1 expression in the raphe, E treatment also increased CRF-BP gene expression, which would prevent activation of CRF-R1, further enhancing serotonin availability.

Chapter 5: The effect of estradiol and progesterone on UCN1 expression in the monkey midbrain

5.1 Introduction

The three other identified neuropeptidergic ligands in the CRF system are urocortin 1 (UCN1), urocortin 2 (UCN2), and urocortin 3 (UCN3). Central production of UCN2 and UCN3 is predominantly in the PVN of the hypothalamus (Reyes et al., 2001; Li et al., 2002), whereas central production of UCN1 is primarily in perioculomotor urocortin population ($pIII_U$) (Ryabinin et al., 2005). UCN1 fibers innervate the primate dorsal raphe nucleus, and evidence suggests that once released into the raphe, UCN1 binds CRF-R1 and CRF-R2 to regulate serotonin neurotransmission (Pernar et al., 2004). In the past ten years, much work has been done to elucidate the unique physiological roles of UCN1, and some of this work (as it pertains to the dorsal raphe) is discussed below. UCN2 and UCN3 were isolated in humans and rats within the last five years, and less is known about the full extent of their physiological functions.

In rodents, ethanol consumption selectively activates UCN1-expressing neurons of the $pIII_u$, and several exposures to ethanol significantly increase CRF-R2 binding in the dorsal raphe (Weitemier and Ryabinin, 2005). Notably, the UCN1-positive innervation to raphe activates ethanol-induced hypothermia (Bachtell et all, 2004;Weitemier and Ryabinin, 2006), and it is thought that UCN1 binds CRF-R2 to mediate this particular behavior. One study attempted to prove that CRF-R2 is necessary for this behavior by measuring ethanol-induced hypothermia in CRF-R2 knockouts and wild-type mice. Surprisingly, the authors reported that CRF-R2 knockouts did not differ from wild-type

mice in sensitivity to hypothermia and several other ethanol-associated behaviors. They suggested that future studies focusing on the role of CRF-R2 in ethanol-associated behaviors should use mice that are stressed or in withdrawal from alcohol (Sharpe et al., 2005), and this merits further investigation. The authors' main interpretation of the lack of phenotype in CRF-R2 knockouts was developmental compensation in these mice.

It is also believed that endogenous UCN1 modulates food consumption because centrally injected UCN1 reduces food consumption, presumably by acting via CRF-R2 (Cullen et al., 2001; Martinez et al., 2004). UCN1 injected directly into the dorsal raphe reduces overnight eating and weight gain in mice (Weitemier and Ryabinin, 2006).

Recent evidence suggests that central UCN2 and UCN3 release may also modulate feeding behaviors, among them cancer cachexia and anorexia (Fekete et al., 2006; Kamdi et al., 2009; Thammacharoen et al., 2009). One such stimulus for hypothalamic UCN2 and UCN3 release is intracerebroventricular injection (icv) of parathyroid hormone-related protein, a protein produced by many tumors (Asakawa et al., 2010). The mechanisms by which UCN2 and UCN3 regulate the downstream effects of cachexia are less clear, but evidence suggests that UCN3-mediated CRF-R2 excitation in the ventromedial hypothalamus modulates feeding behaviors and blood glucose levels in rats through a downstream mechanism involving the melanocortin system (Chen et al., 2005a). A new role for UCN3 is emerging as a neuromodulator linking stress-induced anxiety and energy homeostasis (Jamieson et al., 2006; Kuperman et

al., 2010). In support of this newly emerging role of UCN3, Wittmann et al. report that fibers immunoreactive for both UCN3 and Thyrotropin Releasing Hormone densely innervate brain areas that coordinate feeding and behavioral responses to stress, such as the ventromedial hypothalamic nucleus, the lateral septal nucleus, the posterior bed nucleus of the stria terminalis, the medial amygdalaoid nucleus, the ventral hippocampus, and forebrain areas associated with psychosocial stress and anxiety (Wittmann et al., 2009).

In light of the diverse physiological responses mediated by the urocortins, we sought to determine whether ovarian hormones affect the expression of the urocortins in the midbrain. There is evidence that E positively regulates urocortin 1 gene expression in PC 12 cells transfected with the human UCN promoter via ERα and negatively regulates the human UCN promoter via ERβ (Haeger et al., 2006). In our model, CRF input to the dorsal raphe was decreased with E ± P administration. Because CRF and UCN1 are thought to have opposing actions on the raphe serotonin system (Valentino and Commons, 2005; Waselus et al., 2009), we predicted that E and P treatments would increase UCN1 gene expression in the midbrain block of E±P treated monkeys compared to OVX placebo-treated controls. The primary site of UCN1 production in the monkey and human brains spans an area roughly 2 to 4 mm rostral to the dorsal raphe serotonin system. Because of the close proximity of the $pIII_U$ to the dorsal raphe, we expected to detect a difference in UCN1 mRNA expression between the groups when we performed qRT-PCR on the microdissected raphe area of the ovariectomized placebo-, E-, and E+P- treated animals. In the Sybr Green real time PCR experiments,

we used the microdissected raphe area described in the **General Methods chapter**. In the TaqMan real-time PCR experiment, we isolated RNA from a larger-sized hemi midbrain block that contained more of the $pIII_U$ than the block used in the Sybr Green experiment. We predicted that E and P treatments would increase UCN1 gene expression in these midbrain blocks of ovariectomized monkeys compared to placebo-treated controls.

Although the literature indicates that UCN2 and UCN3 are not highly expressed in the dorsal raphe-containing midbrain block, it was important to examine the expression of these ligands in RNA isolated from the microdissected raphe area of our animals. We used qRT-PCR to assess whether E ± P regulated UCN2 or UCN3 expression in the raphe area of ovariectomized macaques.

5.2 Experiments

Experiment H. *Sybr Green real-time PCR quantifying UCN1, UCN2, and UCN3 in the microdissected raphe area*.

Methods: We hypothesized that E and E+P treatment would increase the abundance of UCN1 in the raphe area of ovariectomized macaques. We used qRT-PCR on the microdissected raphe area collected from 9 monkeys (n=3/group) perfused with RNAlater. Forward and reverse primers were designed from the human sequence of UCN1, UCN2, and UCN3 and qRT-PCR was conducted with the Dynamo Sybr Green

qPCR Mix. **Table 5** includes the primer sequences and gene accession IDs of UCN1, UCN2, and UCN3 used for real time Sybr Green PCR quantification. The primers amplified a 174-bp segment, a 188-bp segment, and a 174-bp segment, respectively, within their corresponding gene sequences.

A standard curve was generated using a pool of rhesus tissues and the slope of the curve was used to calculate the relative pg of UCN1, UCN2, and UCN3 transcript in the total RNA from each animal's midbrain. Then, the ratio of UCN/GAPDH was calculated to determine relative abundance of UCN1, UCN2, and UCN3 in the microdissected raphe -containing area. Finally, the ratio was normalized to the OVX control group.

Results: The results from the Sybr Green real time PCR experiment are illustrated in **Figure 28**. When levels of *UCN1, UCN2,* and *UCN3* cDNA were corrected to GAPDH and normalized to the OVX group, E±P had no significant effect on UCN1, UCN2, or UCN3 production although the E animals showed a trend toward increased expression of UCN1 mRNA compared to the placebo-treated controls, these effects were not significant. In a separate experiment, a TaqMan custom expression array was used to assess UCN1, UCN2, and UCN3 expression in the hemi-midbrain of OVX-, E-, and E+P-treated animals (**Figure 29**). We found that administration of E significantly increased the relative abundance of UCN1 in the hemi-midbrain block of ovariectomized macaques compared to placebo-treated control animals, and supplemental P decreased UCN1 gene expression compared to controls. There was no apparent regulation of UCN2, but E and E+P treatment significantly decreased UCN3 compared

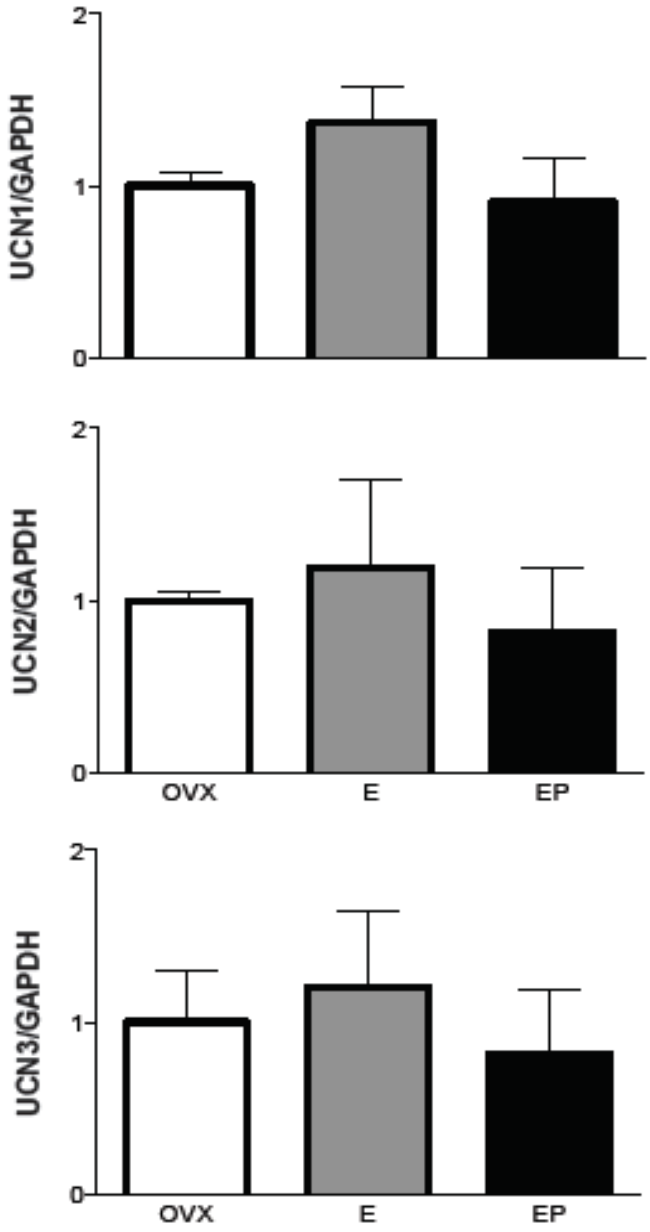

Figure 28. Histograms representing the relative abundance of *UCN1, UCN2,* and *UCN3* in RNA extracted from the microdissected raphe area of OVX female monkeys treated with placebo, E, or E+P for 1 month (n=3 animals/group). E treatment increased expression of *UCN1* compared to the OVX control group, but this difference was not significant. *UCN2* mRNA and *UCN3* mRNA did not appear to be regulated by E or E+P treatments.

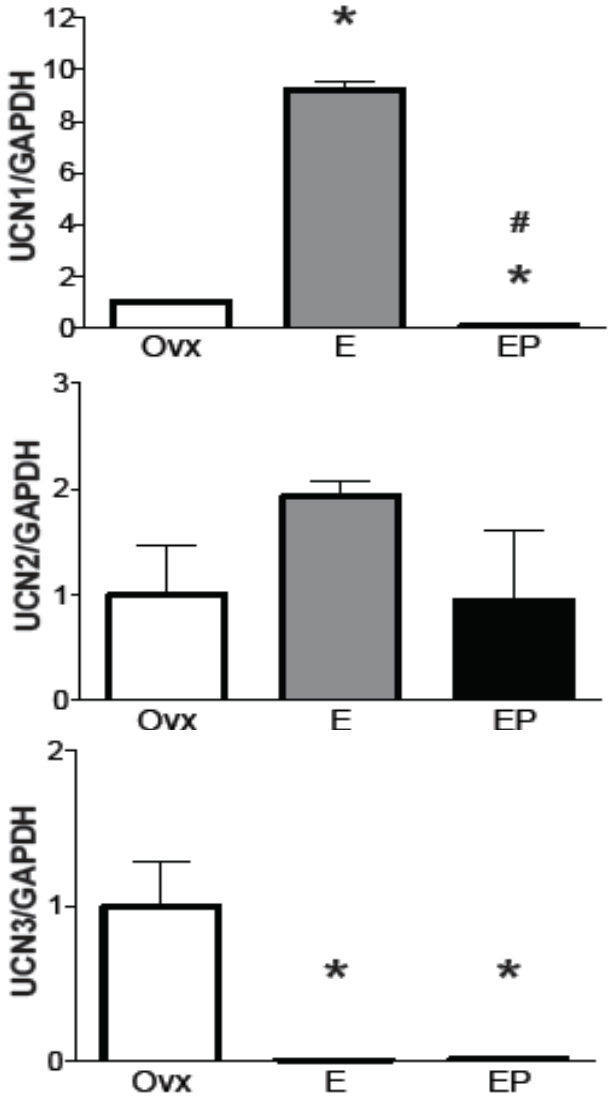

Figure 29. Histograms representing the relative abundance of *UCNs* in RNA extracted from the hemi-midbrain block from three groups of animals (n=4 animals/group). E treatment increased while E+P treatment decreased *UCN1* compared to the OVX control group. E and E+P also significantly decreased *UCN3* expression compared to the control group. The asterisks represent a significant difference from the control group by Student-Neuman-Keuls post-hoc comparison with $p<0.05$.

to controls. Thus, larger hemi-midbrain blocks likely contained more of the $pIII_U$ than the coronal midbrain blocks and it was possible to detect a consistent increase in UCN1 with the better representation of $pIII_U$.

Experiment I. *Immunohistochemistry (IHC) experiment to identify and quantify UCN1-positive cells and pixels in the perioculomotor urocortin population ($pIII_U$).*

Methods: To assess whether E ± P treatments increase mature UCN1 protein expression at the primary site of production within the perioculomotor region, eight sections of the $pIII_U$ at 250 µm intervals from monkeys in each treatment group (n=5/group) were immunostained using an antibody against human UCN1. The primary antibody was made against the C-terminal of human UCN1 (Sigma No. U4757); the immunogen sequence corresponds to pro-urocortin (amino acids 105-120) and is identical in rat urocortin. The number of detectable UCN1-positive neurons were counted and the immunostained UCN1-positive pixel area was quantified with a Marianas Stereology Workstation and Slidebook 4.2. The total area analyzed was recorded to ensure that it did not vary between animals during the analysis. Results are expressed as total number of UCN1-positive neurons and percent UCN1-positive pixels, which were computed by dividing the number of UCN1-positive pixels by the total number of pixels in the area analyzed.

Results: The UCN1 antibody used in this experiment has been well characterized in monkey tissue and matches previously reported morphological maps of the UCN1-

positive neurons in the monkey. The levels of $pIII_U$ analyzed represent the most caudal portions of the urocortin-positive neurons of the $pIII_U$. **Figure 30-B** depicts four of the eight serial sections that were analyzed, and **Figure 30-A** shows the corresponding anatomical levels of UCN1-positive neurons in a diagram of the monkey perioculomotor region. **Figure 31** depicts a high magnification image of the rhesus monkey $pIII_U$ immunostained with the UCN1 antibody. **Figure 32** depicts representative montages of the $pIII_U$ from placebo-, E-, and E+P-treated ovariectomized animals and it appears that UCN1 immunosignal was increased with E±P. When we counted UCN1 positive cells across 8 levels of the $pIII_U$ (serial cross-sections spanning about 2 mm, immediately rostral to the dorsal raphe), we found that animals in the E and E+P groups had significantly more UCN1-positive cells in the $pIII_U$ compared to the OVX control animals. As illustrated in **Figure 33-A** and **33-B**, administration of E and E+P caused a significant increase in the number of detectable UCN1-positive cells in seven of eight of the representative perioculomotor levels analyzed compared to OVX control animals (ANOVAs range $p < 0.0025$ to 0.038; error bars are omitted for clarity) . When the levels were combined, there was an overall increase in the average number of UCN1-positive neurons with administration of E and E+P compared to placebo-treated controls (ANOVA $p< 0.0029$). Likewise, as illustrated in **Figure 33-C** and **33-D**, E and E+P also significantly increased the percent of UCN1-positive pixels in the perioculomotor region in all eight levels analyzed (ANOVAs range $p < 0.0001$ to 0.037; error bars are omitted for clarity). There was an overall increase in the mean percent of UCN1-positive pixels with administration of E and E+P compared to OVX controls (ANOVA $p < 0.0001$).

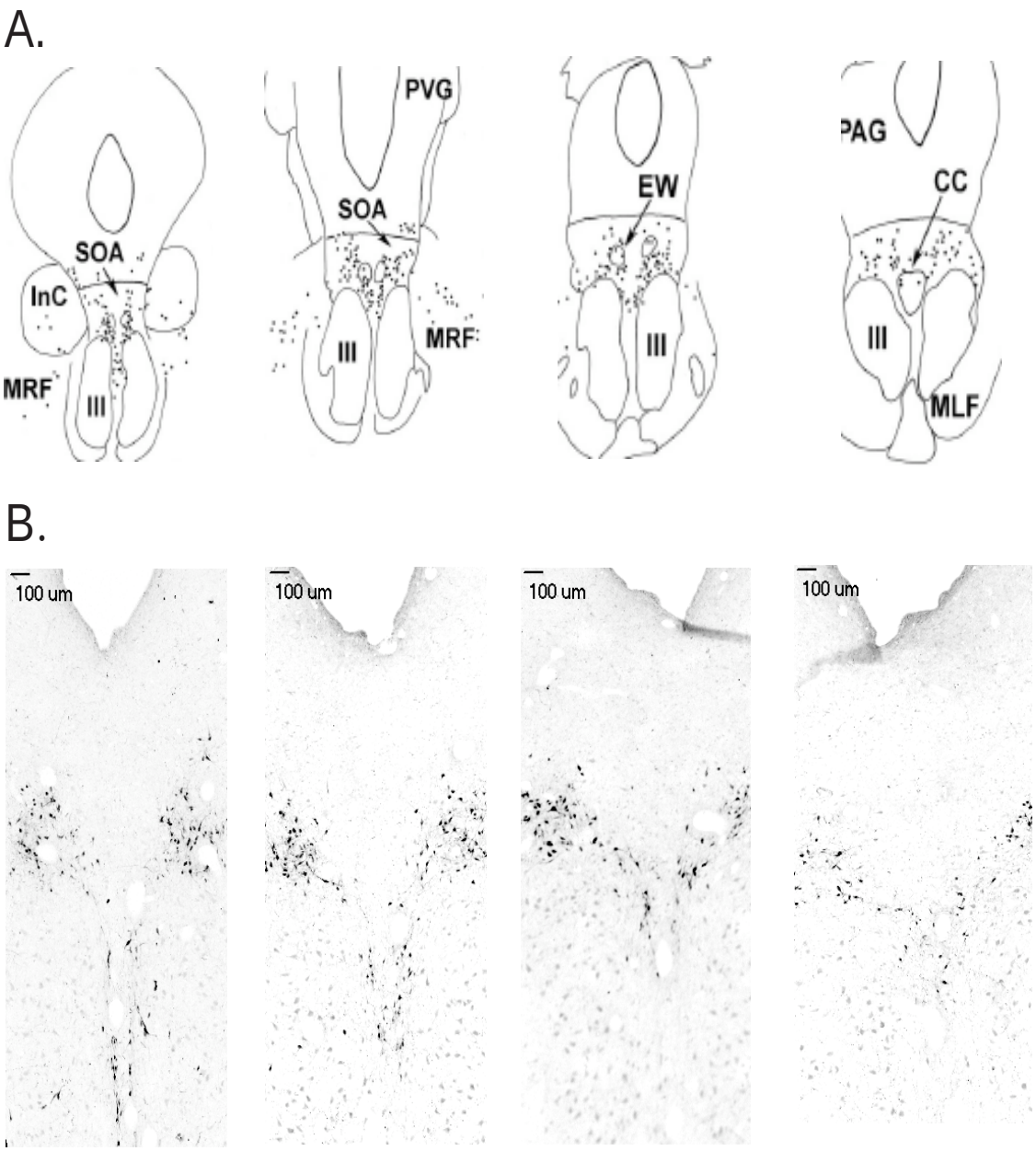

Figure 30. Anatomy of urocortin 1- (UCN1) immunopositive cells in the non-preganglionic Edinger Westphal nucleus of the monkey. **A**. Rostral to caudal charting of the distribution of UCN1-positive neurons in the monkey perioculomotor region reprinted from May et al. (2008) with permission from John Wiley and Sons. **B**. Rostral to caudal serial montages from an E+P-treated immunostained with an antibody raised in rabbit against amino acids 25-40 of the human UCN1 peptide. Each serial montage is 500 μm caudal to the previous montage.

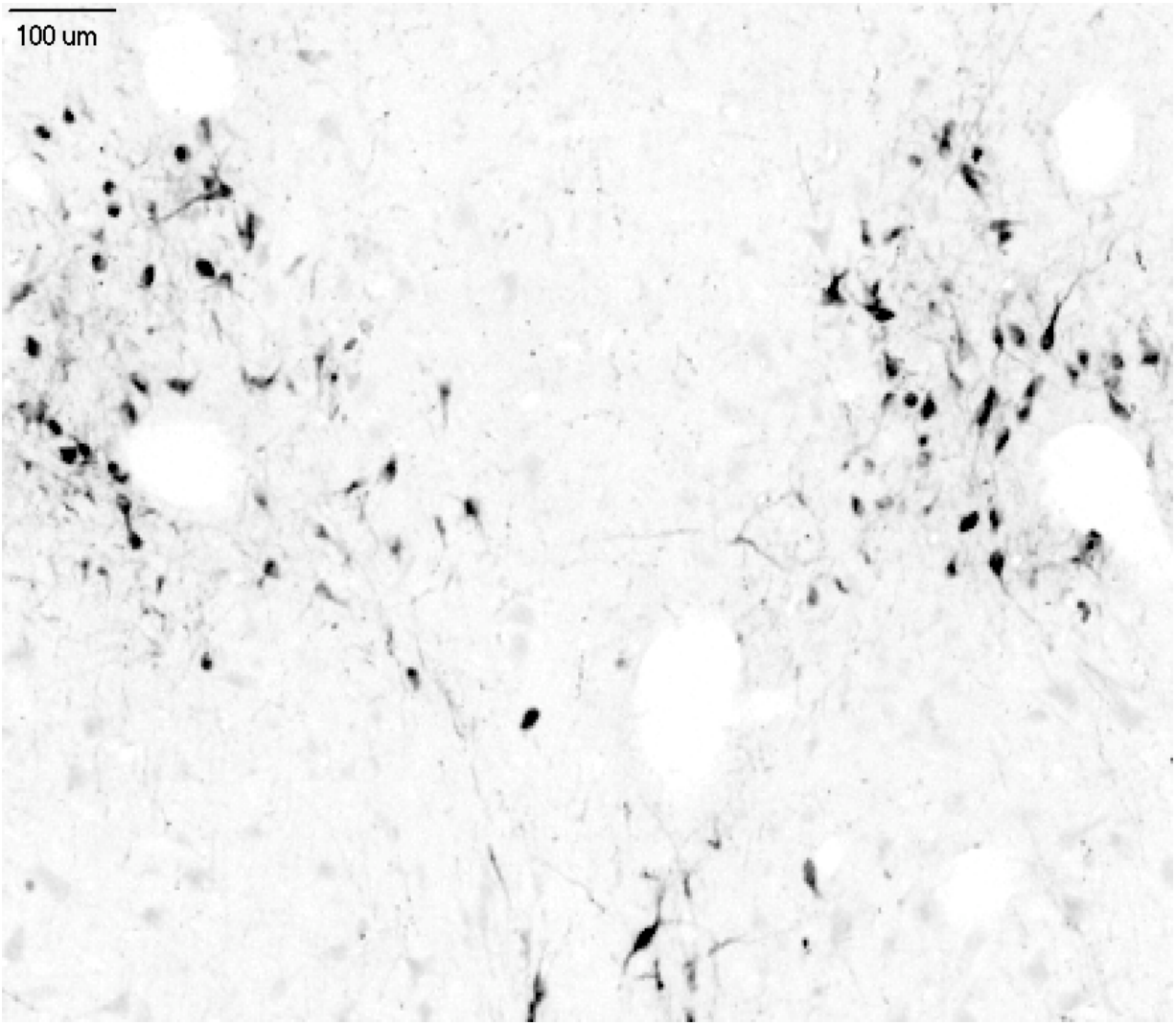

UCN1

Figure 31. High magnification image of UCN1-positive neurons in the monkey perioculomotor region, located about 1 mm rostral to the serial dorsal raphe sections.

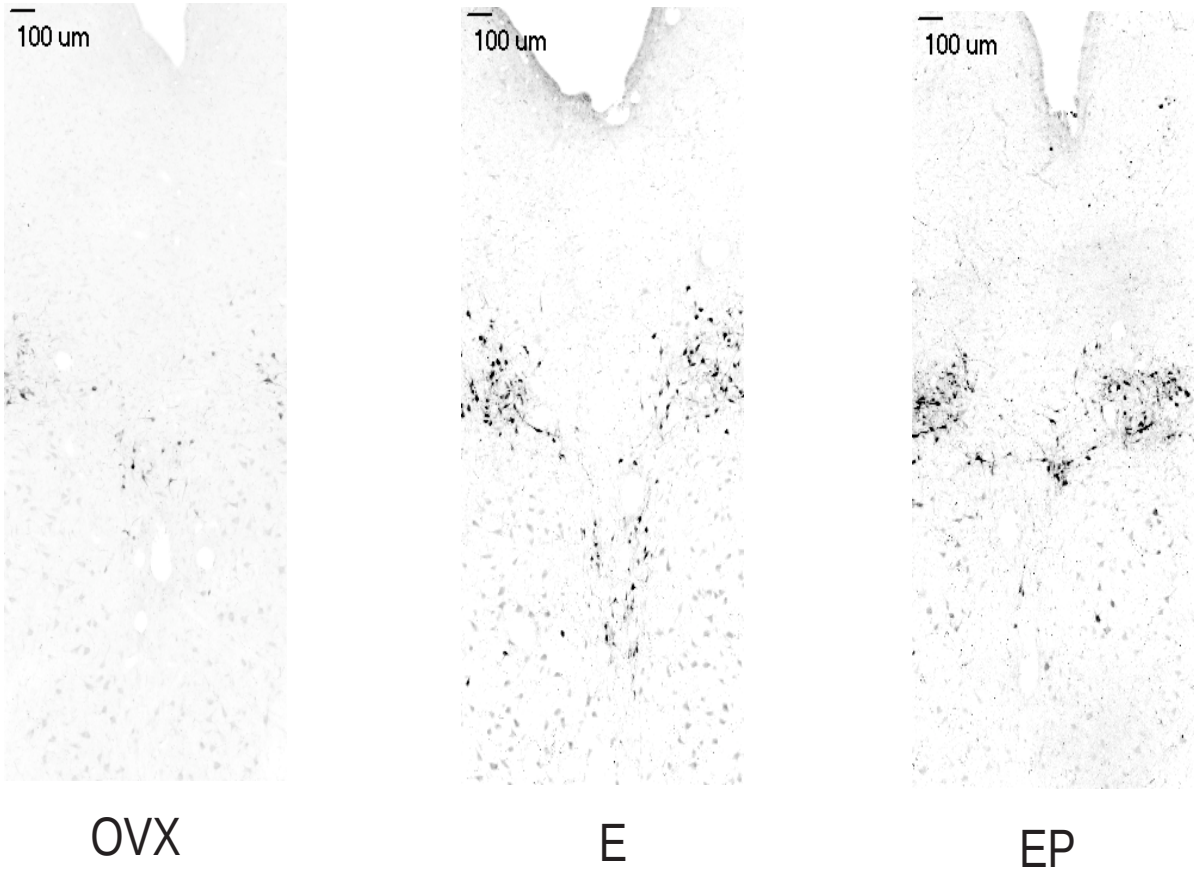

Figure 32. Effects of ovarian steroids on urocortin 1-positive neurons in the monkey perioculomotor region. Representative montages of monkey perioculomotor region immunostained with anti-human UCN1 from an OVX placebo-treated control animal, an E-treated animal, and an E+P-treated animal.

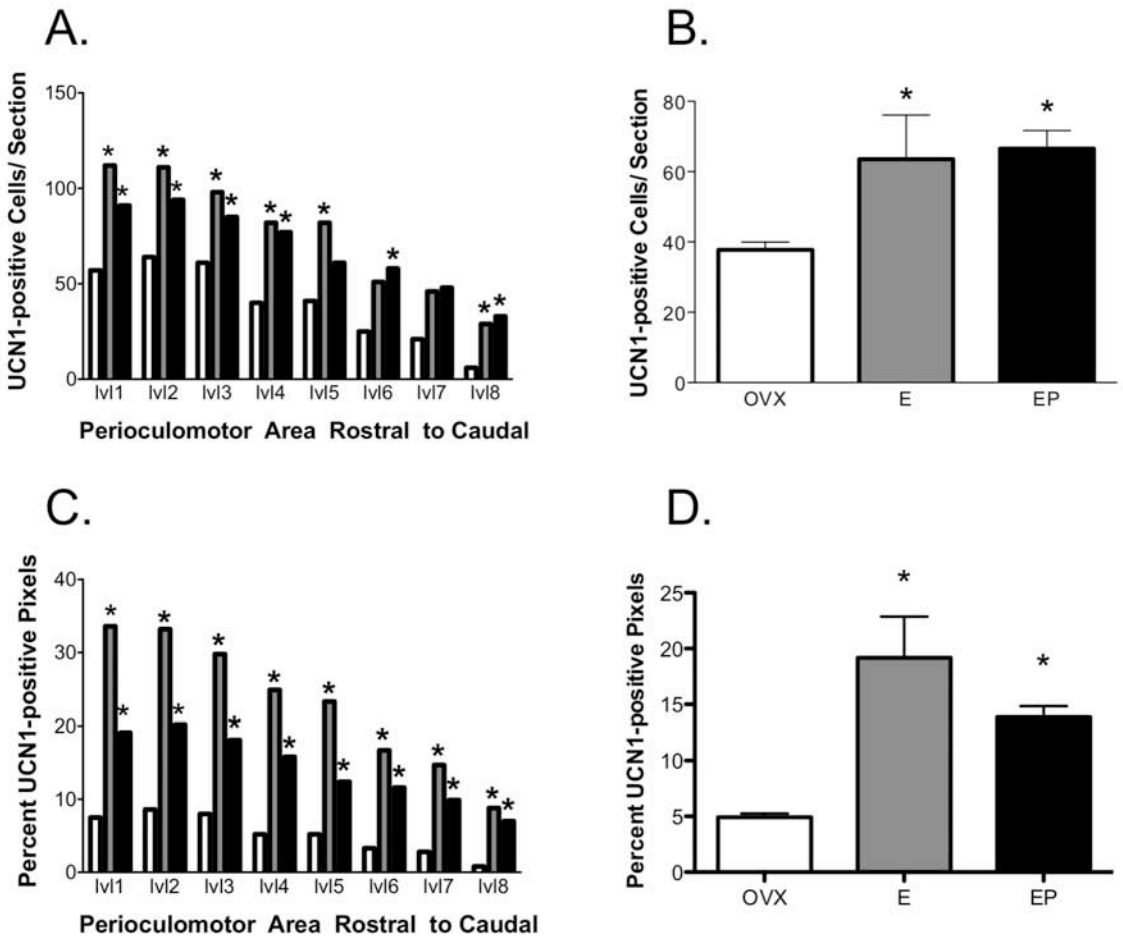

Figure 33. Histograms representing the number of UCN1-positive neurons and percent UCN1-positive pixels within the perioculomotor region in ea ch treatment group (n=5/group). **A**. E or E+P significantly increased the number of UCN1-positive neurons in seven of e ight levels analyzed. **B**. When the levels were combined, E and E+P significantly increased the mean number of UCN1-positive neurons per section compared to p lacebo-treated controls. **C**. E and E+P also significantly increased the percent of UCN1-positive pixels in the perioculomotor region in all eight levels analyzed. **D**. When the levels were combined, E and E+P significantly increased the mean percent of UCN1-positive pixels compared to placebo-treated controls. The asterisk represents a significant difference from the co ntrol group by Student-Neuman-Kuels post hoc comparison with $p<0.05$.

Experiment J. *Double immunohistochemistry for UCN1 and nuclear ERβ.*

Methods: Our results indicate that E±P increased UCN1 in monkey midbrain. Previous studies found that estrogen regulates *UCN1* gene expression in PC 12 cells (Haeger et al., 2006), and that mouse UCN1-positive neurons co-label for nuclear estrogen receptor beta (ERβ). Therefore, we predicted that UCN1-positive neurons in the monkey would also be positive for ERβ. To determine whether monkey UCN1-positive neurons in the perioculomotor area were positive for nuclear ERβ, we double immunostained sections from an E + P-treated animal with an antibody made in mouse against human ERβ IgG (mouse monoclonal, 1:100, Serotec) and the rabbit anti-human UCN1 antibody.

Results: Figure 34 depicts neurons in the perioculomotor area of an E+P-treated ovariectomized monkey double labeled for UCN1 and ERβ. The UCN1-positive immunostain is conjugated to DAB and appears as a reddish-brown precipitate that fills the cytoplasm of the neuron. In contrast, the anti- ERβ immunostain is conjugated to Nickel and DAB and it appears as a purple stain that fills the nucleus of the neuron. The neuron pictured in the right panel of **figure 34** is co-labeled for UCN1 and nuclear ERβ. The result of this double immunohistochemistry experiment implies that gene and protein expression of UCN1 in the perioculomotor UCN1-positive neuron population could be directly regulated by E via ERβ.

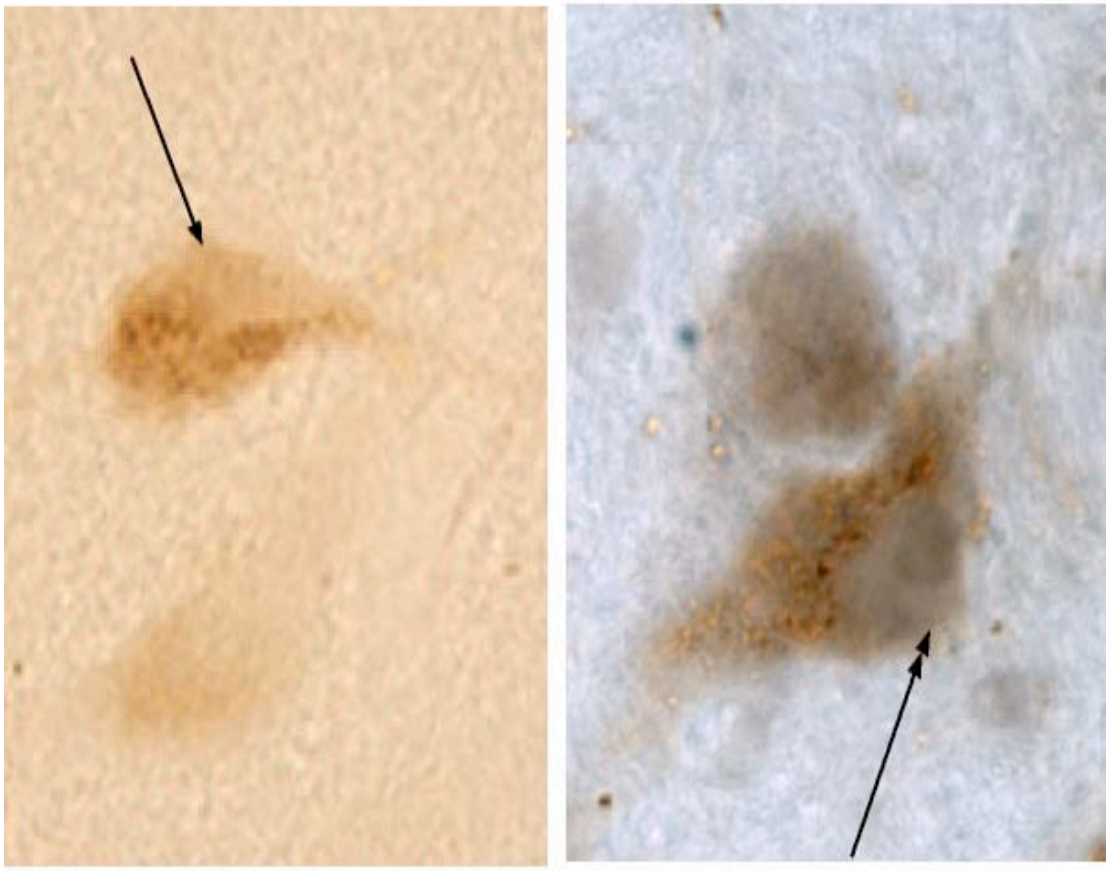

Figure 34. Neurons in the perioculomotor region of an E+P-treated animal double immunostained with antibodies against human UCN1 and nuclear estrogen receptor beta (ERβ). **Left.** Neuron immunostained with the anti-UCN1 antibody, visualized with a reddish-brown precipitate. The single headed arrow depicts the ERβ-negative nucleus. **Right**. Neurons double immunostained with anti-UCN1 and anti-ERβ. The immunostain against human ERβ appears purple and fills the nucleus (double headed arrow), while the reddish-brown anti-UCN1 signal fills the neuronal cell body and cytoplasm.

Experiment K. *Immunochistochemistry (IHC) experiment identifying and quantifying UCN1-positive fibers in caudal linear raphe nucleus*.

Methods: To verify that the E-induced increase in *UCN1* gene and protein expression in the $pIII_U$ was translated to increased UCN1 input to the raphe, we used IHC to identify and quantify UCN1 fibers in the caudal linear raphe nucleus. The caudal linear raphe nucleus contains the most rostral group of serotonin neurons and it exhibited a consistent UCN1 fiber plexus that was amenable to measurement. Three levels of the caudal linear raphe from animals in each treatment group (n=5/group) were immunostained with an antibody against human UCN1. The anti-UCN1 immunostain appeared as beaded varicosities throughout the three serial sections (each 250 μm apart) of the dorsal raphe nucleus. These levels spanned approximately 750 um of the rostral raphe area. A 10X montage of the raphe was constructed and the UCN1-positive pixels were segmented and quantified. **Figure 35** depicts a representative stereology montage of the caudal linear raphe nucleus immunostained with anti-UCN1 and segmented with Slidebook 4.2. The total area analyzed was recorded to ensure that it did not vary between animals during the analysis. Results are expressed in percent UCN1-positive pixels, which were computed by dividing the number of UCN1-positive pixels by the total number of pixels in the area analyzed.

Results: The greatest amount of UCN1-positive fiber staining was in the rostral raphe in a region spanning of approximately 750 μm. We analyzed three levels of the caudal linear raphe nucleus for each animal in the three treatment groups (n=5/group). As

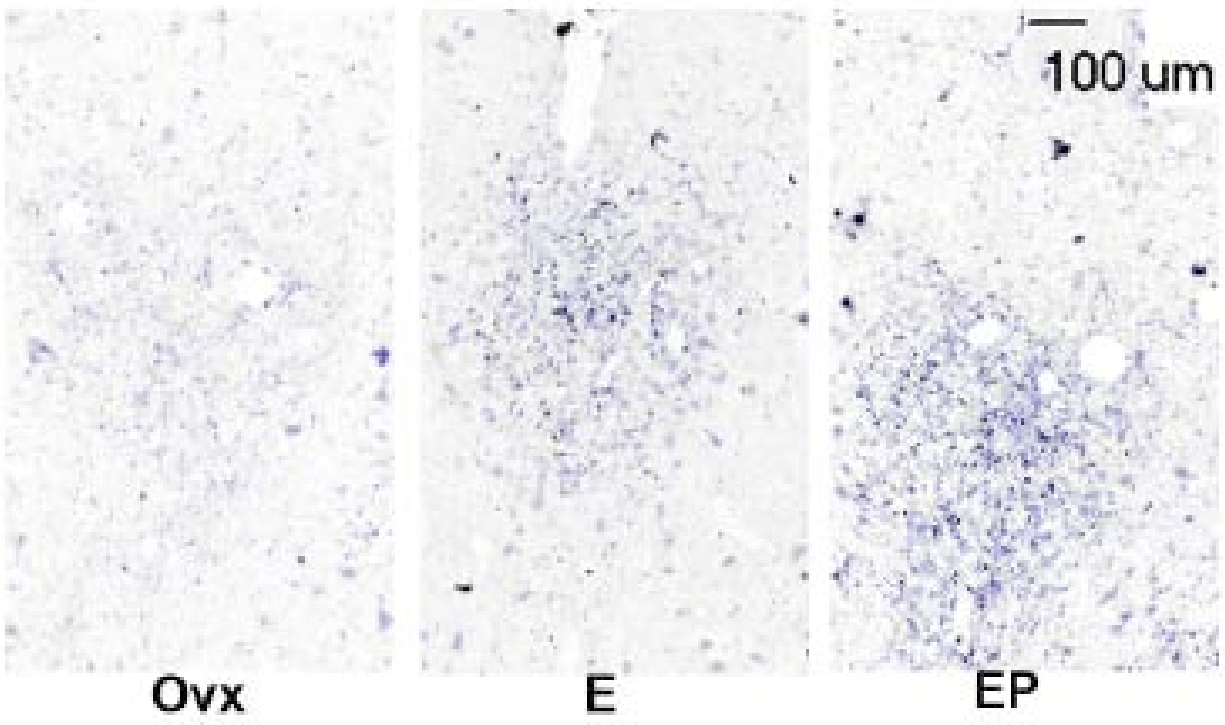

Figure 35. Effects of ovarian steroids on UCN1-positive fibers in the caudal linear raphe nucleus. Montages of UCN1-positive fibers in representative OVX- (control), E-, and E+ P- treated animals after segmentation.

illustrated in **Figure 36**, E or E+P significantly increased the percent of CRF-positive pixels in the caudal linear raphe nucleus at all three levels (ANOVAs range $p < 0.0034$ to 0.0097; error bars are omitted for clarity). When the levels were combined, there was an overall increase in the mean percent positive pixel area per level with administration of E and E+P compared to placebo-treated controls (ANOVA $p < 0.0001$). Thus, E and E + P treatments significantly increased UCN1-positive fibers in the rostral raphe of ovariectomized monkeys.

5.3 Discussion

E alone increased UCN1 expression and P blocked this action at the gene level, but at the protein level there was an increase in UCN1-immunopositive neurons in the perioculomotor region and an increase in fiber density rostral to the raphe nuclei with E and E+P. We cannot explain the disconnection between gene and protein expression with supplemental P. However, because E increased UCN1, we believe this effect is mediated by the classical genomic action of ER. Our colocalization data indicate that part of the action of E was through nuclear ERβ. UCN1 co-localizes with CART (Kozicz, 2003) and we previously detected PR in the same population of UCN1/CART neurons (Lima et al., 2008). Hence, UCN1 neurons have nuclear ERβ and PR, indicating they are direct targets of ovarian steroids.

These data support the notion that ovarian steroids increase serotonin neural function in part by increasing UCN1 gene expression and transportation into the dorsal

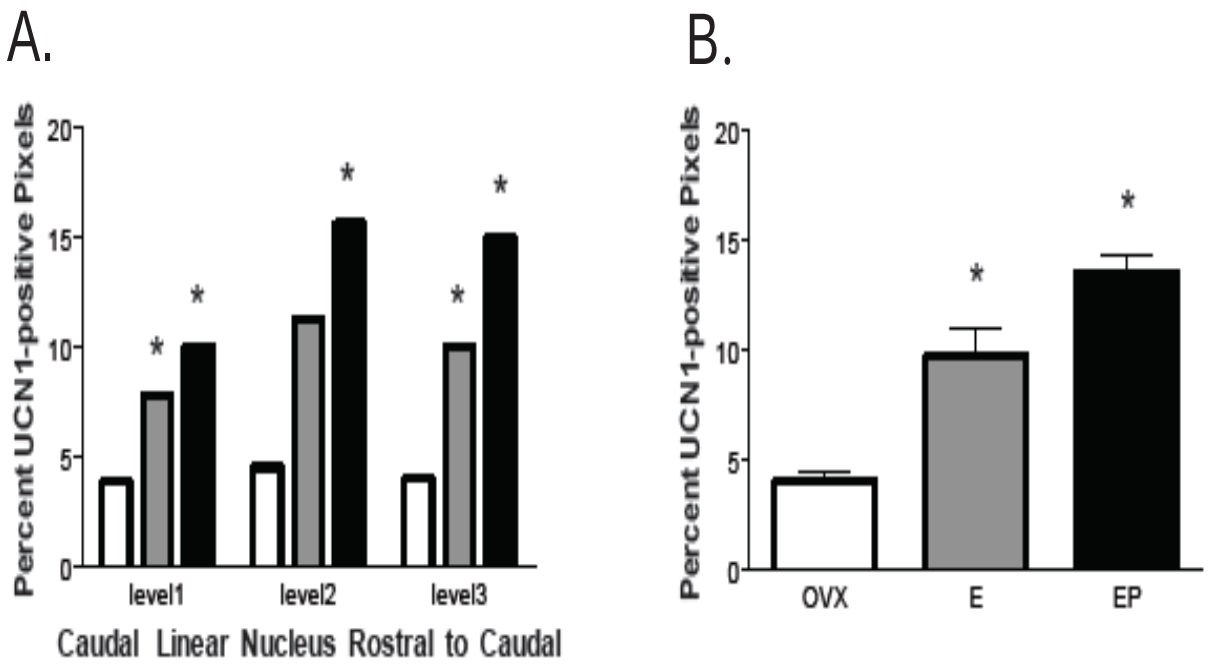

Figure 36. Histograms representing the percent of UCN1-positive pixels within the caudal linear nucleus for the animals in each treatment group (n=5/group). **A**. E or E+ P significantly increased the percent of CRF-positive pixels in the caudal linear raphe nucleus at all three levels. **B**. When caudal linear raphe levels were combined, E and E+P significantly increased the percent of UCN1-positive pixels compared to OVX placebo-treated controls. The asterisks represent a significant difference from the control group by Student-Neuman-Kuels post-hoc comparison with $p<0.05$.

raphe serotonin system and thereby increasing activation of CRF-R2. An increase in serotonin function would elevate mood, increase stress resilience and decrease anxiety. In addition, the E-induced increase in UCN1-input to the raphe may confer protection against hypothermia during stress or alcohol withdrawal because UCN1-positve fibers mediate ethanol-induced hypothermia.

Examination of gene expression for the urocortins indicated that *UCN1* was the predominant transcript in the midbrain and that it was increased by E treatment. The expression of *UCN2* did not appear to be regulated by one month of E or E+P treatment. We were surprised to find that E and E+P treatment significantly decreased overall gene expression *UCN3* compared to controls. This is noteworthy in light of the recent studies indicating that the primary role of UCN3 is as neuromodulator linking stress-induced anxiety and energy homeostasis (Jamieson et al., 2006; Kuperman et al., 2010). This is also surprising because E treatment increases anorexic feeding behaviors, but the E-induced decrease in *UCN3* expression seen here would seem to have the opposite effect. Thus, the finding that one month of E and E+P treatment decrease *UCN3* gene expression merits further mechanistic investigation.

Chapter 6: Discussion

6.1 General Background

During and after menopause a significant number of women report an increase in anxiety and vulnerability to stress (Maki et al., Conde et al., 2006, Heikkinen et al., 2006, Tangen and Mykletun, 2008). Both the CRF and serotonin systems respond to stress and play roles in depression and anxiety disorders (Mann et al., 1996, Holsboer, 1999, Keck and Holsboer, 2001, Arango et al., 2002). Moreover, increasing evidence suggests that their function is inextricably linked. In humans, CRF terminals appose serotonin neurons in the raphe region (Ruggiero et al., 1999), and a postmortem study reported that patients with major depressive disorder had significantly more CRH-positive neurons in the PVN than normal controls (Raadsheer et al., 1994). Antidepressant SSRIs that increase available serotonin reduce the sensitivity of CRF neurons in the PVN (Stout et al., 2002b), and cortisol levels return to normal in depressed patients treated with a variety of antidepressants (Himmerich et al., 2006, Schule et al., 2006). Moreover, repeated citalopram treatment decreased CRF and HPA axis activity in rodents (Moncek et al., 2003). We recently found that 15 weeks of citalopram administration decreased CRF fiber density in the dorsal raphe of stress-sensitive monkeys (Weissheimer et al., 2009).

The impact of ovarian steroids on mental function is of significant importance to women as they transition through menopause. Women without a uterus may be prescribed a formulation of estrogen, whereas women with a uterus may be prescribed

a formulation of estrogen supplemented with progestin to prevent uterine hypertrophy. Therefore, we applied a paradigm in which ovariectomized monkeys are used as a model of surgical menopause and groups treated with placebo, estradiol alone or estradiol supplemented with progesterone were compared.

In the absence of hormone therapy, postmenopausal women exhibit higher release of ACTH and cortisol when administered a challenge of dexamethasone plus CRF (Kudielka et al., 1999) suggesting that their CRF system may be hyperactive. In animal models, the effects of ovarian steroids on the HPA axis are complex. Several studies initially indicated that treatment of ovariectomized female or male rats with estrogen increased CRF (Li et al., 2003, Lund et al., 2004). Subsequently, it was recognized that acute E treatment increases CRF, but low dose chronic E treatment decreased CRH in a stressed rodent model (Dayas et al., 2000). Likewise, 5 days of E treatment to ovariectomized macaques prevented the elevation in cortisol induced by i.c.v. administration of interleukin 1-alpha (Xia-Zhang et al., 1995), and we found that chronic hormone replacement in ovariectomized monkeys decreased CRF mRNA and protein in the PVN (Bethea and Centeno, 2008).

However, CRF expression is widespread in the brain and within the limbic system there is evidence that the CRF system modulates behavioral traits such as locomotor activity, sleep, addictive behavior and in particular, anxiety related behavior (Dunn and Berridge, 1990, Liebsch et al., 1995). Indeed, we found that in stress-sensitive macaques, CRF mRNA was elevated in the subthalamic nucleus as well as the PVN,

and that CRF fiber density was greater in the central nucleus of the amygdala compared to stress-resilient macaques (Centeno et al., 2007) .

The knowledge of CRF innervation of the serotonergic raphe nuclei (Sakanaka et al., 1987, Ruggiero et al., 1999) coupled with the detection of CRF receptors in the raphe (Chalmers et al., 1995, Van Pett et al., 2000) forged the link between the CRF and serotonin systems. Subsequently, the opposing effects of CRF and UCN on serotonin were established in rodents. Administration of CRF directly into the DRN inhibits serotonergic activity, and CRF-R1 antagonists block this effect (Denihan et al., 2000). Conversely, the stimulatory effect of UCN and CRF-R2 is supported by increased 5-HT efflux in the basolateral amygdala (a projection region of the DRN) with intra-DRN administration of the CRF-R2 agonist, UCN2. This effect was completely blocked by antisauvagine-30 (ASV-30), a relatively selective CRF-R2 antagonist (Amat et al., 2004).

6.2 The effect of ovarian steroids on CRF innervation of the dorsal raphe

This study in monkeys shows that E±P decreased CRF fiber density in the dorsal, interfascicular and median raphe suggesting that CRF transport to the serotonin system is lower in the presence of ovarian steroids. The origin of the CRF fibers in the raphe nuclei is likely the PVN, but it is premature to rule out other areas of origin given the expression of CRF in amygdala and subthalamic nuclei. Previous work also traced CRF terminals in the raphe to cell bodies in the dorsolaterial tegmental field (Sakai et al., 1977). These data raise the question of whether the CRF cell bodies contain any form

of estrogen receptors, and/or whether CRF neurons may differ in their expression of receptors from region to region? One study reported ERα in CRF neurons in human hypothalamus (Bao et al., 2005). A recent report in rodents showed that ERα agonists activate c-fos expression in CRF neurons of the PVN to decrease feeding behaviors (Thammacharoen et al., 2009). Also in rodents, Laflamme et al (Laflamme et al., 1998) reported that non-neuroendocrine CRF neurons in the caudal PVN expressed ERβ [these neurons project to the raphe (Luiten et al., 1985, Portillo et al., 1998)]. However, few neuroendocrine CRF neurons in the medial PVN expressed ERβ [project to the median eminence and regulate ACTH]. This means that in the rodent, local, non-neuroendocrine CRF-positive neurons that project to raphe and presumably regulate serotonin release may be differentially modulated by estrogen than their neighboring neuroendocrine counterparts. This has important implications because it provides an avenue where estrogen can modulate behavioral responses to stress but have no effect on the hypothalamic-pituitary-adrenal response to stress. Nonetheless, whether CRF neurons in the PVN contain ERα or ERβ or whether there are differences in the steroid receptor compliment of CRF neurons between species has not been adequately resolved.

In addition, the mechanism of action of estrogen on CRF gene expression in the hypothalamus is not well understood because the CRF gene lacks a classical palindromic ERE site. *In vitro* studies in HeLA cells suggested that agonist mediated ERβ and ERα activation of CRF transcription requires protein/protein interaction with other transcription factors and associated complexes, and is mediated through a cAMP

regulatory element (Miller et al., 2004; Ni and Nicholson, 2006). Lalmansingh and Uht reported increased levels of CRF mRNA in an amygdaloid cell line after 1 minute of estrogen treatment, suggesting CRF behaves as an immediate early gene (Lalmansingh and Uht, 2008). CRF mRNA peaked at 3 minutes after estradiol treatment in amygdaloid cells, returned to baseline, and then increased again at 60 minutes after estradiol treatment. The results of Lalmansingh and Uht suggest that ERα and ERβ associate with different proteins to activate the cAMP regulatory element regulating CRF mRNA expression, and that the ERα- and ERβ -activation of CRF gene expression may occur at temporally distinct time points. Ogura et al. demonstrated that ERβ agonists stimulated gene transcription of CRF in hypothalamic cells, which are known to express dramatically more ERβ than ERα (Ogura et al., 2008). These *in vitro* data cannot be reconciled with our observations that estrogen decreases CRF in primates (Bethea and Centeno, 2008) and serve to highlight the problems with transfected cell models. We speculate that E±P increases serotonin directly, which in turn, decreases CRF in the PVN via inhibitory interneurons. This is reflected by a decrease in fiber density in the raphe that allows serotonin to increase further. In our model, it is not clear whether E acts via ERα or via ERβ to decrease CRF-fiber innervation in the raphe, and the mechanism of action of E on CRF gene expression needs further clarification.

The questions of whether other CNS CRF neurons contain ERs, and whether CRF neurons may differ in their expression of receptors from region to region are also unresolved. These questions were not addressed by the work reported here, but they underscore the importance of determining E-induced CRF gene expression from region

to region. Biochemical evidence, such as mass spectroscopy, is also required to determine whether ERα and ERβ are present in the alternate complexes forming at the CRF promoter.

6.3 The effect of ovarian steroids on CRF-R1 and CRF-R2 expression in the dorsal raphe serotonin system.

We found that E±P decreased CRF-R1 at the gene and protein levels in the raphe nuclei suggesting that ovarian steroids downregulate expression of the anxiogenic receptor. In contrast, E increased CRF-R2 in the dorsal raphe nucleus suggesting that estrogens increase expression of the anxiolytic receptor. We have shown that serotonin neurons express ERβ and PR (Bethea, 1993, Gundlah et al., 2001), which could regulate CRF-R1 or R2 expression. However, our immunocytochemical studies do not reveal whether the receptors are expressed on serotonin neurons. However, the pattern of the staining and the type of large neurons stained were highly indicative of serotonin neurons. In addition, RNA from laser captured serotonin neurons contains CRF-R1 and R2 mRNAs according to microarray analysis (unpublished). In rodents, double ISH revealed that CRF-R2 was expressed exclusively in serotonin neurons at midlevels of the dorsal raphe, whereas, at caudal levels, CRF-R2 was expressed in both serotonin and GABAergic neurons (Day et al., 2004). In addition, administration of UCN2 into the DRN increased c-fos expression in labeled 5-HT neurons (Amat et al., 2004). Together the data suggest that serotonin neurons express CRF-R1 and CRF-R2. Since serotonin neurons also express ERβ and PR, it follows that the CRF receptors could be directly regulated by the steroid receptors.

CRF-R1 was not detectable by autoradiography or ISH in the raphe of rats (Day et al., 2004) or monkeys (Sanchez et al., 1999), but CRF-R1 immunostaining was demonstrated in the raphe of monkeys with a well-characterized and highly specific antibody (Kostich et al., 2004). In our study, CRF-R1 immunostaining was clearly present, but we also detected CRF-R1 mRNA suggesting that the Taqman qPCR may be more sensitive than the other approaches.

Whether E decreases gene expression of CRF-R1 directly via ERs, or via some (as yet) unknown mechanism, our results indicate that ovarian hormone treatment after ovariectomy reduces CRF-R1 gene and protein expression in the raphe. Our results are significant because they indicate that ovarian hormone treatment may decrease stress-induced activation of CRF-R1 in the dorsal raphe. This may be an avenue whereby E ± P decrease inhibition of serotonin neural activity. E ± P treatments would therefore be expected to increase serotonin availability and ameliorate depressive symptoms. In support of this theory, rats that exhibit proactive behavior in resisting defeat to a social stressor show signs of decreased efficacy of both CRF receptors (Wood et al., 2009).

Conversely, we saw that E treatment increased CRF-R2 mRNA expression in the microdissected midbrain block in both qRT-PCR experiments and increased CRF-R2 protein in IHC assays. As presented in Chapter 5 and discussed below, there is reason to believe that CRF-R2 is expressed and regulated on serotonin neurons in monkeys, which contain ERβ and PR. Along this line of reasoning, E could act via ERβ in

serotonin neurons to increase expression of CRF-R2. This is the simplest explanation of the data and therefore the most acceptable. Future experiments with ERβ conditional knock out mice may provide direct evidence for this speculation.

Alternatively, the effect of E on overall midbrain gene expression of CRF-R2 could be secondary to E-induced upregulation of the CRF-R2 agonist, UCN1. It is also possible that E treatment regulates CRF receptor expression through a membrane-bound, g-protein coupled ER, but this mechanism would not be detectable in our model. Therefore, there exists an inherent bias in our model towards measuring the effects of estrogen on the CRF system via its nuclear receptors (i.e., the classical mechanism of E action on ERα and ERβ), which involves binding of an estrogen response element (ERE) and initiating transcription that will generate a response in the target cell 24 to 48 hours later.

Supplemental progesterone abolished the effects of E on midbrain gene expression CRF-R2. When E stimulates gene expression, supplemental P administration can have different effects depending on the gene, the ratio of E/P achieved in the serum, and the isoforms of progestin receptor (PR) in the cell type. Another mechanism where P may indirectly reverse E-induced elevation of CRF-R2 gene expression is via its effects on cocaine amphetamine related transcript (CART) expression in the perioculomotor region. In our model of ovarian hormone treatment after surgical menopause in the monkey, we have shown that one month of P-treatment increases cocaine amphetamine related transcript (CART) in the perioculomotor region and that CART-

positive perioculomotor neurons colocalize with the nuclear progesterone receptor (Lima et al., 2008). Work in rodents indicates that an intraperitoneal injection of amphetamine (Pringle et al., 2008) decreases CRF-R2 density in the rat dorsal raphe nucleus. We speculate that the P-induced increase in CART expression in our animals may be responsible for lowering CRF-R2 gene expression in the raphe and reversing the effects of E.

The increase observed in CRFBP with E treatment could also have anxiolytic effects. CRFBP is thought to bind CRF and prevent it from binding to receptors. Since CRF has the highest affinity at CRF-R1, any decrease in CRF due to CRFBP binding would first prevent its activation of the preferred anxiogenic CRF-R1 receptors. CRFBP mRNA and immunostaining were reported in the trigeminal nuclei and in some raphe nuclei of pontine midbrain (Potter et al., 1992), which are present in our hemi-midbrain block. The regulation of CRF-BP gene expression in the raphe-containing midbrain by estrogen is a novel finding and merits further investigation.

To date, very little is known about what factors affect the expression of sCRFR2α. It is highly expressed in rat midbrain (Chen et al., 2005b), and may be present in macaque midbrain as well. If E and E + P modulate sCRFR2α gene expression, then this would be an avenue where ovarian hormones regulate activation of CRF-R2 and serotonin release in the dorsal raphe nucleus.

6.4 Ovarian steroid effects on UCN1

E alone increased UCN1 expression and P blocked this action at the gene level, but at the protein level there was an increase in immunostained neurons in the $pIII_u$ and an increase in fiber density rostral to the raphe nuclei with E alone and E+P. We cannot explain the disconnection between gene and protein expression with supplemental P, but our data indicate that part of the action of E was through nuclear ERβ. *In vivo* and *in vitro* evidence in rodents supports the notion that estrogens exert a direct and differential transcriptional regulation of the urocortin gene (Haeger et al., 2006). We previously detected PR in the same population of UCN1 neurons (Lima et al., 2008) that also colocalize with CART (Kozicz, 2003). Hence, UCN1 neurons have nuclear ERβ and PR, indicating they are direct targets of ovarian steroids. These data support the notion that ovarian steroids increase serotonin neural function in part by increasing *UCN1* gene expression and transportation into the dorsal raphe serotonin system. An increase in serotonin function would elevate mood, increase stress resilience and decrease anxiety.

Examination of gene expression for the urocortins indicated that *UCN1* was the predominant transcript in the midbrain and that it was increased by E treatment. The expression of *UCN2* was too low to warrant pursuit at the protein level, and it did not appear to be regulated by E ± P. It is noteworthy that E ± P treatments decreased the overall midbrain gene expression of *UCN3* in light of the recent evidence suggesting that the primary role of UCN3 is as a neuromodulator linking stress-induced anxiety and energy homeostasis (Jamieson et al., 2006; Kuperman et al., 2010). However, *UCN3* is

not abundant in the raphe-containing midbrain block of female monkeys treated with placebo, E, or E+P for one month and we therefore could not extrapolate meaningful information from the low levels of *UCN3* gene expressed in the animals within our study.

It would be important to discern whether *UCN2* and *UCN3* are also regulated by estrogen in their respective areas of production in light of newly distinguished roles of UCN2 and UCN3 as modulators of stress-induced food intake in rodents (Asakawa et al., 2010). We determine gene expression in our animals after one month of placebo, E, or E+P treatment to more precisely model the effects of long-term use of ovarian hormone treatment on gene and protein expression in monkeys. Therefore, an inherent bias exists in our model because the immediate early gene effects caused by E (or P) may be occluded after one month of continuous E treatment.

6.5 Differential actions of estradiol and progesterone

The mechanisms of action of E and P on the different components under study may differ from gene to gene. Classically E acts through nuclear ERs that bind to E response elements (EREs) and stimulate gene transcription. The stimulatory effect of E was observed in the expression of CRF-R2 and UCN1 at gene levels, which was translated to the protein level. When E stimulates gene expression, supplemental P administration can have different effects depending on the gene, the ratio of E/P achieved in the serum and the isoforms of progestin receptor (PR) in the cell type. At the ratio of 1/50 typically achieved with our implants, P has been observed to block E -stimulated PR gene expression in the pituitary, but to have no effect on E-stimulated PR gene expression in

the hypothalamus of the same animals (Bethea et al., 1996). This may be due to the differential prevalence of PR-A and PR-B in pituitary and brain (Bethea and Widmann, 1998). Likewise, P had no effect on E –stimulated TPH2 gene expression in the raphe (Sanchez et al., 2005). In this study, P was observed to block the effect of E on CRF-R2 gene and protein expression, and to block the effect of E on UCN1 and CRFBP gene expression. However, P did not block the effect of E on UCN1 protein expression and we have no ready explanation for the disconnection between UCN1 gene and protein expression.

In contrast, E±P decreased gene and protein expression of CRF-R1. The ability of E to decrease gene expression appears to rely on indirect mechanisms. In one pathway, ligand activated steroid receptors sequester NFkB and thereby decrease gene transcription that is dependent upon binding of NFkB to its response element, NRE (Cerillo et al., 1998, McKay and Cidlowski, 1999). Hence, genes that are driven by NFkB can be deactivated with E treatment. Thus, there is precedence to speculate that stress signals induce translocation of NFkB to the nucleus where it drives CRF-R1 gene expression, and that E decreases this action by incapacitating NFkB. Indeed, we have shown that E treatment decreases NFkB translocation to the nucleus in serotonin neurons of the dorsal raphe (Bethea et al., 2006).

Another factor that needs further consideration is the role of allopregnanolone, a metabolite of progesterone that binds to the GABA-A receptor and exhibits anti-anxiety effects similar to benzodiazepines. This has been a particularly difficult action to isolate

from the nuclear actions of progesterone. However, a group of ovariectomized animals that are treated with P alone may be informative. In the absence of E, nuclear PR expression would be very low. Hence, treatment of ovariectomized animals with P could reveal actions of allopregnanolone. In select other studies in the Bethea laboratory, the inclusion of a P treated group has yielded mixed results depending upon the end point examined. P alone had no effect on NFkB translocation (Bethea et al., 2006) or on kyurenin mono-oxygenase expression (Bethea et al., 2009). However, TPH2 expression was increased (Sanchez et al., 2005), and CRF expression in the PVN was decreased (Centeno et al., 2007) by P in a manner similar to E. Thus, we predict that P would decrease CRF fibers in the dorsal raphe as well. The effect of P on the expression of CRF-R1 and CRF-R2 is harder to predict.

6.6 Future directions of this work.

The research presented in this dissertation will make a significant contribution to our understanding of ovarian steroids, the CRF system and serotonin. Behavioral observations were not conducted on the animals used in this study. The animals were in single cages and treated for a short period of time. Previous attempts to monitor behavior under these conditions indicated that the individual temperaments of the animals outweighed any effect of treatment. However, a study of the behavior of ovariectomized and intact Japanese macaques in a semi-free ranging troop has recently been completed and the results indicate that ovariectomy increased several behaviors that are indicative of anxiety (manuscript in preparation). This data supports the inferences of this study in which a short-term single caged model was used.

However, questions remain. As noted above, experiments to define the colocalization of CRF-R1 and CRF-R2 on serotonin neurons with double immunolabeling or double *in situ* hybridization are warranted. Important information may be obtained with ERα and ERβ knock out mice on the specific steroid receptor regulation of *CRF, CRF-R1, CRF-R2* and *UNC1*. Further investigation of the regulation of the different components of the stress system by P alone may provide insight into the role of alloprenanolone in the effects of ovarian steroids. The use of older monkeys that could be treated for longer periods of time with lower doses of ovarian steroids would provide a more accurate translational model. And of course, time courses and dose response curves are always desirous but prohibitively expensive with monkey models.

The largest female population segment in the US, the 'baby boomers' are in perimenopause or menopause, and the life expectancy of women is currently 81 years. Hence, they will live 30 or more years without ovarian steroids. Preserving brain function in this population is absolutely critical from an economic and an interpersonal perspective.

The Women's Health Initiative found that administration of conjugated equine estrogens (CEE, containing largely estriol) supplemented with medroxyprogesterone acetate (MPA; Prempro^{TR}) were detrimental to aspects of cognitive function and increased risk of breast cancer and cardiovascular events. The WHI study has prevented many women from using hormone therapy (HRT), even though low doses of

the bioidentical formulations are more efficacious and safer than Prempro^{TR}, especially when administered via skin or vagina. Perhaps more importantly, community gynecologists discourage HRT even after surgical menopause due to ongoing reliance on misinterpretation of the WHI. Even now, the benefits and risks of HRT in menopausal women are the subjects of ongoing debate in academic circles (Shapiro, 2007) and clinical studies continue to conflict with basic science studies. The "window of opportunity" hypothesis suggests that administration of HRT during the perimenopause is beneficial, whereas administration of HRT long after menopause is detrimental to women's health (Lemay, 2002). The risks of starting HRT long after menopause appeared largely due to cardiovascular problems. However, there were reports of cognitive problems as well (Rossouw et al., 2002, Espeland et al., 2004, Shumaker et al., 2004). But, the cognitive problems could be related to cerebral vascular issues. Moreover in the WHI, general aging and various pre-existing conditions were confounds that could not be discriminated from long-term lack of ovarian steroids. A critical barrier in the field is the execution of a clinical trial that adequately controls these variables. Future studies in the Bethea laboratory intend to test the window of opportunity hypothesis with older monkeys.

The discovery of other compounds that act like estrogen in the brain, but lack the peripheral side effects, is of great importance. In the stress system, agents that block CRF-R1 are highly sought. Current CRF-R1 antagonists have poor clearance in the primate, and provide no immediate hope for success. Considering the evidence in rodents that CRF-R2 mediates depressive behavior after uncontrollable stress, it may

be useful to develop pharmaceutical treatments that antagonize CRF-R2 during chronic or uncontrollable stressful events that precipitate post-traumatic stress syndrome. Presumably, this would prevent the uncontrollable stress-induced release of serotonin into the amygdala, thereby preserving serotonin stores for future use when serotonin is needed for learning, cognition, emotional processing, sleeping, etc. A major obstacle preventing the use of CRF-R2 antagonist therapeutically in humans is evidence in rodents that acute stress reverses the distribution of CRF-receptors in the raphe (Waselus et al., 2009). If acute stress similarly reverses CRF receptor distribution in the human, then the use of R1 and R2 antagonists is fraught with problems.

We have shown that ovariectomy increases CRF-R1 expression, which may translate to fight-or-flight responses to stress. Another way for women entering menopause to ameliorate CRF-R1-induced anxious behaviors may be to increase their daily exercise. Recent evidence in rodents suggests that treadmill exercise recovers corticosterone-induced dysregulation of CRF production in the hypothalamus (Kim et al., 2008). Although the investigators were measuring hypothalamic CRF production as a means to gauge hypothalamic-pituitary-adrenal axis dysregulation, the discovery that exercise can rescue hypothalamic CRF gene expression from dysregulation is a novel finding that could help menopausal women. However, along with the other myriad beneficial effects of exercise, it is doubtful that this result will prompt more people to exercise in our culture.

6.7 Summary

Altogether, in addition to direct actions of E and P on serotonin related gene expression, these data support the notion that ovarian steroids increase serotonin neural function by actions through the CRF system, which include decreased CRF transported to serotonin neurons and a decrease in CRF-R1 expression, in conjunction with an increase in UCN1 transported caudally and an increase in CRF-R2 and CRFBP expression. An increase in serotonin function would elevate mood, increase stress resilience and decrease anxiety (Graeff, 2002, Hammack et al., 2002, Hanley and Van de Kar, 2003, Hendricks et al., 2003, Lowry et al., 2009). From the opposite perspective, stress increases CRF production, which under chronic conditions could decrease serotonin neurotransmission resulting in depression and anxiety (Stout et al., 2002a, Valentino et al., 2009). Our data indicate that ovarian steroids may be protective by ameliorating (not necessarily blocking) these effects of stress, and that the absence of ovarian steroids, as in menopause, would increase sensitivity to stress.

In conclusion, it is well accepted that CRF regulates serotonin and conversely, serotonin regulates CRF. As illustrated in **Figure 37**, our data strongly indicate that ovarian steroids regulate both systems in primates in a synergistic manner. That is, either E alone or E+P act through nuclear, and perhaps other, receptors in serotonin neurons to increase serotonin function. At the same time, they act either directly or indirectly to decrease CRF, to decrease CRF-R1, to increase UCN1 and to increase CRF-R2 in the raphe terminal fields. The mechanism of ER regulation of CRF remains unclear; the CRF gene contains ERE half-sites, but cellular studies indicate that ER

regulation of CRF takes place through an alternate pathway involving protein-protein interactions with other transcription factor complexes (Miller et al., 2004). Therefore, we speculate that the steroid induced increase in serotonin acts to decrease CRF in the PVN via interneurons (Bethea and Centeno, 2008). This in turn, results in less CRF delivered back to the serotonin neurons, further removing inhibition and increasing serotonin delivered to CRF neurons. Perhaps we can cautiously surmise that ovarian steroids start and/or optimally maintain a critical feed-forward loop between the serotonin and CRF neural systems in primates, which is beneficial to mental health and coping strategies.

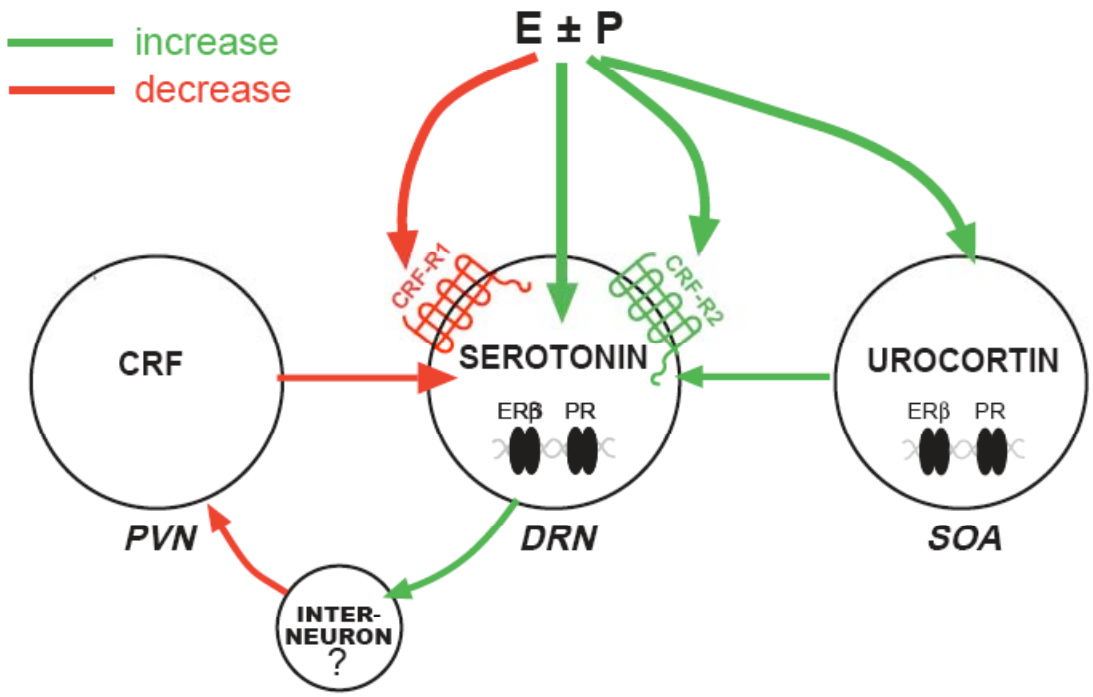

Figure 37. Potential interactions of E & P with serotonin neurons, CRF neurons, and UCN1 neurons. Previous work in our lab indicates that E ± P increases serotonin-related gene expression in the dorsal raphe (green arrow pointing downward). E increased gene transcription of the CRF system ligand UCN1 (green arrow pointing down and right) in the supraoculomotor area (SOA) of the perioculomotor urocortin population, potentially through nuclear estrogen receptors (pictured). E ± P treatment had opposing effects on CRF receptor expression where E ± P decreased the expression of mature CRF-R1 and increased the expression of mature CRF-R2. CRF preferentially binds CRF-R1 while UCN1 preferentially binds CRF-R2. PVN refers to the hypothalamic paraventricular nucleus, DRN refers to the dorsal raphe nucleus, and SOA is the the supraoculomotor area containing the perioculomotor UCN1 population.

References Cited

Amat J, Tamblyn JP, Paul ED, Bland ST, Amat P, Foster AC, Watkins LR, Maier SF (2004) Microinjection of urocortin 2 into the dorsal raphe nucleus activates serotonergic neurons and increases extracellular serotonin in the basolateral amygdala. Neuroscience 129:509-519.

Arango V, Underwood MD, Mann JJ (2002) Serotonin brain circuits involved in major depression and suicide. Prog Brain Res 136:443-453.

Asakawa A, Fujimiya M, Niijima A, Fujino K, Kodama N, Sato Y, Kato I, Nanba H, Laviano A, Meguid MM, Inui A (2010) Parathyroid hormone-related protein has an anorexigenic activity via activation of hypothalamic urocortins 2 and 3. Psychoneuroendocrinology 35:1178-116.

Austin MC, Janosky JE, Murphy HA (2003) Increased corticotropin-releasing hormone immunoreactivity in monoamine-containing pontine nuclei of depressed suicide men. Molecular psychiatry 8:324-332.

Austin MC, Rhodes JL, Lewis DA (1997) Differential distribution of corticotropin-releasing hormone immunoreactive axons in monoaminergic nuclei of the human brainstem. Neuropsychopharmacology 17:326-341.

Bachtell RK, Weitemier AZ, Ryabinin AE (2004) Lesions of the Edinger-Westphal nucleus in C57BL/6J mice disrupt ethanol-induced hypothermia and ethanol consumption. Eur J Neurosci 20:1613-1623.

Bale TL, Vale WW (2004) CRF and CRF receptors: role in stress responsivity and other behaviors. Annu Rev Pharmacol Toxicol 44:525-557.

Bao AM, Hestiantoro A, Van Someren EJ, Swaab DF, Zhou JN (2005) Colocalization of corticotropin-releasing hormone and oestrogen receptor-alpha in the paraventricular nucleus of the hypothalamus in mood disorders. Brain 128:1301-1313.

Baptista T, Reyes D, Hernandez L (1999) Antipsychotic drugs and reproductive hormones: relationship to body weight regulation. Pharmacol Biochem Behav 62:409-417.

Bartolomucci A, Carola V, Pascucci T, Puglisi-Allegra S, Cabib S, Lesch KP, Parmigiani S, Palanza P, Gross C (2010) Increased vulnerability to psychosocial stress in heterozygous serotonin transporter knockout mice. Dis Model Mech 3:459-70.

Bassett JL, Foote SL (1992) Distribution of corticotropin-releasing factor-like immunoreactivity in squirrel monkey (Saimiri sciureus) amygdala. J Comp Neurol 323:91-102.

Behan DP, De Souza EB, Lowry PJ, Potter E, Sawchenko P, Vale WW (1995) Corticotropin releasing factor (CRF) binding protein: a novel regulator of CRF and related peptides. Frontiers in Neuroendocrinology 16:362-382.

Behan DP, De Souza EB, Potter E, Sawchenko P, Lowry PJ, Vale WW (1996) Modulatory actions of corticotropin-releasing factor-binding protein. Annals of the New York Academy of Sciences 780:81-95.

Bellino FL, Wise PM (2003) Nonhuman primate models of menopause workshop. Biol Reprod 68:10-18.

Berod A, Hartman Bk, Pujol Jf (1981) Importance of fixation in immunohistochemistry: use of formaldehyde solutions at variable pH for the localization of tyrosine hydroxylase. J Histochem Cytochem 29:844-850

Bethea CL (1993) Colocalization of progestin receptors with serotonin in raphe neurons of macaque. Neuroendocrinology 57:1-6.

Bethea CL, Brown NA, Kohama SG (1996) Steroid regulation of estrogen and progestin receptor messenger ribonucleic acid in monkey hypothalamus and pituitary. Endocrinology 137:4372-4383.

Bethea CL, Centeno ML (2008) Ovarian steroid treatment decreases corticotropin-releasing hormone (CRH) mRNA and protein in the hypothalamic paraventricular nucleus of ovariectomized monkeys. Neuropsychopharmacology 33:546-556.

Bethea CL, Lu NZ, Gundlah C, Streicher JM (2002) Diverse actions of ovarian steroids in the serotonin neural system. Frontiers in Neuroendocrinology 23:41-100.

Bethea CL, Mirkes SJ, Shively CA, Adams MR (2000) Steroid regulation of tryptophan hydroxylase protein in the dorsal raphe of macaques. Biol Psychiatry 47:562-576.

Bethea CL, Reddy AP, Smith LJ (2006) Nuclear factor kappa B in the dorsal raphe of macaques: an anatomical link for steroids, cytokines and serotonin. J Psychiatry Neurosci 31:105-114.

Bethea CL, Reddy AP, Tokuyama Y, Henderson JA, Lima FB (2009) Protective actions of ovarian hormones in the serotonin system of macaques. Frontiers in Neuroendocrinology 30:212-238.

Bethea CL, Widmann AA (1998) Differential espression of progestin receptor isoforms in the hypothalamus, pituitary, and endometrium of rhesus macaques. Endocrinology 139:677-687.

Bittencourt JC, Vaughan J, Arias C, Rissman RA, Vale WW, Sawchenko PE (1999) Urocortin expression in rat brain: evidence against a pervasive relationship of urocortin-containing projections with targets bearing type 2 CRF receptors. J Comp Neurol 415:285-312.

Bodo C, Rissman EF (2006) New roles for estrogen receptor beta in behavior and neuroendocrinology. Frontiers in Neuroendocrinology 27:217-232.

Brenner RM, Resko JA, West NB (1974) Cyclic changes in oviductal morphology and residual cytoplasmic estradiol binding capacity induced by sequential estradiol--progesterone treatment of spayed rhesus monkeys. Endocrinology 95:1094-1104.

Centeno ML, Reddy AP, Smith LJ, Sanchez RL, Henderson JA, Salli NC, Hess DJ, Pau FK, Bethea CL (2007) Serotonin in microdialysate from the mediobasal hypothalamus increases after progesterone administration to estrogen primed macaques. Eur J Pharm 555:67-75.

Cerillo G, Rees A, Manchanda N, Reilly C, Brogan I, White A, Needham M (1998) The oestrogen receptor regulates NFkappaB and AP-1 activity in a cell-specific manner. J Steroid Biochem Mol Biol 67:79-88.

Chalmers DT, Lovenberg TW, De Souza EB (1995) Localization of novel corticotropin-releasing factor receptor (CRF2) mRNA expression to specific subcortical nuclei in rat brain: comparison with CRF1 receptor mRNA expression. J Neurosci 15:6340-6350.

Chen A, Perrin M, Brar B, Li C, Jamieson P, Digruccio M, Lewis K, Vale W (2005a) Mouse corticotropin-releasing factor receptor type 2alpha gene: isolation, distribution, pharmacological characterization and regulation by stress and glucocorticoids. Mol Endocrinol 19:441-458.

Chen AM, Perrin MH, Digruccio MR, Vaughan JM, Brar BK, Arias CM, Lewis KA, Rivier JE, Sawchenko PE, Vale WW (2005b) A soluble mouse brain splice variant of type 2alpha corticotropin-releasing factor (CRF) receptor binds ligands and modulates their activity. PNAS USA 102:2620-2625.

Clarkson TB (2007) Estrogne effects on arteries vary with stage of reproductive life and extent of subclinical atherosclerosis progression. Menopause 14:373-384.

Commons KG, Connolley KR, Valentino RJ (2003) A neurochemically distinct dorsal raphe-limbic circuit with a potential role in affective disorders. Neuropsychopharmacology 28:206-215.

Conde DM, Pinto-Neto AM, Santos-Sa D, Costa-Paiva L, Martinez EZ (2006) Factors associated with quality of life in a cohort of postmenopausal women. Gynecol Endocrinol 22:441-446.

Cowen PJ (1993) Serotonin receptor subtypes in depression: evidence from studies in neuroendocrine regulation. Clin Neuropharmacol 16 Suppl 3:S6-18.

Cullen MJ, Ling N, Foster AC, Pelleymounter MA (2001) Urocortin, corticotropin releasing factor-2 receptors and energy balance. Endocrinology 142:992-999.

Dautzenberg FM, Hauger RL (2002) The CRF peptide family and their receptors: yet more partners discovered. Trends Pharmacol Sci 23:71-77.

Day HE, Greenwood BN, Hammack SE, Watkins LR, Fleshner M, Maier SF, Campeau S (2004) Differential expression of 5HT-1A, alpha 1b adrenergic, CRF-R1, and CRF-R2 receptor mRNA in serotonergic, gamma-aminobutyric acidergic, and catecholaminergic cells of the rat dorsal raphe nucleus. J Comp Neurol 474:364-378.

Dayas CV, Xu Y, Buller KM, Day TA (2000) Effects of chronic oestrogen replacement on stress-induced activation of hypothalamic-pituitary-adrenal axis control pathways. J Neuroendocrinol 12:784-794.

Denihan A, Kirby M, Bruce I, Cunningham C, Coakley D, Lawlor BA (2000) Three-year prognosis of depression in the community-dwelling elderly. British J Psychiatry 176:453-457.

Desan PH, Silbert LH, Maier SF (1988) Long-term effects of inescapable stress on daily running activity and antagonism by desipramine. Pharmacol Biochem Behav 30:21-29.

Deussing JM, Breu J, Kuhne C, Kallnik M, Bunck M, Glasl L, Yen YC, Schmidt MV, Zurmuhlen R, Vogl AM, Gailus-Durner V, Fuchs H, Holter SM, Wotjak CT, Landgraf R, de Angelis MH, Holsboer F, Wurst W (2010) Urocortin 3 modulates social discrimination abilities via corticotropin-releasing hormone receptor type 2. J Neurosci 30:9103-9116.

Drugan RC, Skolnick P, Paul SM, Crawley JN (1989) A pretest procedure reliably predicts performance in two animal models of inescapable stress. Pharmacol Biochem Behav 33:649-654.

Dunn AJ, Berridge CW (1990) Physiological and behavioral responses to corticotropin-releasing factor administration: is CRF a mediator of anxiety or stress responses? Brain Res Brain Res Rev 15:71-100

Espeland MA, Rapp SR, Shumaker SA, Brunner R, Manson JE, Sherwin BB, Hsia J, Margolis KL, Hogan PE, Wallace R, Dailey M, Freeman R, Hays J (2004) Conjugated equine estrogens and global cognitive function in postmenopausal women: Women's Health Initiative Memory Study. JAMA 291:2959-2968.

Fekete EM, Inoue K, Zhao Y, Rivier JE, Vale WW, Szucs A, Koob GF, Zorrilla EP (2007) Delayed satiety-like actions and altered feeding microstructure by a selective type 2 corticotropin-releasing factor agonist in rats: Intra-hypothalamic Urocortin 3 administration reduces food intake by prolonging the post-meal interval. Neuropsychopharmacology 32:1052-1068.

Freeman EW, Sammel MD, Lin H, Nelson DB (2006) Associations of hormones and menopausal status with depressed mood in women with no history of depression. Arch Gen Psychiatry 63:375-382.

Graeff FG (2002) On serotonin and experimental anxiety. Psychopharmacology 163:467-476.

Gundlah C, Kohama SG, Mirkes SJ, Garyfallou VT, Urbanski HF, Bethea CL (2000) Distribution of estrogen receptor beta (ERbeta) mRNA in hypothalamus, midbrain and temporal lobe of spayed macaque: continued expression with hormone replacement. Brain Res Mol Brain Res 76:191-204.

Gundlah C, Lu NZ, Mirkes SJ, Bethea CL (2001) Estrogen receptor beta (ERβ) mRNA and protein in serotonin neurons of macaques. Molecular Brain Research 91:14-22.

Haeger P, Andres ME, Forray MI, Daza C, Araneda S, Gysling K (2006) Estrogen receptors alpha and beta differentially regulate the transcriptional activity of the Urocortin gene. J Neurosci 26:4908-4916.

Hammack SE, Pepin, JL, DesMarteau, J.S., Watkins LR, Maier, SF (2003) Low doses of corticotropin-releasing hormone injected into the dorsal raphe nucleus block the behavioral consequences of uncontrollable stress. Behavioral Brain Research 147:55-64.

Hammack SE, Richey KJ, Schmid MJ, LoPresti ML, Watkins LR, Maier SF (2002) The role of corticotropin-releasing hormone in the dorsal raphe nucleus in mediating the behavioral consequences of uncontrollable stress. J Neurosci 22:1020-1026.

Hammack SE, Schmid MJ, LoPresti ML, Der-Avakian A, Pellymounter MA, Foster AC, Watkins LR, Maier SF (2003) Corticotropin releasing hormone type 2 receptors in the dorsal raphe nucleus mediate the behavioral consequences of uncontrollable stress. J Neurosci 23:1019-1025.

Hanley NR, Van de Kar LD (2003) Serotonin and the neuroendocrine regulation of the hypothalamic--pituitary-adrenal axis in health and disease. Vitam Horm 66:189-255.

Harman SM, Naftolin F, Brinton EA, Judelson DR (2005b) Is the estrogen controversy over? Deconstructing the Women's Health Initiative Study: A critical evaluation of the evidence. Ann NY Acad Sci 1052:43-56.

Harman SM, Brinton EA, Cedars M, Lobo R, Manson JE, Merriam GR, Miller VM, Naftolin F, Santoro N. KEEPS: The Kronos Early Estrogen Prevention Study (2005b) Cimacteric 8:3-12.

Heikkinen J, Vaheri R, Timonen U (2006) A 10-year follow-up of postmenopausal women on long-term continuous combined hormone replacement therapy: Update of safety and quality-of-life findings. J Br Menopause Soc 12:115-125.

Hendricks TJ, Fyodorov DV, Wegman LJ, Lelutiu NB, Pehek EA, Yamamoto B, Silver J, Weeber EJ, Sweatt JD, Deneris ES (2003) Pet-1 ETS gene plays a critical role in 5-HT neuron development and is required for normal anxiety-like and aggressive behavior. Neuron 37:233-247.

Himmerich H, Binder EB, Kunzel HE, Schuld A, Lucae S, Uhr M, Pollmacher T, Holsboer F, Ising M (2006) Successful antidepressant therapy restores the disturbed interplay between TNF-alpha system and HPA axis. Biol Psychiatry 60:882-888.

Herringa RJ, Nanda SA, Hsu DT, Roseboom PH, Kalin NH (2004) The effects of acute stress on the regulation of central and basolateral amygdala CRF-binding protein gene expression. Brain Res Mol Brain Res 131:17-25.

Hoffman JF, Linderman JJ, Omann GM (1996) Receptor up-regulation, internalization, and interconverting receptor states. Critical components of a quantitative description of N-formyl peptide-receptor dynamics in the neutrophil. J Biol Chem 271:18394-18404.

Holsboer F (1999) The rationale for corticotropin-releasing hormone receptor (CRH-R) antagonists to treat depression and anxiety. J Psychiatr Res 33:181-214.

Hotchkiss JaK, E. (1994) The Menstrual Cycle and Its Neuroendocrine Control. In: Knobil and Neill's Physiology of Reproduciton, 2nd Edition, vol. 2 (Wassarman, P., ed), p 712 New York, NY: Raven Press, Ltd.

Hsu SY, Hsueh AJ (2001) Human stresscopin and stresscopin-related peptide are selective ligands for the type 2 corticotropin-releasing hormone receptor. Nat Med 7:605-611.

Jamieson PM, Li C, Kukura C, Vaughan J, Vale W (2006) Urocortin 3 modulates the neuroendocrine stress response and is regulated in rat amygdala and hypothalamus by stress and glucocorticoids. Endocrinology 147:4578-4588.

Kalin NH, Shelton SE, Davidson RJ (2000) Cerebrospinal fluid corticotropin-releasing hormone levels are elevated in monkeys with patterns of brain activity associated with fearful temperament. Biol Psychiatry 47:579-585.

Kamdi SP, Nakhate KT, Dandekar MP, Kokare DM, Subhedar NK (2009) Participation of corticotropin-releasing factor type 2 receptors in the acute, chronic and withdrawal actions of nicotine associated with feeding behavior in rats. Appetite 53:354-362.

Keck ME, Holsboer F (2001) Hyperactivity of CRH neuronal circuits as a target for therapeutic interventions in affective disorders. Peptides 22:835-844.

Keck ME, Ohl F, Holsboer F, Muller MB (2005) Listening to mutant mice: a spotlight on the role of CRF/CRF receptor systems in affective disorders. Neurosci Biobehav Rev 29:867-889.

Kelly MJ, Ronnekleiv OK (2008) Membrane-initiated estrogen signaling in hypothalamic neurons. Mol Cell Endocrinol 290:14-23.

Kemp CF, Woods RJ, Lowry PJ (1998) The corticotrophin-releasing factor-binding protein: an act of several parts. Peptides 19:1119-1128.

Kendler KS, Karkowski LM, Prescott CA (1999) Causal relationship between stressful life events and the onset of major depression. The Am J Psychiatry 156:837-841.

Kendler KS, Kuhn JW, Vittum J, Prescott CA, Riley B (2005) The interaction of stressful life events and a serotonin transporter polymorphism in the prediction of episodes of major depression: a replication. Arch Gen Psychiatry 62:529-535.

Kim HG, Lim EY, Jung WR, Shin MK, Ann ES, Kim KL (2008) Effects of treadmill exercise on hypoactivity of the hypothalamo-pituitary-adrenal axis induced by chronic administration of corticosterone in rats. Neurosci Lett 434:46-49.

Kirby LG, Rice KC, Valentino RJ (2000) Effects of corticotropin-releasing factor on neuronal activity in the serotonergic dorsal raphe nucleus. Neuropsychopharmacology 22:148-162.

Kostich WA, Grzanna R, Lu NZ, Largent BL (2004) Immunohistochemical visualization of corticotropin-releasing factor type 1 (CRF1) receptors in monkey brain. J Comp Neurol 478:111-125.

Kozicz T (2003) Neurons colocalizing urocortin and cocaine and amphetamine-regulated transcript immunoreactivities are induced by acute lipopolysaccharide stress in the Edinger-Westphal nucleus in the rat. Neuroscience 116:315-320.

Kozicz T (2010) The missing link; the significance of urocortin 1/urocortin 2 in the modulation of the dorsal raphe serotoninergic system. Mol Psychiatry 15:340-341.

Kozicz T, Arimura A, Maderdrut JL, Lazar G (2002) Distribution of urocortin-like immunoreactivity in the central nervous system of the frog Rana esculenta. J Comp Neurol 453:185-198.

Kudielka BM, Schmidt-Reinwald AK, Hellhammer DH, Kirschbaum C (1999) Psychological and endocrine responses to psychosocial stress and dexamethasone/corticotropin-releasing hormone in healthy postmenopausal women and young controls: the impact of age and a two-week estradiol treatment. Neuroendocrinology 70:422-430.

Kuiper GG, Enmark E, Pelto-Huikko M, Nilsson S, Gustafsson JA (1996) Cloning of a novel receptor expressed in rat prostate and ovary. PNAS USA 93:5925-5930.

Kuo J, Hariri OR, Bondar G, Ogi J, Micevych P (2009) Membrane estrogen receptor-alpha interacts with metabotropic glutamate receptor type 1a to mobilize intracellular calcium in hypothalamic astrocytes. Endocrinology 150:1369-1376.

Kuperman Y, Issler O, Regev L, Musseri I, Navon I, Neufeld-Cohen A, Gil S, Chen A (2010) Perifornical Urocortin-3 mediates the link between stress-induced anxiety and energy homeostasis. PNAS USA 107:8393-8398.

Laflamme N, Nappi RE, Drolet G, Labrie C, Rivest S (1998) Expression and neuropeptidergic characterization of estrogen receptors (ERalpha and ERbeta) throughout the rat brain: anatomical evidence of distinct roles of each subtype. J Neurobiol 36:357-378.

Lalmansingh AS, Uht RM (2008) Estradiol regulates corticotropin-releasing hormone gene (crh) expression in a rapid and phasic manner that parallels estrogen receptor-alpha and -beta recruitment to a 3',5'-cyclic adenosine 5'-monophosphate regulatory region of the proximal crh promoter. Endocrinology 149:346-357.

Lesch KP (2001) Serotonergic gene expression and depression: implications for developing novel antidepressants. J Affect Disord 62:57-76.

Lewis K, Li C, Perrin MH, Blount A, Kunitake K, Donaldson C, Vaughan J, Reyes TM, Gulyas J, Fischer W, Bilezikjian L, Rivier J, Sawchenko PE, Vale WW (2001) Identification of urocortin III, an additional member of the corticotropin-releasing factor (CRF) family with high affinity for the CRF2 receptor. PNAS USA 98:7570-7575.

Lemay A (2002) The relevance of the Women's Health Initiative results on combined hormone replacement therapy in clinical practice. J Obstet Gynaecol Can 24:711-715.

Li C, Vaughan J, Sawchenko PE, Vale WW (2002) Urocortin III-immunoreactive projections in rat brain: partial overlap with sites of type 2 corticotrophin-releasing factor receptor expression. J Neurosci 22:991-1001.

Li XF, Mitchell JC, Wood S, Coen CW, Lightman SL, O'Byrne KT (2003) The effect of oestradiol and progesterone on hypoglycaemic stress-induced suppression of pulsatile luteinizing hormone release and on corticotropin-releasing hormone mRNA expression in the rat. J Neuroendocrinol 15:468-476.

Liebsch G, Landgraf R, Gerstberger R, Probst JC, Wotjak CT, Engelmann M, Holsboer F, Montkowski A (1995) Chronic infusion of a CRH1 receptor antisense oligodeoxynucleotide into the central nucleus of the amygdala reduced anxiety-related behavior in socially defeated rats. Regul Pept 59:229-239.

Lim MM, Tsivkovskaia NO, Bai Y, Young LJ, Ryabinin AE (2006) Distribution of corticotropin-releasing factor and urocortin 1 in the vole brain. Brain Behav Evol 68:229-240.

Lima FB, Henderson JA, Reddy AP, Tokuyama Y, Hubert GW, Kuhar MJ, Bethea CL (2008) Unique responses of midbrain CART neurons in macaques to ovarian steroids. Brain Research 1227:76-88.

Lowry CA, Hale MW, Plant A, Windle RJ, Shanks N, Wood SA, Ingram CD, Renner KJ, Lightman SL, Summers CH (2009) Fluoxetine inhibits corticotropin-releasing factor (CRF)-induced behavioural responses in rats. Stress 12:225-239.

Lowry CA, Moore FL (2006) Regulation of behavioral responses by corticotropin-releasing factor. Gen Comp Endocrinol 146:19-27.

Luiten PG, Koolhaas JM, de Boer S, Koopmans SJ (1985a) The cortico-medial amygdala in the central nervous system organization of agonistic behavior. Brain Research 332:283-297.

Luiten PG, ter Horst GJ, Karst H, Steffens AB (1985b) The course of paraventricular hypothalamic efferents to autonomic structures in medulla and spinal cord. Brain Research 329:374-378.

Lund TD, Munson DJ, Haldy ME, Handa RJ (2004) Androgen inhibits, while oestrogen enhances, restraint-induced activation of neuropeptide neurones in the paraventricular nucleus of the hypothalamus. J Neuroendocrinol 16:272-278.

Lukkes JL, Forster GL, Renner KJ, Summers CH (2008) Corticotropin-releasing factor 1 and 2 receptors in the dorsal raphe differentially affect serotonin release in the nucleus accumbens. Eur J Pharmacology 578:185-193.

Maier SF, Drugan RC, Grau JW (1982) Controllability, coping behavior, and stress-induced analgesia in the rat. Pain 12:47-56.

Maier SF, Watkins LR (2005) Stressor controllability and learned helplessness: the roles of the dorsal raphe nucleus, serotonin, and corticotropin-releasing factor. Neurosci Biobehav Rev 29:829-841.

Maki PM, Freeman EW, Greendale GA, Henderson VW, Newhouse PA, Schmidt PJ, Scott NF, Shively CA, Soares CN Summary of the National Institute on Aging-sponsored conference on depressive symptoms and cognitive complaints in the menopausal transition. Menopause 17:815-822.

Mani S (2008) Progestin receptor subtypes in the brain: the known and the unknown. Endocrinology 149:2750-2756.

Mann JJ, Malone KM, Diehl DJ, Perel J, Cooper TB, Mintun MA (1996) Demonstration in vivo of reduced serotonin responsivity in the brain of untreated depressed patients. Am J Psychiatry 153:174-182.

Martinez V, Wang L, Rivier J, Grigoriadis D, Tache Y (2004) Central CRF, urocortins and stress increase colonic transit via CRF1 receptors while activation of CRF2 receptors delays gastric transit in mice. J Physiol 556:221-234.

May PJ, Reiner AJ, Ryabinin AE (2008) Comparison of the distributions of urocortin-containing and cholinergic neurons in the perioculomotor midbrain of the cat and macaque. J Comp Neurol 507:1300-1316.

McKay LI, Cidlowski JA (1999) Molecular control of immune/inflammatory responses: interactions between nuclear factor-kappa B and steroid receptor-signaling pathways. Endocr Rev 20:435-459.

McKinlay SM, Brambilla DJ, Posner JG (2008) The normal menopause transition. Maturitas 61:4-16.

Micevych PE, Mermelstein PG (2008) Membrane estrogen receptors acting through metabotropic glutamate receptors: an emerging mechanism of estrogen action in brain. Mol Neurobiol 38:66-77.

Miller WJ, Suzuki S, Miller LK, Handa R, Uht RM (2004) Estrogen receptor (ER)beta isoforms rather than ERalpha regulate corticotropin-releasing hormone promoter activity through an alternate pathway. J Neurosci 24:10628-10635.

Minor TR, Dess NK, Ben-David E, Chang WC (1994) Individual differences in vulnerability to inescapable shock in rats. J Exp Psychol Anim Behav Process 20:402-412.

Moncek F, Duncko R, Jezova D (2003) Repeated citalopram treatment but not stress exposure attenuates hypothalamic-pituitary-adrenocortical axis response to acute citalopram injection. Life Sci 72:1353-1365.

Muller MB, Zimmermann S, Sillaber I, Hagemeyer TP, Deussing JM, Timpl P, Kormann MS, Droste SK, Kuhn R, Reul JM, Holsboer F, Wurst W (2003) Limbic corticotropin-releasing hormone receptor 1 mediates anxiety-related behavior and hormonal adaptation to stress. Nature Neuroscience 6:1100-1107.

Neufeld-Cohen A, Evans AK, Getselter D, Spyroglou A, Hill A, Gil S, Tsoory M, Beuschlein F, Lowry CA, Vale W, Chen A (2010) Urocortin-1 and -2 double-deficient mice show robust anxiolytic phenotype and modified serotonergic activity in anxiety circuits. Mol Psychiatry 15:426-441, 339.

Ni X, Nicholson RC (2006) Steroid hormone mediated regulation of corticotropin-releasing hormone gene expression. Front Biosci 11:2909-2917.

Nisar N, Sohoo NA (2009) Frequency of menopausal symptoms and their impact on the quality of life of women: a hospital based survey. J Pak Med Assoc 59:752-756.

O'Connor KA, Ferrell R, Brindle E, Trumble B, Shofer J, Holman DJ, Weinstein M (2009) Progesterone and ovulation across stages of the transition to menopause. Menopause 16:1178-1187.

O'Connor TG, Cameron JL (2006) Translating research findings on early experience to prevention: animal and human evidence on early attachment relationships. Am J Prev Med 31:S175-181.

Ogura E, Kageyama K, Hanada K, Kasckow J, Suda T (2008) Effects of estradiol on regulation of corticotropin-releasing factor gene and interleukin-6 production via estrogen receptor type beta in hypothalamic 4B cells. Peptides 29:456-464.

Osterlund MK, Gustafsson JA, Keller E, Hurd YL (2000) Estrogen receptor beta (ERbeta) messenger ribonucleic acid (mRNA) expression within the human forebrain: distinct distribution pattern to ERalpha mRNA. J Clin Endocrinol Metab 85:3840-3846.

Owens MJ, Nemeroff CB (1994) Role of serotonin in the pathophysiology of depression: focus on the serotonin transporter. Clin Chem 40:288-295.

Pastor R, McKinnon CS, Scibelli AC, Burkhart-Kasch S, Reed C, Ryabinin AE, Coste SC, Stenzel-Poore MP, Phillips TJ (2008) Corticotropin-releasing factor-1 receptor involvement in behavioral neuroadaptation to ethanol: a urocortin1-independent mechanism. PNAS USA105:9070-9075.

Paxinos G (1990) The Human Nervous System. San Diego, CA: Academic Press Inc.

Pernar L, Curtis AL, Vale WW, Rivier JE, Valentino RJ (2004) Selective activation of corticotropin-releasing factor-2 receptors on neurochemically identified neurons in the rat dorsal raphe nucleus reveals dual actions. J Neurosci 24:1305-1311.

Petrov T, Krukoff TL, Jhamandas JH (1992) The hypothalamic paraventricular and lateral parabrachial nuclei receive collaterals from raphe nucleus neurons: a combined double retrograde and immunocytochemical study. J Comp Neurol 318:18-26.

Pezawas L, Meyer-Lindenberg A, Drabant EM, Verchinski BA, Munoz KE, Kolachana BS, Egan MF, Mattay VS, Hariri AR, Weinberger DR (2005) 5-HTTLPR polymorphism impacts human cingulate-amygdala interactions: a genetic susceptibility mechanism for depression. Nature Neuroscience 8:828-834.

Pinto-Meza A, Usall J, Serrano-Blanco A, Suarez D, Haro JM (2006) Gender differences in response to antidepressant treatment prescribed in primary care. Does menopause make a difference? J Affect Disord 93:53-60.

Ponchel F, Toomes C, Bransfield K, Leong FT, Douglas SH, Field SL, Bell SM, Combaret V, Puisieux A, Mighell AJ, Robinson PA, Inglehearn CF, Isaacs JD, Markham AF (2003) Real-time PCR based on SYBR-Green I fluorescence: an alternative to the TaqMan assay for a relative quantification of gene rearrangements, gene amplifications and micro gene deletions. BMC Biotechnol 3:18.

Portillo F, Carrasco M, Vallo JJ (1998) Separate populations of neurons within the paraventricular hypothalamic nucleus of the rat project to vagal and thoracic autonomic preganglionic levels and express c-Fos protein induced by lithium chloride. J Chem Neuroanat 14:95-102.

Potter E, Behan DP, Linton EA, Lowry PJ, Sawchenko PE, Vale WW (1992) The central distribution of a corticotropin-releasing factor (CRF)-binding protein predicts multiple sites and modes of interaction with CRF. PNAS USA 89:4192-4196.

Poulin JF, Castonguay-Lebel Z, Laforest S, Drolet G (2008) Enkephalin co-expression with classic neurotransmitters in the amygdaloid complex of the rat. J Comp Neurol 506:943-959.

Prather AA, Carroll JE, Fury JM, McDade KK, Ross D, Marsland AL (2009) Gender differences in stimulated cytokine production following acute psychological stress. Brain Behav Immun 23:622-628.

Price ML, Lucki I (2001) Regulation of serotonin release in the lateral septum and striatum by corticotropin-releasing factor. J Neurosci 21:2833-2841.

Pringle RB, Mouw NJ, Lukkes JL, Forster GL (2008) Amphetamine treatment increases corticotropin-releasing factor receptors in the dorsal raphe nucleus. Neuroscience research 62:62-65.

Raadsheer FC, Hoogendijk WJ, Stam FC, Tilders FJ, Swaab DF (1994) Increased numbers of corticotropin-releasing hormone expressing neurons in the hypothalamic paraventricular nucleus of depressed patients. Neuroendocrinology 60:436-444.

Refojo D, Echenique C, Muller MB, Reul JM, Deussing JM, Wurst W, Sillaber I, Paez-Pereda M, Holsboer F, Arzt E (2005) Corticotropin-releasing hormone activates ERK1/2 MAPK in specific brain areas. PNAS USA 102:6183-6188.

Reyes TM, Lewis K, Perrin MH, Kunitake KS, Vaughan J, Arias CA, Hogenesch JB, Gulyas J, Rivier J, Vale WW, Sawchenko PE (2001) Urocortin II: a member of the corticotropin-releasing factor (CRF) neuropeptide family that is selectively bound by type 2 CRF receptors. PNAS USA 98:2843-2848.

Risch N, Herrell R, Lehner T, Liang KY, Eaves L, Hoh J, Griem A, Kovacs M, Ott J, Merikangas KR (2009) Interaction between the serotonin transporter gene (5-HTTLPR), stressful life events, and risk of depression: a meta-analysis. Jama 301:2462-2471.

Roepke TA, Xue C, Bosch MA, Scanlan TS, Kelly MJ, Ronnekleiv OK (2008) Genes associated with membrane-initiated signaling of estrogen and energy homeostasis. Endocrinology 149:6113-6124.

Rossouw JE, Anderson GL, Prentice RL, LaCroix AZ, Kooperberg C, Stefanick ML, Jackson RD, Beresford SA, Howard BV, Johnson KC, Kotchen JM, Ockene J (2002) Risks and benefits of estrogen plus progestin in healthy postmenopausal women: principal results from the Women's Health Initiative randomized controlled trial. JAMA 288:321-333.

Roy BN, Reid RL, Van Vugt DA (1999) The effects of estrogen and progesterone on corticotropin-releasing hormone and arginine vasopressin messenger ribonucleic acid levels in the paraventricular nucleus and supraoptic nucleus of the rhesus monkey. Endocrinology 140:2191-2198.

Ruggiero DA, Underwood MD, Rice PM, Mann JJ, Arango V (1999) Corticotropic-releasing hormone and serotonin interact in the human brainstem: behavioral implications. Neuroscience 91:1343-1354.

Ryabinin AE, Tsivkovskaia NO, Ryabinin SA (2005) Urocortin 1-containing neurons in the human Edinger-Westphal nucleus. Neuroscience 134:1317-1323.

Sakai K, Salvert D, Touret M, Jouvet M (1977) Afferent connections of the nucleus raphe dorsalis in the cat as visualized by the horseradish peroxidase technique. Brain Research 137:11-35.

Sakanaka M, Shibasaki T, Lederis K (1987) Corticotropin releasing factor-like immunoreactivity in the rat brain as revealed by a modified cobalt-glucose oxidase-diaminobenzidine method. J Comp Neurol 260:256-298.

Sanchez MM, Young LJ, Plotsky PM, Insel TR (1999) Autoradiographic and in situ hybridization localization of corticotropin-releasing factor 1 and 2 receptors in nonhuman primate brain. J Comp Neurol 408:365-377.

Sanchez RL, Reddy AP, Centeno ML, Henderson JA, Bethea CL (2005) A second tryptophan hydroxylase isoform, TPH-2 mRNA, is increased by ovarian steroids in the raphe region of macaques. Brain Res Mol Brain Res 135:194-203.

Santoro N (2005) The menopausal transition. Am J Med 118 Suppl 12B:8-13.

Schule C, Baghai TC, Eser D, Zwanzger P, Jordan M, Buechs R, Rupprecht R (2006) Time course of hypothalamic-pituitary-adrenocortical axis activity during treatment with reboxetine and mirtazapine in depressed patients. Psychopharmacology (Berl) 186:601-611.

Schunkert H, Danser AH, Hense HW, Derkx FH, Kurzinger S, Riegger GA (1997) Effects of estrogen replacement therapy on the renin-angiotensin system in postmenopausal women. Circulation 95:39-45.

Shaaban AM, O'Neill PA, Davies MP, Sibson R, West CR, Smith PH, Foster CS (2003) Declining estrogen receptor-beta expression defines malignant progression of human breast neoplasia. Am J Surg Pathol 27:1502-1512.

Shapiro S (2007) Recent epidemiological evidence relevant to the clinical management of the menopause. Climacteric 10 Suppl 2:2-15.

Sharpe AL, Coste SC, Burkhart-Kasch S, Li N, Stenzel-Poore MP, Phillips TJ (2005) Mice deficient in corticotropin-releasing factor receptor type 2 exhibit normal ethanol-associated behaviors. Alcohol Clin Exp Res 29:1601-1609.

Shumaker SA, Legault C, Kuller L, Rapp SR, Thal L, Lane DS, Fillit H, Stefanick ML, Hendrix SL, Lewis CE, Masaki K, Coker LH (2004) Conjugated equine estrogens and incidence of probable dementia and mild cognitive impairment in postmenopausal women: Women's Health Initiative Memory Study. JAMA 291:2947-2958.

Simmons DM, Arriza JL, Swanson LW (1989) A complete protocol for in situ hybridization of messenger RNAs in brain and other tissues with radio-labeled single-stranded RNA probes. J Histotechnol 12:169-181.

Smith GW, Aubry JM, Dellu F, Contarino A, Bilezikjian LM, Gold LH, Chen R, Marchuk Y, Hauser C, Bentley CA, Sawchenko PE, Koob GF, Vale W, Lee KF (1998) Corticotropin releasing factor receptor 1-deficient mice display decreased anxiety, impaired stress response, and aberrant neuroendocrine development. Neuron 20:1093-1102.

Soares CN, Frey BN (2010) Challenges and opportunities to manage depression during the menopausal transition and beyond. Psychiatr Clin North Am 33:295-308.

Staub DR, Spiga F, Lowry CA (2005) Urocortin 2 increases c-Fos expression in topographically organized subpopulations of serotonergic neurons in the rat dorsal raphe nucleus. Brain Research 1044:176-189.

Stout SC, Owens MJ, Nemeroff CB (2002a) Regulation of corticotropin-releasing factor neuronal systems and hypothalamic-pituitary-adrenal axis activity by stress and chronic antidepressant treatment. J Pharmacol Exp Ther 300:1085-1092.

Stout SC, Owens MJ, Nemeroff CB (2002b) Regulation of corticotropin-releasing factor neuronal systems and hypothalamic-pituitary-adrenal axis activity by stress and chronic antidepressant treatment. J Pharmacol Exper Ther 300:1085-1092.

Tangen T, Mykletun A (2008) Depression and anxiety through the climacteric period: an epidemiological study (HUNT-II). J Psychosom Obstet Gynaecol 29:125-131.

Tetel MJ (2009) Modulation of steroid action in the central and peripheral nervous systems by nuclear receptor coactivators. Psychoneuroendocrinology 34 Suppl 1:S9-19.

Thammacharoen S, Geary N, Lutz TA, Ogawa S, Asarian L (2009) Divergent effects of estradiol and the estrogen receptor-alpha agonist PPT on eating and activation of PVN CRH neurons in ovariectomized rats and mice. Brain Research 1268:88-96.

Thomas RF, Holt BD, Schwinn DA, Liggett SB (1992) Long-term agonist exposure induces upregulation of beta 3-adrenergic receptor expression via multiple cAMP response elements. PNAS USA 89:4490-4494.

Timpl P, Spanagel R, Sillaber I, Kresse A, Reul JM, Stalla GK, Blanquet V, Steckler T, Holsboer F, Wurst W (1998) Impaired stress response and reduced anxiety in mice lacking a functional corticotropin-releasing hormone receptor 1. Nature Genetics 19:162-166.

Tokuyama Y, Reddy AP, Bethea CL (2008) Neuroprotective actions of ovarian hormones without insult in the raphe region of rhesus macaques. Neuroscience 154:720-731.

Tsai MJ, O'Malley BW (1994) Molecular mechanisms of action of steroid/thyroid receptor superfamily members. Annu Rev Biochem 63:451-486.

Vale W, Spiess J, Rivier C, Rivier J (1981) Characterization of a 41-residue ovine hypothalamic peptide that stimulates secretion of corticotropin and beta-endorphin. Science 213:1394-1397.

Valentino RJ, Commons KG (2005) Peptides that fine-tune the serotonin system. Neuropeptides 39:1-8.

Valentino RJ, Lucki I, Van Bockstaele E (2009) Corticotropin-releasing factor in the dorsal raphe nucleus: Linking stress coping and addiction. Brain Research 1314:29-37.

Vamvakopoulos NC, Chrousos GP (1993) Evidence of direct estrogenic regulation of human corticotropin-releasing hormone gene expression. Potential implications for the sexual dimophism of the stress response and immune/inflammatory reaction. J Clin Invest 92:1896-1902.

van de Stolpe A, Slycke AJ, Reinders MO, Zomer AW, Goodenough S, Behl C, Seasholtz AF, van der Saag PT (2004) Estrogen receptor (ER)-mediated transcriptional regulation of the human corticotropin-releasing hormone-binding protein promoter: differential effects of ERalpha and ERbeta. Mol Endocrinology 18:2908-2923.

Van Den Eede F, Van Broeckhoven C, Claes SJ (2005) Corticotropin-releasing factor-binding protein, stress and major depression. Ageing Res Rev 4:213-239.

Van Pett K, Viau V, Bittencourt JC, Chan RK, Li HY, Arias C, Prins GS, Perrin M, Vale W, Sawchenko PE (2000) Distribution of mRNAs encoding CRF receptors in brain and pituitary of rat and mouse. J Comp Neurol 428:191-212.

Vasconcelos LA, Donaldson C, Sita LV, Casatti CA, Lotfi CF, Wang L, Cadinouche MZ, Frigo L, Elias CF, Lovejoy DA, Bittencourt JC (2003) Urocortin in the central nervous system of a primate (Cebus apella): sequencing, immunohistochemical, and hybridization histochemical characterization. J Comp Neurol 463:157-175.

Vaughan J, Donaldson C, Bittencourt J, Perrin MH, Lewis K, Sutton S, Chan R, Turnbull AV, Lovejoy D, Rivier C, et al. (1995) Urocortin, a mammalian neuropeptide related to fish urotensin I and to corticotropin-releasing factor. Nature 378:287-292.

Waselus M, Nazzaro C, Valentino RJ, Van Bockstaele EJ (2009) Stress-induced redistribution of corticotropin-releasing factor receptor subtypes in the dorsal raphe nucleus. Biol Psychiatry 66:76-83.

Waselus M, Van Bockstaele EJ (2007) Co-localization of corticotropin-releasing factor and vesicular glutamate transporters within axon terminals of the rat dorsal raphe nucleus. Brain Research 1174:53-65.

Weiss JM (1971) Effects of coping behavior with and without a feedback signal on stress pathology in rats. J Comp Physiol Psychol 77:22-30.

Weitemier AZ, Ryabinin AE (2005) Brain region-specific regulation of urocortin 1 innervation and corticotropin-releasing factor receptor type 2 binding by ethanol exposure. Alcohol Clin Exp Res 29:1610-1620.

Weitemier AZ, Ryabinin AE (2006) Urocortin 1 in the dorsal raphe regulates food and fluid consumption, but not ethanol preference in C57BL/6J mice. Neuroscience 137:1439-1445.

Whiteaker P, Sharples CG, Wonnacott S (1998) Agonist-induced up-regulation of alpha4beta2 nicotinic acetylcholine receptors in M10 cells: pharmacological and spatial definition. Mol Pharmacol 53:950-962.

Wittmann G, Fuzesi T, Liposits Z, Lechan RM, Fekete C (2009) Distribution and axonal projections of neurons coexpressing thyrotropin-releasing hormone and urocortin 3 in the rat brain. J Comp Neurol 517:825-840.

Wood SK, Baez MA, Bhatnagar S, Valentino RJ (2009) Social stress-induced bladder dysfunction: potential role of corticotropin-releasing factor. Am J Physiol Regul Integr Comp Physiol 296:R1671-1678.

Wood SK, Walker HE, Valentino RJ, Bhatnagar S (2010) Individual differences in reactivity to social stress predict susceptibility and resilience to a depressive phenotype: role of corticotropin-releasing factor. Endocrinology 151:1795-1805.

Xia-Zhang L, Xiao E, Ferin M (1995) A 5-day estradiol therapy, in amounts reproducing concentrations of the early-mid follicular phase, prevents the activation of the hypothalamo-pituitary-adrenal axis by interleukin-1 alpha in the ovariectomized rhesus monkey. J Neuroendocrinol 7:387-392.

Xu J, Hennebold JD, Stouffer RL (2006) Dynamic expression and regulation of the corticotropin-releasing hormone/urocortin-receptor-binding protein system in the primate ovary during the menstrual cycle. J Clin Endocrinol Metab 91:1544-1553.

Zhao L, Donaldson CJ, Smith GW, Vale WW (1998) The structures of the mouse and human urocortin genes (Ucn and UCN). Genomics 50:23-33.